National Library of Canada
Bibliothèque nationale du Canada

Canadian Theses Service
Service des thèses canadiennes

Ottawa, Canada
K1A 0N4

NOTICE

The quality of this microform is heavily dependent upon the quality of the original thesis submitted for microfilming. Every effort has been made to ensure the highest quality of reproduction possible.

If pages are missing, contact the university which granted the degree.

Some pages may have indistinct print especially if the original pages were typed with a poor typewriter ribbon or if the university sent us an inferior photocopy.

Previously copyrighted materials (journal articles, published tests, etc.) are not filmed.

Reproduction in full or in part of this microform is governed by the Canadian Copyright Act, R.S.C. 1970, c. C-30.

AVIS

La qualité de cette microforme dépend grandement de la qualité de la thèse soumise au microfilmage. Nous avons tout fait pour assurer une qualité supérieure de reproduction.

S'il manque des pages, veuillez communiquer avec l'université qui a conféré le grade.

La qualité d'impression de certaines pages peut laisser à désirer, surtout si les pages originales ont été dactylographiées à l'aide d'un ruban usé ou si l'université nous a fait parvenir une photocopie de qualité inférieure.

Les documents qui font déjà l'objet d'un droit d'auteur (articles de revue, tests publiés, etc.) ne sont pas microfilmés.

La reproduction, même partielle, de cette microforme est soumise à la Loi canadienne sur le droit d'auteur, SRC 1970, c. C-30.

NL-339 (r. 88/04)

Canada

THE UNIVERSITY OF ALBERTA

SOME PROBLEMS OF HYPERBOLIC WAVES IN SOLID MECHANICS

BY

JOANNE LAURA WEGNER

A THESIS
SUBMITTED TO THE FACULTY OF GRADUATE STUDIES AND RESEARCH
IN PARTIAL FULFILMENT OF THE REQUIREMENTS FOR THE DEGREE OF
DOCTOR OF PHILOSOPHY

DEPARTMENT OF MECHANICAL ENGINEERING

EDMONTON, ALBERTA

FALL, 1988

Permission has been granted to the National Library of Canada to microfilm this thesis and to lend or sell copies of the film.

The author (copyright owner) has reserved other publication rights, and neither the thesis nor extensive extracts from it may be printed or otherwise reproduced without his/her written permission.

L'autorisation a été accordée à la Bibliothèque nationale du Canada de microfilmer cette thèse et de prêter ou de vendre des exemplaires du film.

L'auteur (titulaire du droit d'auteur) se réserve les autres droits de publication; ni la thèse ni de longs extraits de celle-ci ne doivent être imprimés ou autrement reproduits sans son autorisation écrite.

ISBN 0-315-45738-4

THE UNIVERSITY OF ALBERTA

RELEASE FORM

NAME OF AUTHOR JOANNE LAURA WEGNER

TITLE OF THESIS SOME PROBLEMS OF HYPERBOLIC WAVES IN SOLID MECHANICS

DEGREE FOR WHICH THESIS WAS PRESENTED DOCTOR OF PHILOSOPHY

YEAR THIS DEGREE GRANTED FALL 1988

Permission is hereby granted to THE UNIVERSITY OF ALBERTA LIBRARY to reproduce single copies of this thesis and to lend or sell such copies for private, scholarly or scientific purposes only.

The author reserves other publication rights, and neither the thesis nor extensive extracts from it may be printed or otherwise reproduced without the author's written permission.

(SIGNED) Joanne Wegner

PERMANENT ADDRESS:

22350 TWP Rd. 522
Sherwood Park
Alberta T8C 1G3

DATED August 23 19 88

The University of Alberta

Faculty of Graduate Studies and Research

The undersigned certify that they have read, and recommend to the Faculty of Graduate Studies and Research for acceptance, a thesis entitled

Some Problems of Hyperbolic Waves in Solid Mechanics

submitted by

Joanne Laura Wegner

in partial fulfilment of the requirements for the degree of

Doctor of Philosophy

James B. Haddow
(Supervisor)

Millard F. Beatty

R J Dart

J R Colbourne

Date: 19th August 1988

To my son Nikolaos

Abstract

Some problems of propagation of linear and nonlinear hyperbolic waves in solids are investigated, namely the propagation of plane waves in a linear viscoelastic solid with more than one relaxation time, wave propagation in a linear non-dissipative dispersive system governed by the Klein-Gordon equation and nonlinear wave propagation in hyperelastic strings. A new formulation of a hyperbolic system of first order governing equations for the viscoelastic problem is proposed. Numerical results obtained for the linear problems are based on purely mechanical theory, however some aspects of the thermodynamics of rubberlike materials are investigated in connection with the string problem. Numerical solutions are presented for the linear problems and exact similarity solutions are presented for the nonlinear problems of transverse impact of a stretched string and response of a plucked string. Some of the theoretical results obtained for the string problems are compared with experimental results and the agreement is satisfactory.

Acknowledgements

I would like to express my appreciation to Dr. J.B. Haddow for his excellent guidance and supervision of this thesis. I would also like to thank Dr. A. Mioduchowski and Dr. R.J. Tait for their many helpful suggestions.

I would also like to express my gratitude to Mr. Bernie Faulkner who provided valuable assistance with the experimental work, and to Miss Gail Anderson for word processing the manuscript.

Appreciation is extended to the Province of Alberta, Department of Mechanical Engineering and NSERC for the financial support received during the course of this research.

Table of Contents

PAGE

Chapter I - Introduction 1

Chapter II - Linear Hyperbolic Dispersive Systems 6

2.1 Introduction 6

2.2 Method of Solution for Semi-Infinite Interval 8

2.3 Method of Solution for Finite Interval 12

2.4 Numerical Results 15

Chapter III - Plane Wave Propagation in a Linear Viscoelastic Solid 29

3.1 Introduction 29

3.2 Governing Equations 30

3.3 Numerical Techniques 37

3.3.1 Application of MacCormack's Scheme 37

3.3.2. Method of Characteristics 40

3.4 Numerical Results 43

Chapter IV - Thermomechanics of Hyperelastic Solids 60

4.1 Constitutive Assumptions 60

4.2 Mechanical Incompressibility 64

4.3 Strictly Entropic Elasticity 66

4.4 Modified Entropic and Peizotropic Elasticity 70

Chapter V - Finite Amplitude Wave Propagation in a Stretched Hyperelastic String 74

5.1 Governing Equations 74

5.2 Discontinuity Relations 79

5.3 Exceptional Condition and Genuine Non-Linearity 82

5.4 Similarity Solutions 83

5.5 Solutions 84

5.5.1 Mooney-Rivlin String 87

5.5.2 Three Term Strain Energy Function 90

5.6 Estimate of Validity of the Thermodynamic Approximations 94

5.6.1 Strictly Entropic Material 96

5.6.2 Piezotropic Material 99

5.7 Reflection Problem for Unloaded String 102

5.8 Application of Godunov's Method 103

Chapter VI - Transverse Impact and Plucked String Problems 111

6.1 Transverse Impact Problem 111

6.1.1 Mooney-Rivlin String 113

6.1.2 Three Term Ogden String 123

6.2 Symmetrically Plucked String 137

6.3.1 Mooney-Rivlin String 139

6.3.2 Three Term Ogden String 143

6.3 Analogy with Propagation of Waves in Elastic Half Space . 148

Chapter VII - Experimental Results 154

7.1 Experimental Procedure 154

7.1.1 Transverse Impact Problem 154

7.1.2 Plucked String 156

7.2 Results for Transverse Impact Problem 159

7.3 Results for Plucked String Problem 162

7.4 Concluding Remarks 176

Bibliography 177

List of Tables

Table		Page
3.1	Calculation of nondimensional stress at $x = t^+$ for $N = 2$, with $\sigma(0,t) = \sigma_o H(t)$, $\bar{\sigma}_o = 1$, and quiescent initial conditions, for $\nu = 1.0$ (Refer to Figure 3.8)	44
5.1	Comparison of wave speeds for strictly entropic and piezotropic cases.	101
5.2	Comparison of results for strictly entropic and piezotropic cases. Adiabatic stretch to λ_1	102
7.1	Transverse Impact Problem: Measured final angle θ_f for impact velocities $Q \cong 85$ and 49 m/s, and $\lambda_o = 3.2$.	162
7.2	Experimental values of velocity of the central flat portion of the string, v_f, compared to the theoretical value of v_f, with $\lambda_o = 2.0$, $\theta_1 = 45°$ and $\lambda_1 = 2.83$.	164

List of Figures

Figure		Page
2.1	Problem geometry of finite interval initial-boundary value problem.	13
2.2	Solution of Klein-Gordon equation by FFT algorithm with quiescent initial conditions and boundary condition $\phi(0,t) = \sin \pi t\ H(t)\ H(1-t)$, T = 70, and N = 2048.	17
2.3	Solution of Klein-Gordon equation by FFT algorithm with quiescent initial conditions and boundary condition $\phi(0,t) = \sin \pi t\ H(t)\ H(1-t)$, T = 200, N = 2048.	18
2.4	Solution of Klein-Gordon equation by FFT algorithm with quiescent initial conditions and boundary condition $\phi(0,t) = \sin \pi t\ H(t)\ H(1-t)$, T = 300, and N = 4096.	19
2.5	Solution of Klein-Gordon equation by FFT algorithm with quiescent initial conditions and boundary condition $\phi(0,t) = \sin \pi t\ H(t)\ H(1-t)$, T = 100, and N = 2048. Aliasing is apparent.	20
2.6	Solution of Klein-Gordon equation by FFT algorithm with quiescent initial conditions and boundary condition $\phi(0,t) = \sin \pi t\ H(t)\ H(1-t)$, T = 600, N = 4096.	21
2.7	Solution of Klein-Gordon equation by FFT algorithm with quiescent initial conditions and boundary condition $\phi(0,t) = H(t)\ H(1-t)$, T = 200, and N = 16384.	22
2.8	Solution of Klein-Gordon equation by FFT algorithm with quiescent initial conditions and boundary condition $\phi(0,t) = H(t)\ H(1-t)$, T = 200, and N = 16384.	23
2.9	Solution of Klein-Gordon equation by FFT algorithm with quiescent initial conditions and boundary condition $\phi(0,t) = H(t)\ H(1-t)$, T = 200 and N = 16384.	24

2.10 Solution of Klein-Gordon equation by FFT algorithm with quiescent initial conditions and boundary condition $\phi(0,t) = H(t)\ H(1-t)$, T = 100, and N = 16384. Aliasing is apparent. 25

2.11 Solution of Klein-Gordon equation by FFT algorithm with quiescent initial conditions and boundary condition $\phi(0,t) = H(t)\ H(1-t)$, T = 600 and N = 16384. 26

2.12 Solution of Klein-Gordon equation by FFT algorithm with quiescent initial conditions and boundary condition $\phi(0,t) = H(t)$, T = 600 and N = 16384. 27

2.13 Solution of Klein-Gordon equation by FFT algorithm with quiescent initial conditions and boundary condition $\phi(0,t) = H(t)$, T = 600 and N = 16384. 28

3.1 A second order viscoelastic fluid represented by a Kelvin element in series with a Maxwell element. 33

3.2 A second order viscoelastic fluid represented by a standard model in series with a dashpot. 33

3.3 The solid lines represent the mesh used for the method of characteristics. If a wavefront expansion technique is incorporated at the wavefront x = t, the mesh would be modified at x = t as indicated by the dashed lines. 42

3.4 Standard Model $\alpha_o = 1.0$ - Nondimensional σ versus nondimensional x for $\sigma(0,t) = \sigma_o H(t)$, with $\sigma_o = 1$ and $\nu = 1.0$. 45

3.5 Standard Model $\alpha_o = 1.0$ - Nondimensional σ versus nondimensional x for $\sigma(0,t) = \sigma_o H(t)$, with $\sigma_o = 1$ and $\nu = 0.99$. 46

3.6 Standard Model $\alpha_o = 0.9$ - Nondimensional σ versus nondimensional x for $\sigma(0,t) = \sigma_o H(t)$, with $\sigma_o = 1$ and $\nu = 1$. 47

3.7 Standard Model $\alpha_o = 0.9$ - Nondimensional σ versus nondimensional x for $\sigma(0,t) = \sigma_o H(t)$, with $\sigma_o = 1$ and $\nu = 0.99$. 48

3.8 Extended Model (N = 2) α_o = 0.9 - Nondimensional σ versus nondimensional x for $\sigma(0,t) = \sigma_o H(t)$, with σ_o = 1 and ν = 1.0. 49

3.9 Extended Model (N = 2) α_o = 0.9 - Nondimensional σ versus nondimensional x for $\sigma(0,t) = \sigma_o H(t)$, with σ_o = 1 and ν = 0.99. 50

3.10 Standard Model - α_o = 0.1 - Nondimensinal σ versus nondimensional x for $\sigma(0,t) = \sigma_o H(t)$, with σ_o = 1, ν = 1. 51

3.11 Extended Model (N = 2) α_o = 0.1 - Nondimensional σ versus nondimensional x for $\sigma(0,t) = \sigma_o H(t)$, with σ_o = 1 and ν = 0.99. 52

3.12 Standard Model α_o = 1.0 - Nondimensional σ versus nondimensional x for $\sigma(0,t) = \sigma_o \sin \pi t\, H(t)\, H(1-t)$, with σ_o = 1 and ν = 1.0. 53

3.13 Standard Model α_o = 0.9 - Nondimensional σ versus nondimensional x for $\sigma(0,t) = \sigma_o \sin \pi t\, H(t)\, H(1-t)$, with σ_o = 1 and ν = 1.0. 54

3.14 Extended Model (N = 2) α_o = 0.9 - Nondimensional σ versus nondimensional x for $\sigma(0,t) = \sigma_o \sin \pi t\, H(t)\, H(1-t)$, with σ_o = 1 and ν = 1.0. 55

3.15 Standard Model α_o = 0.1 - Nondimensional σ versus nondimensional x for $\sigma(0,t) = \sigma_o \sin \pi t\, H(t)\, H(1-t)$, with σ_o = 1 and ν = 1.0. 56

3.16 Standard Model α_o = 0.1 - Nondimensional σ versus nondimensional x for $\sigma(0,t) = \sigma_o \sin \pi t\, H(t)\, H(1-t)$, with σ_o = 1 and ν = 0.99. 57

3.17 Extended Model (N = 2) α_o = 0.1 - Nondimensional σ versus nondimensional x for $\sigma(0,t) = \sigma_o \sin \pi t\, H(t)\, H(1-t)$, with σ_o = 1 and ν = 1.0. 58

3.18 Extended Model (N = 2) α_o = 0.1 - Nondimensional σ versus nondimensional x for $\sigma(0,t) = \sigma_o \sin \pi t\, H(t)\, H(1-t)$, with σ_o = 1 and ν = 0.99. 59

4.1 Isothermal nominal stress-stretch relation for Ogden's 3 term strain energy function with parameters (4.18), and Mooney-Rivlin strain energy function with $\alpha = 0.6$. 65

5.1 Problem geometry 75

5.2 Problem geometry of simple tension problem. 85

5.3 Similarity solution for simple tension loading problem when $P_f > P_o$, valid for Mooney-Rivlin strain energy function, and 3 term strain energy function when $\lambda_i > \lambda_f > \lambda_o \geq 1$. The solution is valid for $tc_L(\lambda_o) \leq 1$. 89

5.4 Isothermal stress-stretch relation for Ogden's 3 term strain energy function with parameters (4.18). 91

5.5 Similarity solution for simple tension loading problem when $P_f > P_o$, valid for 3 term strain energy function when $\lambda_f > \lambda_i$ and $\lambda_T > \lambda_o \geq 1$. Solution is valid for $tc_L(\lambda_o) \leq 1$. 92

5.6 Similarity solution for simple tension loading problem when $P_f > P_o$, valid 3 term strain energy function when $\lambda_f > \lambda_i$ and $\lambda_o \geq \lambda_T \geq 1$. Solution is valid for $tV_L \leq 1$. 92

5.7 Solution with reflection for simple tension loading problem when $P_f > P_o$, valid for 3 term strain energy function when $\lambda_f > \lambda_i$ and $\lambda_o \geq \lambda_T \geq 1$. Solution is valid for $0 \leq t \leq 1/V_L^{(r)}$. 95

5.8 The possible similarity solutions for simple tension problem of a neo-Hookean strain energy function string. 105

5.9 Godunov's method applied to the simple tension problem of a neo-Hookean string, with initial conditions $u(X,0) = 0$, $\lambda(X,0) = 1 + \cos 2\pi X$, and boundary conditions $u(-2,t) = u(2,t) = 0$. 108

5.10 Godunov's method applied to simple tension problems of a neo-Hookean string, with initial conditions $u(X,0)=0$, $\lambda(X,0) = 1 + \cos 2\pi X$, and boundary conditions $u(-2,t) = u(2,t) = 0$. 109

5.11 Godunov's method applied to simple tension problems of a neo-Hookean string, with initial conditions $u(X,0) = 0$, $\lambda(X,0) = 1 + \cos 2\pi X$, and boundary conditions $u(-2,t) = u(2,t) = 0$. 110

6.1 Problem geometry of transverse impact problem. 112

6.2 Isothermal stress-stretch relation for Mooney-Rivlin material with $\alpha = 0.6$. 115

6.3 Transverse Impact Problem - Solution valid for Mooney-Rivlin string if $\lambda_f < \lambda_{c1}$. 116

6.4 Transverse Impact Problem - Region of validity in (Q,λ_o) plane for solution of a Mooney-Rivlin string valid if $\lambda_f < \lambda_{c1}$. 118

6.5 Transverse Impact Problem - Solution valid for Mooney-Rivlin string if $\lambda_o < \lambda_{c1}$ and $\lambda_f > \lambda_{c1}$. 119

6.6 Transverse Impact Problem - Solution valid for Mooney-Rivlin string if $\lambda_o > \lambda_{c1}$. 121

6.7 Isothermal stress-stretch relation for 3 term strain energy function with parameters (4.18). 124

6.8 Isothermal stress-stretch relation (schematic) for 3 term strain energy function showing λ_o in region (c), that is $\lambda_i < \lambda_o < \lambda_{c2}$, and $V_T(\lambda_o) = V_T(\lambda_*)$. 125

6.9 Transverse Impact Problem - Solution valid for 3 term Ogden string when $\lambda_o \geq \lambda_{c2}$. 126

6.10 Transverse Impact Problem - Solution valid for 3 term Ogden string when $\lambda_i < \lambda_o < \lambda_{c2}$ and $\lambda_f < \lambda_*$. 129

6.11 Isothermal stress-stretch relation (schematic) for 3 term strain energy function showing λ_o in region (b), that is $\lambda_{c1} < \lambda_o < \lambda_i$, and $V_T(\lambda_o) = V_T(\lambda_*)$. 130

6.12 Isothermal stress-stretch relation (schematic) for 3 term strain energy function showing λ_o in region (b), that is $\lambda_{c1} < \lambda_o < \lambda_i$, and $\lambda_f < \lambda_*$. 131

6.13 Transverse Impact Problem - Solution valid for 3 term Ogden string when $\lambda_{c1} < \lambda_o < \lambda_T$ and $\lambda_f < \lambda_*$. 132

6.14 Isothermal stress-stretch relation (schematic) for 3 term strain energy function showing λ_o in region (a), that is $1 < \lambda_o < \lambda_{c1}$, and $V_T(\lambda_{c1}) = V_T(\lambda_{**})$. 133

6.15 Transverse Impact Problem - Solution valid for 3 term Ogden string when $1 < \lambda_o < \lambda_{c1}$ and $\lambda_i < \lambda_f < \lambda_{**}$. 134

6.16 Isothermal stress-stretch relation (schematic) for 3 term strain energy function showing λ_o in region (a), that is $1 < \lambda_o < \lambda_{c1}$, and $\lambda_f > \lambda_{**}$. 135

6.17 Transverse Impact Problem - Solution valid for 3 term Ogden string when $\lambda_o < \lambda_T < \lambda_{c1}$ and $\lambda_f > \lambda_{**}$. 136

6.18 Transverse Impact Problem - Solution valid for 3 term Ogden string when $\lambda_o = \lambda_T < \lambda_{c1}$ and $\lambda_f > \lambda_{**}$. 136

6.19 Deformed configuration of the string before it is released at time $t = 0$. 138

6.20 Deformed configuration of the string for time $t > 0$. 138

6.21 Plucked String Problem - Solution valid for Mooney-Rivlin string if $\lambda_1 < \lambda_{c1}$ or if $\lambda_1 > \lambda_{c1}$ and $\lambda_f < \hat{\lambda}_T$. 140

6.22 Plucked String Problem - Solution valid if $\lambda_f > \lambda_{c1}$ or if $\lambda_1 > \lambda_{c1}$ and $\lambda_f > \hat{\lambda}_T$. 142

6.23 Plucked String Problems - Regions of validity for Mooney-Rivlin string with $\alpha = 0.6$. 144

6.24 Plucked String Problem - Solution valid for 3 term Ogden string if $\lambda_1 > \lambda_f > \lambda_{c2}$. 145

6.25 Plucked String Problem - Solution valid for 3 term Ogden string if $\lambda_1 > \lambda_{c2} > \lambda_f > \lambda_i$. 147

6.26 Plucked String Problem - Regions of validity for 3 term Ogden string with parameters (4.18). 149

6.27 Relation between resultant shear stress and shear strain due to Treloar (1975). 153

7.1 Experimental setup for transverse impact problem. 155

7.2 Another view of the experimental setup for transverse impact problem. 155

7.3 Experimental setup for plucked string problem. 157

7.4 Deformed configuration of the string before it is released at time t = 0. 157

7.5 An example of a photograph with double exposure which is used to calculate the velocity of the central flat portion of the string. 158

7.6 Isothermal nominal stress-stretch relation obtained from 3 term strain energy function with parameters (4.18) compared to experimental values. Young's modulus for infinitesimal deformations was experimentally determined to be equal to 1570 kPa. 160

7.7 Transverse Impact Problem - Example of a photograph taken for a time before the first reflection occurs with impact velocity Q = 85.1 m/s. 163

7.8 Transverse Impact Problem - Example of a photograph taken for a time before the first reflection occurs with impact velocity Q = 48.6 m/s. 163

7.9 Plucked String Problem - A photograph with double exposure showing the initial deformed shape of the string before it is released at time t = 0, and the subsequent deformed shape of the string after it is released. 165

7.10 Plucked String Problem - An example of a photograph taken at a time before the first reflection occurs. The double exposure is used to determine the velocity of the central flat portion of the string. 166

7.11 Plucking String Problem - the final stretch λ_f and λ_1 satisfy condition $V_T(\lambda_f) = V_T(\lambda_1)$ and the discontinuities of λ and θ coincide. This solution is valid for $tV_T(\lambda_1) \leq 1$. 167

7.12 Plucking String Problem - The solution with reflection for $0 \leq t \leq L/c_L(\lambda_o) + L/V_T(\lambda_1)$, when $V_T(\lambda_f) = V_T(\lambda_1)$ and the discontinuities of λ and θ coincide for $tV_T(\lambda_1) \leq 1$. 167

7.13 Plucking String Problem - Deformed configuration of the string when $V_T(\lambda_f) = V_T(\lambda_1)$, shown before and after the first reflection occurs. 168

7.14 Plucking String Problem - experimental results taken for a time after the first reflection occurs, with $\lambda_o = 2$ and $\theta_1 = 45°$. The form after the reflection is similar to that before the reflection. 169

7.15 Plucking String Problem - Experimental results taken for a time after the first reflection occurs, with evidence of a double kink. 171

7.16 Plucking String Problem - Experimental results taken for a time after the first reflection occurs, with evidence if a double kink. 172

7.17 Plucking String Problem - Solution for Mooney-Rivlin string with $\alpha = 0.6$, and $\lambda_1 = \lambda_{c1}$. The solution is valid for $tV_L \leq 1$. 174

7.18 Plucking String Problem - Solution with reflection for Mooney-Rivlin string with $\alpha = 0.6$, and $\lambda_1 \leq \lambda_{c1}$. The solution is valid for $t \leq t^*$. 174

7.19 Plucking String Problem - Experimental results for $\lambda_o = 1$, $\theta = 45°$, at time $t = 3.9$ ms. The longitudinal shock has reflected from the ends resulting in instability since the string cannot sustain compression. 175

Chapter I

Introduction

The purpose of this thesis is to investigate some problems of solid mechanics which involve the propagation of hyperbolic waves. Hyperbolic waves are described mathematically by hyperbolic partial differential equations (Whitham, 1974). Solutions are obtained for problems involving a linear dispersive system, a linear dissipative medium and nonlinear finite deformation of a hyperelastic string.

In Chapter II a method of solution, of problems of linear hyperbolic dispersive equations, by using Fourier transforms is proposed as an alternative to the method of characteristics or Laplace transform techniques. Solutions are obtained for the Klein-Gordon equation which governs the propagation of transverse waves in an elastically supported string. The application of the Fourier transform technique to the Klein-Gordon equation was considered by Havelock (1914) who obtained solutions in terms of Bessel Functions, for a pure initial value problem, by the analytical inversion of the Fourier transform. In Chapter II solutions are obtained for boundary-initial value problems by the numerical inversion of Fourier transforms. Havelock used Fourier transforms with respect to the spatial variable. This procedure is also given in detail by Whitham (1974) for initial value wave propagation problems which are not necessarily hyperbolic. However in Chapter II Fourier transforms with respect to time are used to obtain solutions for initial boundary value problems.

investigated. Solutions are obtained by the application of a modification of MacCormack's scheme (Lorimer, 1986) and also by the method of characteristics. A vast amount of work has been done in this area (Christensen, 1982), however the approach presented in this study to obtain solutions for plane wave propagation in linear viscoelastic materials with more than one relaxation time appears to be new. This investigation is a preliminary for the possible application of MacCormack's scheme to problems of finite amplitude wave propagation in nonlinear viscoelastic materials with suitable constitutive equations. MacCormack's scheme is a shock capturing technique and would be a useful alternative to the method of characteristics since for nonlinear problems the position of the shock front is not known a priori. For many nonlinear problems, the method of characteristics is almost intractable, because, in general, the characteristic curves are not straight lines and a shock front does not coincide with a characteristic.

The remaining chapters investigate finite amplitude wave propagation in a stretched hyperelastic string. The dynamic finite deformation of flexible strings has been studied extensively. Karman and Duwez (1950) and Taylor (1942) considered elastic-plastic longitudinal waves, in Lagrangian and Eulerian forms respectively. Provided no unloading occurs, the elastic-plastic problem is similar to the finite deformation, nonlinear elasticity problem. Cristescu (1964) considered the interaction of longitudinal and transverse waves during both propagation and reflection from the ends of a string fixed at one end while the other end is subjected to a velocity boundary condition,

both propagation and reflection from the ends of a string fixed at one end while the other end is subjected to a velocity boundary condition, however he considered a linear constitutive relation. Nowinski (1965) considered the propagation of finite amplitude longitudinal waves in bars. Recently, Beatty and Haddow (1985) considered the transverse impact problem of a stretched string, and this paper contains numerous references. The work presented in this thesis is an extension of the above paper, however the Lagrangian system of governing equations is obtained in conservation form. Also, the discontinuity relations are treated in greater detail than previously given. In this study, the dynamic simple tension problem is considered as a preliminary to problems of transverse impact and plucking of a stretched string.

In Chapters II and III the solutions are based on purely mechanical theory, however, thermodynamical considerations are introduced in Chapters IV and V. The elastic string is assumed to possess rubberlike elasticity, and some aspects of the thermodynamics associated with the deformation are investigated for the simple tension problem. In formulating the problem, the deformation is assumed to be adiabatic, that is we neglect the heat conduction or assume a nonconducting material. This is intuitively a good approximation since rubberlike materials are relatively poor conductors of heat. Also, it is shown, in Chapter V, that the temperature variations are very small for the deformations considered in the string problem. The validity of the isentropic approximation, which is the neglect of the effect of the jump in entropy across a shock on the constitutive equation, is also

investigated in Chapter V. The adiabatic and isentropic approximations have been discussed in some detail by Bland (1964).

In Chapter IV, adiabatic stress-stretch relations are obtained for strictly entropic and piezotropic materials which are the two limiting cases of modified entropic elasticity proposed by Chadwick and Creasy (1984). In obtaining solutions, isothermal stress-stretch relations are used. There is no difficulty in principle in using an adiabatic constitutive equation rather than an isothermal one, however, it is shown in Chapter V for the simple tension problem, that for the range of deformation considered in this thesis, the errors resulting from using isothermal rather than adiabatic stress-stretch relations are negligible.

The form of the system of Lagrangian governing equations for simple tension is similar to the system of equations which governs finite amplitude plane wave propagation in gases. Riemann (1860) considered this problem in Eulerian coordinates and although he did not succeed in integrating the general nonlinear wave equation in closed form, his methods of solution have since been used by other researchers. Earnshaw (1858) worked with the Lagrangian form of the equations and obtained complete solutions for progressive waves travelling in one direction. Rayleigh (1910) also considered finite amplitude wave propagation in a gas in Eulerian coordinates.

Since then, finite amplitude wave propagation in gas dynamics has been considered by many others including (Courant, Friedrichs, 1948) and (Whitham, 1974). The methods developed to obtain solutions for the problem of finite amplitude wave propagation in a gas can be adapted to

the problem of finite amplitude wave propagation in isotropic hyperelastic solids.

In Chapter VI, similarity solutions are obtained for the wave propagation resulting when a prestretched string fixed at both ends is suddenly subjected to a transverse impact, and when a symmetrically plucked string fixed at both ends is suddenly released. The similarity solutions obtained are valid for times before reflections occur at the fixed ends of the strings.

Experimental results are presented in Chapter VII for the transverse impact and plucking problems, and compared to results obtained from similarity solutions outlined in Chapter VI.

Chapter II

Linear Hyperbolic Dispersive Systems

2.1 Introduction

According to Whitham (1974), a one spatial dimension linear dispersive system admits solutions of the form

$$\phi(x,t) = Ae^{i(\omega t - kx)} \tag{2.1}$$

where A is the amplitude, k is the wave number, ω is the circular frequency, and the quantity $\theta = kx - \omega t$ is the phase. To satisfy the governing partial differential equation or equations, the frequency ω is a function of the wave number k and is given by dispersion relations of the form $\omega = W(k)$, which are determined by substitution of equation (2.1) into the governing partial differential equation or equations. A one dimensional system is dispersive if W(k) is not a linear function of k, that is if $W''(k) \neq 0$.

The phase speed,

$$c_p = \frac{W(k)}{k} \tag{2.2}$$

is the speed of propagation of a constant value of θ and for a dispersive system is not constant but is a function of the wave number k, consequently harmonic waves with different wave numbers propagate at different speeds, resulting in dispersion since the various Fourier components of an initial disturbance propagate at different speeds.

The group velocity is given by,

$$c_g(k) = \frac{dW}{dk} \tag{2.3}$$

and $c_g(k_o)$ is the speed at which the wave number k_o propagates. It can also be shown that the total energy between points $x_1(t)$ and $x_2(t)$, moving with group velocities $c_g(k_1)$ and $c_g(k_2)$, remains constant (Whitham, 1974).

It is possible for a hyperbolic system also to be dispersive, and an example is the Klein-Gordon equation which governs the propagation of transverse waves in an elastically supported string. The Klein-Gordon equation, suitably normalized, is

$$\frac{\partial^2 \phi}{\partial t^2} - \frac{\partial^2 \phi}{\partial x^2} + \phi = 0 \ , \tag{2.4}$$

and the dispersion relation W(k) is,

$$\omega = \pm (k^2 + 1)^{1/2} \ . \tag{2.5}$$

Since we consider only waves travelling in the positive x direction, we take the positive root.

The purpose of this chapter is to investigate solutions of initial-boundary value problems of linear hyperbolic dispersive equations by numerical inversions of Fourier transforms, with respect to time, as an alternative to the method of characteristics, finite difference techniques and Laplace transform techniques. The solution of pure initial value problems using Fourier transform techniques is given in detail (Whitham, 1974), however in this study solutions of the Klein-Gordon equation are obtained for initial-boundary value problems.

The method of solution of the Klein-Gordon equation is outlined for initial-boundary value problems, for the intervals $x\epsilon[0,\infty)$, and $x\epsilon[0,\ell]$, where the latter includes the effects of reflections. Numerical solutions are obtained for the interval $x\epsilon[0,\infty)$ with quiescent initial conditions and three different boundary conditions.

2.2 Method of Solution for Semi-Infinite Interval

Solutions of the Klein-Gordon equation are obtained for the interval $x\epsilon[0,\infty)$ and initial conditions,

$$\phi(x,0) = 0, \quad \frac{\partial\phi}{\partial t}(x,0) = 0 , \tag{2.6}$$

and three different boundary conditions,[1]

$$\begin{aligned} &\phi(0,t) = g(t) = \sin \pi t\, H(t)\, H(1-t), \\ &\phi(0,t) = g(t) = H(t)\, H(1-t), \\ &\phi(0,t) = g(t) = H(t), \end{aligned} \tag{2.7}$$

where $H(t)$ is the unit step function.

A formal solution for the initial-boundary value problem is,

$$\phi(x,t) = \frac{1}{2\pi}\int_{-\infty}^{\infty} \bar{G}(\omega) e^{i(\omega t - k(\omega)x)} d\omega , \tag{2.8}$$

since waves propagate only in the positive x direction. Herein $\bar{G}(\omega)$ is a certain function to be determined by the boundary conditions. It follows from the dispersion relation (2.5) that,

---

[1] The boundary conditions $(2.7)_{2,3}$ are not physically admissible if ϕ represents the deflection of an elastically supported string, however the Klein-Gordon equation is a model for other physical systems for which $(2.7)_{2,3}$ are physically reasonable boundary conditions.

$$k = \pm(\omega^2-1)^{1/2}, \qquad |\omega| > 1 ,$$

$$k = \pm i(1-\omega^2)^{1/2}, \qquad |\omega| < 1 , \tag{2.9}$$

where only the positive sign in equation $(2.9)_1$ is considered since for this problem waves can propagate only in the positive x direction, and the negative sign in equation $(2.9)_2$ is taken for the solution to be bounded. For $|\omega| < 1$, k is imaginary and the harmonic waves cannot propagate but exist as standing waves.

The boundary condition $\phi(0,t) = g(t)$ may be expressed as a Fourier integral

$$g(t) = \frac{1}{2\pi}\int_{-\infty}^{\infty} \bar{G}(\omega)e^{i\omega t}d\omega , \tag{2.10a}$$

where

$$\bar{G}(\omega) = \int_{-\infty}^{\infty} g(t)e^{-i\omega t}dt , \tag{2.10b}$$

and

$$\bar{G}(\omega) = \left\{ \frac{\sin((\omega-\pi/2)}{\omega - \pi} + \frac{\sin((\omega+\pi)/2)}{\omega + \pi} \right\} e^{-i\omega/2} , \tag{2.11}$$

for boundary condition $(2.7)_1$, and

$$\bar{G}(\omega) = \frac{i}{\omega}\left\{ e^{-i\omega}-1 \right\} , \tag{2.12}$$

for boundary condition $(2.7)_2$.

A sufficient, but not necessary, condition for existence of a Fourier transform of the function g(t) is,

$$\int_{-\infty}^{\infty} |g(t)|\, dt < \infty \ .$$

Boundary condition equation $(2.7)_3$ does not satisfy the above condition and determination of its Fourier transform involves theory of distributions. Therefore, for the purpose of the numerical computation, boundary condition $(2.7)_3$ is written as

$$\phi(0,t) = H(t)\ H(t^* - t),$$

and the corresponding Fourier integral is,

$$\bar{G}(\omega) = \frac{i}{\omega}\left[e^{-i\omega t^*} - 1\right] \ . \qquad (2.13)$$

Equation (2.13) reduces to eqn. (2.12) when $t^* = 1$. The solution for the boundary condition $(2.7)_3$ is then obtained for $t < t^*$.

A formal solution is,

$$\phi(x,t) = \frac{1}{2\pi}\int_{-\infty}^{\infty} \bar{G}(\omega) e^{i(\omega^2-1)^{1/2}x}\ e^{i\omega t}\ d\omega \ , \qquad (2.14)$$

where $\bar{G}(\omega)$ is given by equations (2.11), (2.12), (2.13) for boundary conditions $(2.7)_{1,2,3}$ respectively.

In order to evaluate equation (2.14) numerically using a discrete Fourier transform, equation (2.14) is expressed as

$$\phi(x,t) = \frac{1}{2\pi}\left\{\int_{-\infty}^{-1}\bar{G}(\omega)e^{-i(\omega^2-1)^{1/2}x}e^{i\omega t}d\omega + \int_{-1}^{1}\bar{G}(\omega)e^{-(1-\omega^2)^{1/2}x}e^{i\omega t}d\omega\right.$$

$$\left. + \int_{1}^{\infty}\bar{G}(\omega)e^{-i(\omega^2-1)^{1/2}x}e^{i\omega t}d\omega\right\}. \qquad (2.15)$$

Consider equation (2.8) in the form

$$\phi(x,t) = \frac{1}{2\pi}\int_{-\infty}^{\infty}\bar{G}(\omega)\exp\left[i\omega\left(t - \frac{x}{c_p(\omega)}\right)\right]d\omega. \qquad (2.16)$$

Boundary conditions g(t) are causal functions, that is g(t) is zero for $t < 0$, consequently it follows from (2.10a) and Jordan's Lemma that singularities of $\bar{G}(\omega)$ are located on or above the real axis in the complex ω plane (Morse, 1968)[2]. Also,

$$c_p(\omega) = \frac{\omega}{(\omega^2-1)^{1/2}},$$

and the singularities of $c_p(\omega)$ are ± 1 and are located on the real axis in the complex ω plane. Therefore, if the contour of integration in the complex ω plane for (2.16) is taken with the line integral just below the real axis and closed by a semi-circular arc of radius $R \to \infty$ in the lower half of the plane it follows that $\phi(x,t)$ is zero if $tc_p(\infty)$

[2]Morse defines the Fourier transform as $\int_{-\infty}^{\infty}g(t)e^{i\omega t}dt$ so that the singularities of $G(\omega)$ are then on or below the real axis.

$x < 0$ or $x > t\, c_p(\infty)$. This means that the wave front propagates with speed

$$c_p(\infty) = \lim_{\omega \to \infty} c_p(\omega) = 1 \tag{2.17}$$

2.3 Method of Solution for Finite Interval

Consider the initial-boundary value problem shown in Figure 2.1, with quiescent conditions,

$$\phi(x,0) = 0, \quad \phi_t(x,0) = 0 , \tag{2.18}$$

and boundary conditions,

$$\phi(0,t) = g(t), \quad \phi(\ell,t) = 0 . \tag{2.19}$$

To avoid considering reflected waves at $x = \ell$ we propose the following procedure.

First, consider steady state solution for boundary condition $g(t) = \Phi_o e^{i\omega t}$, where Φ_o is a constant and we seek a solution of the form

$$\phi(x,t) = \Phi(x) e^{i\omega t} . \tag{2.20}$$

Substituting (2.20) into the governing partial differential equation (2.4) gives,

$$\Phi'' + (\omega^2 - 1)\Phi = 0 . \tag{2.21}$$

Equation (2.21) is an ordinary differential equation which has solutions,

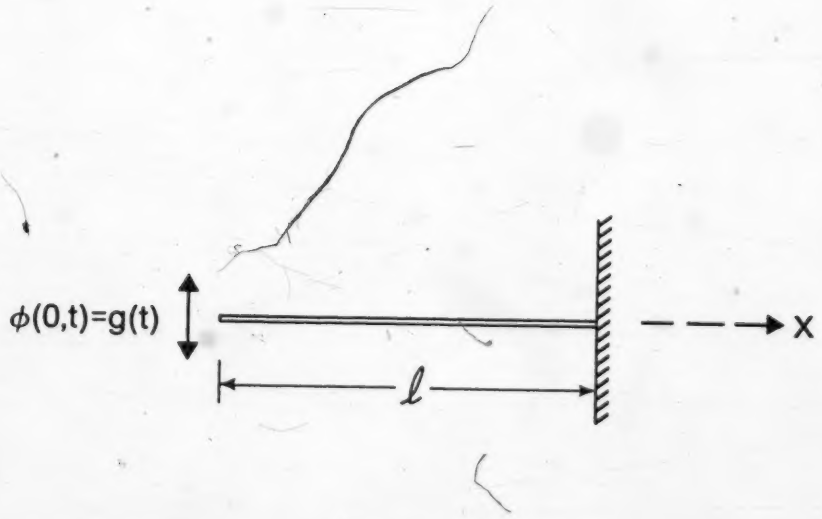

Figure 2.1 Problem geometry of finite interval initial-boundary value problem.

$$\Phi(x) = A \cos (\omega^2-1)^{1/2} x + B \sin (\omega^2-1)^{1/2} x, \quad |\omega| > 1 ,$$
$$\Phi(x) = A \cosh (1-\omega^2)^{1/2} x + B \sinh (1-\omega^2)^{1/2} x, \quad |\omega| < 1 ,$$
$$\Phi(x) = Ax + B , \quad |\omega| = 1 . \qquad (2.22)$$

The constants A,B are determined from the boundary conditions $\Phi(0) = \Phi_o$ and $\Phi(\ell) = 0$, so that the solutions (2.22) are,

$$\Phi(x) = \Phi_o \{\cos(\omega^2-1)^{1/2}x - \cot(\omega^2-1)^{1/2}\ell \sin(\omega^2-1)^{1/2}x\}, \quad |\omega| > 1,$$
$$\Phi(x) = \Phi_o\{\cosh(1-\omega^2)^{1/2}x - \coth(1-\omega^2)^{1/2}\ell \sinh(1-\omega^2)^{1/2}x\}, \quad |\omega| < 1,$$
$$\Phi(x) = \Phi_o \left\{ 1 - \frac{x}{\ell} \right\}, \quad |\omega| = 1 . \qquad (2.23)$$

Then the solution for the interval $x \in [0,\ell]$ is,

$$\phi(x,t) = \frac{1}{2\pi} \int_{-\infty}^{\infty} \bar{G}(\omega)\, f(\omega,x) e^{i\omega t} d\omega \qquad (2.24)$$

where $\bar{G}(\omega)$ is given by equation (2.10b) and,

$$f(\omega,x) = \cos(\omega^2-1)^{1/2}x - \cot(\omega^2-1)^{1/2}\ell \sin(\omega^2-1)^{1/2}x, \quad |\omega| > 1,$$
$$f(\omega,x) = \cosh(1-\omega^2)^{1/2}x - \coth(1-\omega^2)^{1/2}\ell \sinh(1-\omega^2)^{1/2}x, \quad |\omega| < 1,$$
$$f(\omega,x) = (1-x/\ell), \quad |\omega| = 1 . \qquad (2.25)$$

2.4 Numerical Results

Equation (2.15) is written as an inverse discrete Fourier transform for a fixed value of x,

$$\phi(x,KT) = \frac{1}{T}\sum_{n=0}^{N-1}[R(x,n\,\Delta\omega + iI(x,n\,\Delta\omega]e^{\frac{inK}{N}}, \quad K = 0,1, \ldots N-1, \tag{2.26}$$

where T is the period, $R(x,n\,\Delta\omega)$ and $I(x,n\,\Delta\omega)$ are the real and imaginary parts respectively of the complex frequency function to be inverted as given by equations (2.15), $\Delta\omega = 2\pi/T$ is the sample interval in the frequency domain and N is the number of sampled intervals. The inverse discrete Fourier transform is computed numerically through the use of a FFT algorithm (Brigham, 1974).

Figures 2.2 to 2.6 show the results obtained with boundary condition $(2.7)_1$. In Figure 2.2, the sine pulse boundary condition is recovered when x = 0 as expected. In Figure 2.5, for x = 15, 25 and T = 100, aliasing is apparent which is eliminated by an increase in the length of the period as shown in Figure 2.6 (T = 600).

In all of these examples, with the exception of Figure 2.5, there is a sharp wavefront that propagates with velocity $c_p(\infty) = 1$ as predicted by equation (2.17).

Figures 2.7 to 2.11 show results obtained with boundary condition $(2.7)_2$, and again the boundary condition is recovered with x = 0 as expected (Figure 2.7). For greater values of x, (x = 15,25) a larger period (T = 600) is required to eliminate aliasing as is demonstrated in Figures 2.10 and 2.11. A sharp wavefront propagating with velocity $c_p(\infty) = 1$ is observed.

The results for boundary condition $(2.7)_3$ are shown in Figures (2.12) to (2.13), and again, a sharp wavefront travelling with velocity $c_p(\infty) = 1$ is observed.

With boundary conditions $(2.7)_{2,3}$, Figures 2.7 to 2.13, Gibbs' phenomenon is observed, and the amount of overshoot is approximately 9% of the discontinuity as predicted by Bracewell (1986).

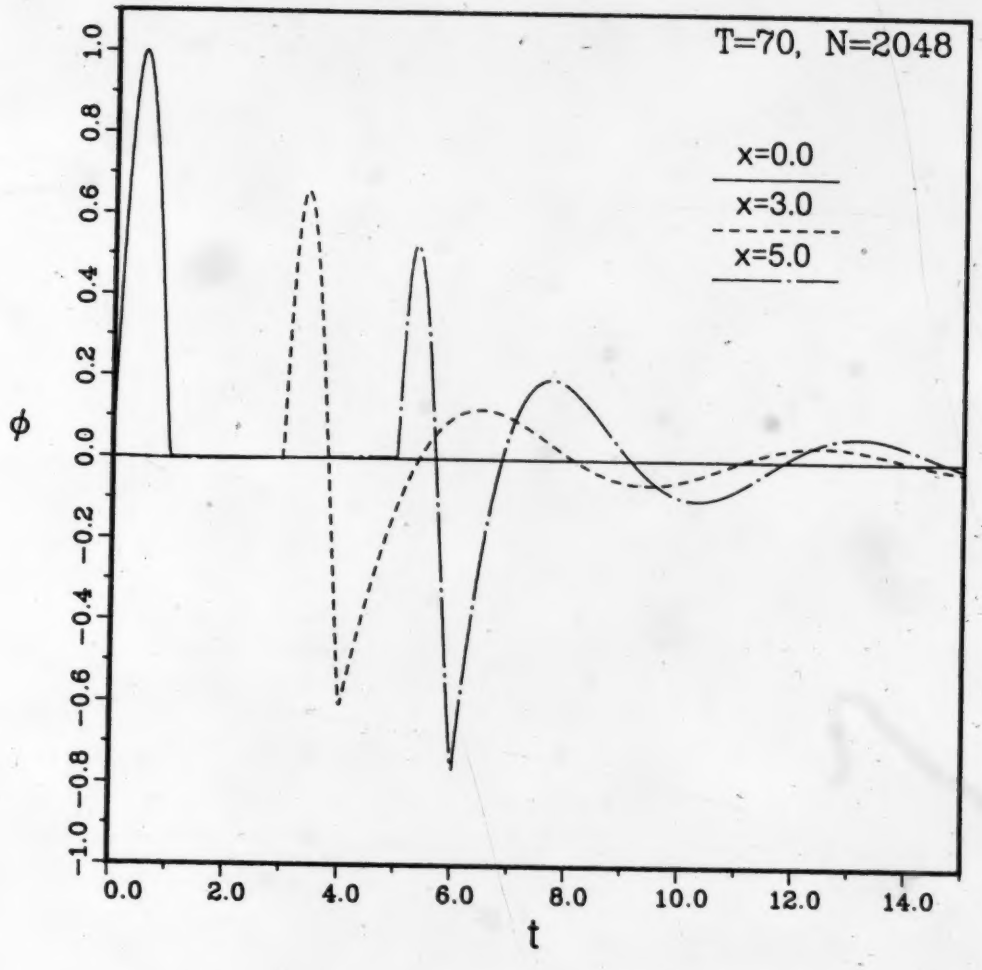

Figure 2.2 Solution of Klein-Gordon equation by FFT algorithm with quiescent initial conditions and boundary condition $\phi(0,t) = \sin \pi t \, H(t) \, H(1-t)$, T = 70, and N = 2048.

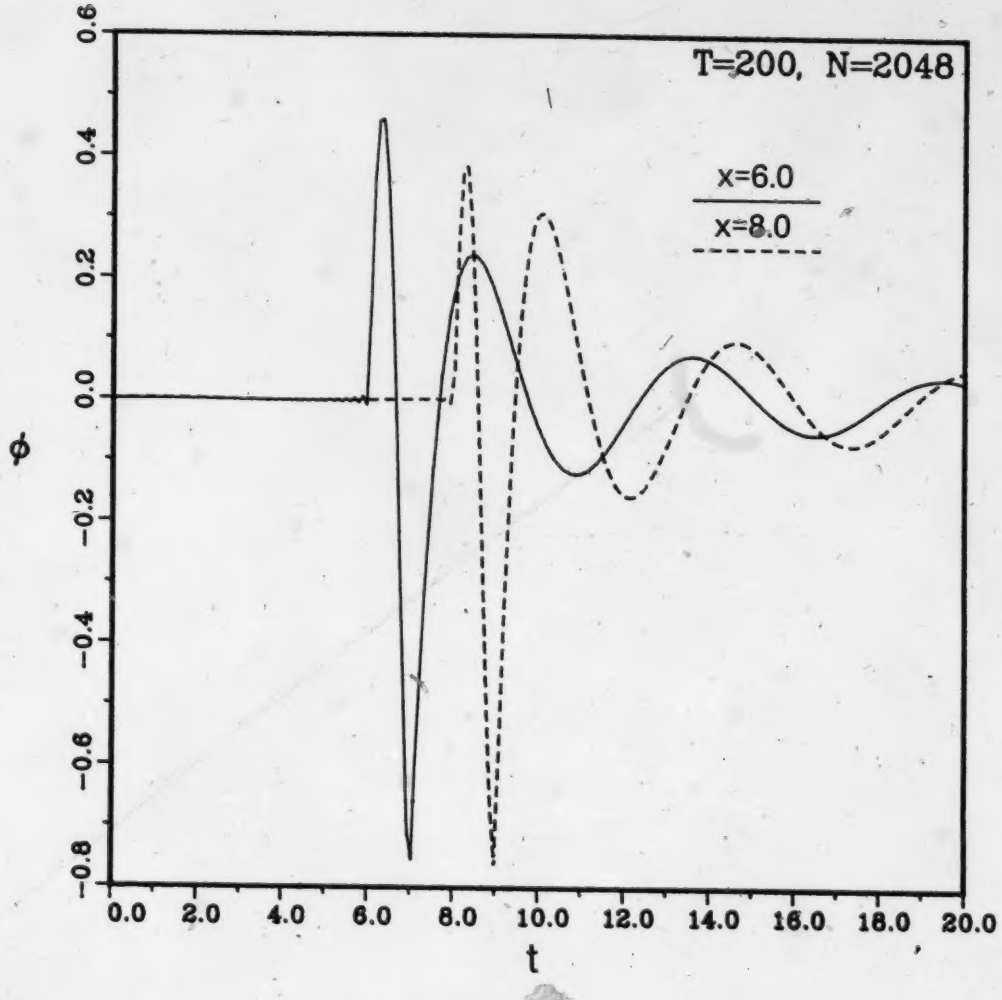

Figure 2.3 Solution of Klein-Gordon equation by FFT algorithm with quiescent initial conditions and boundary condition $\phi(0,t) = \sin \pi t\ H(t)\ H(1-t)$, T = 200, N = 2048.

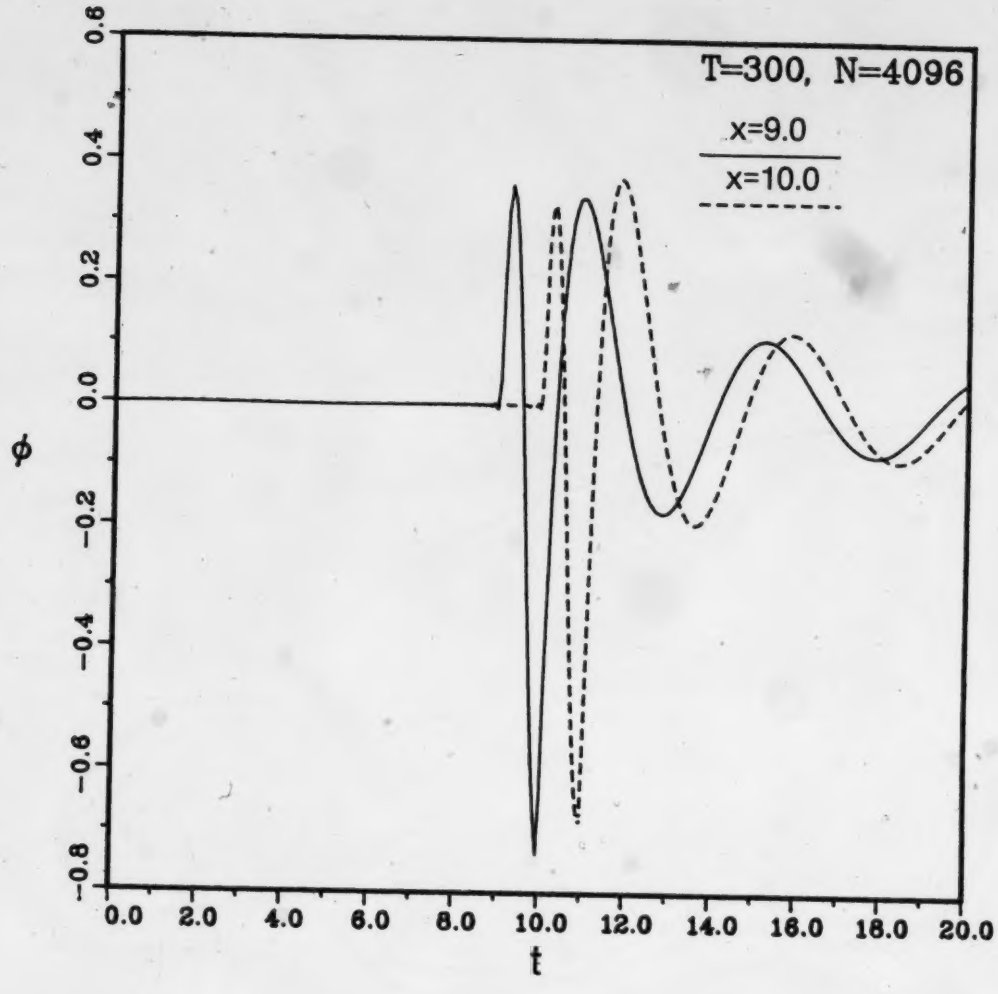

Figure 2.4 Solution of Klein-Gordon equation by FFT algorithm with quiescent initial conditions and boundary condition $\phi(0,t) = \sin \pi t\ H(t)\ H(1-t)$, T = 300, and N = 4096.

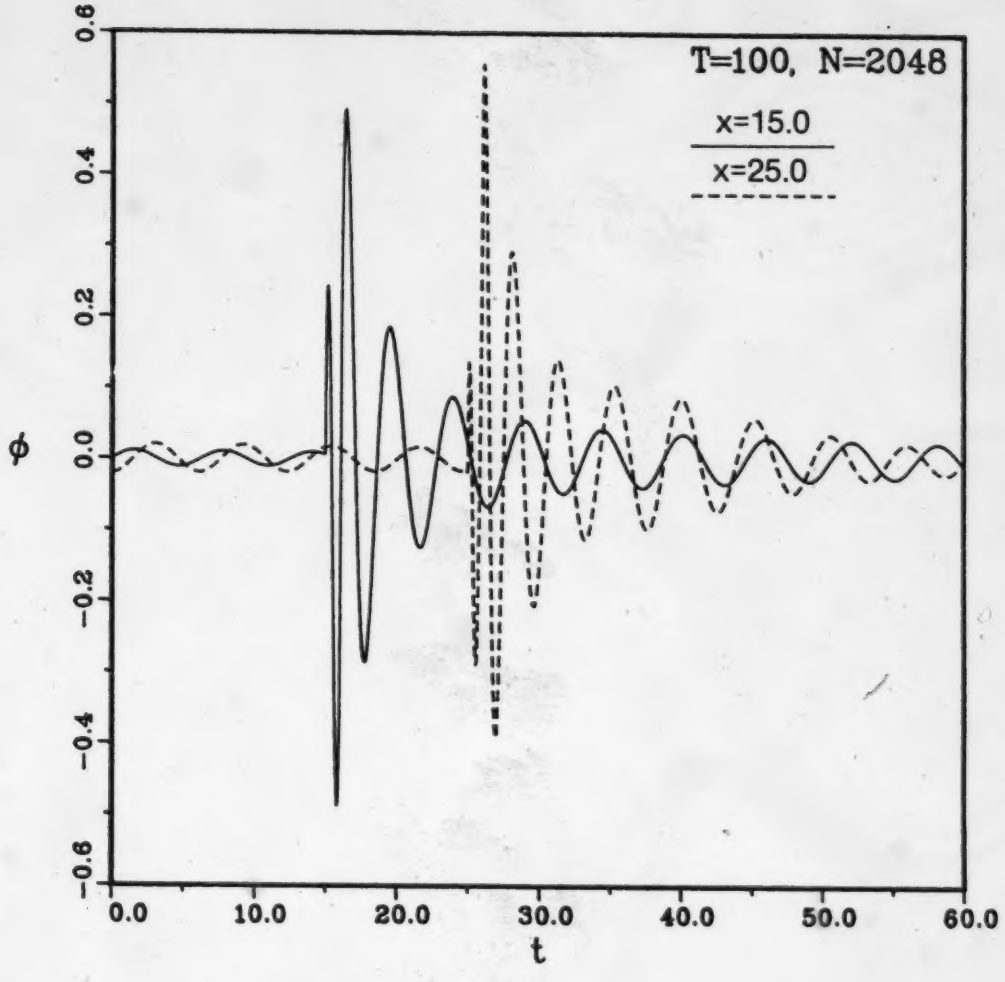

Figure 2.5 Solution of Klein-Gordon equation by FFT algorithm with quiescent initial conditions and boundary condition $\phi(0,t) = \sin \pi t\ H(t)\ H(1-t)$, T = 100, and N = 2048. Aliasing is apparent.

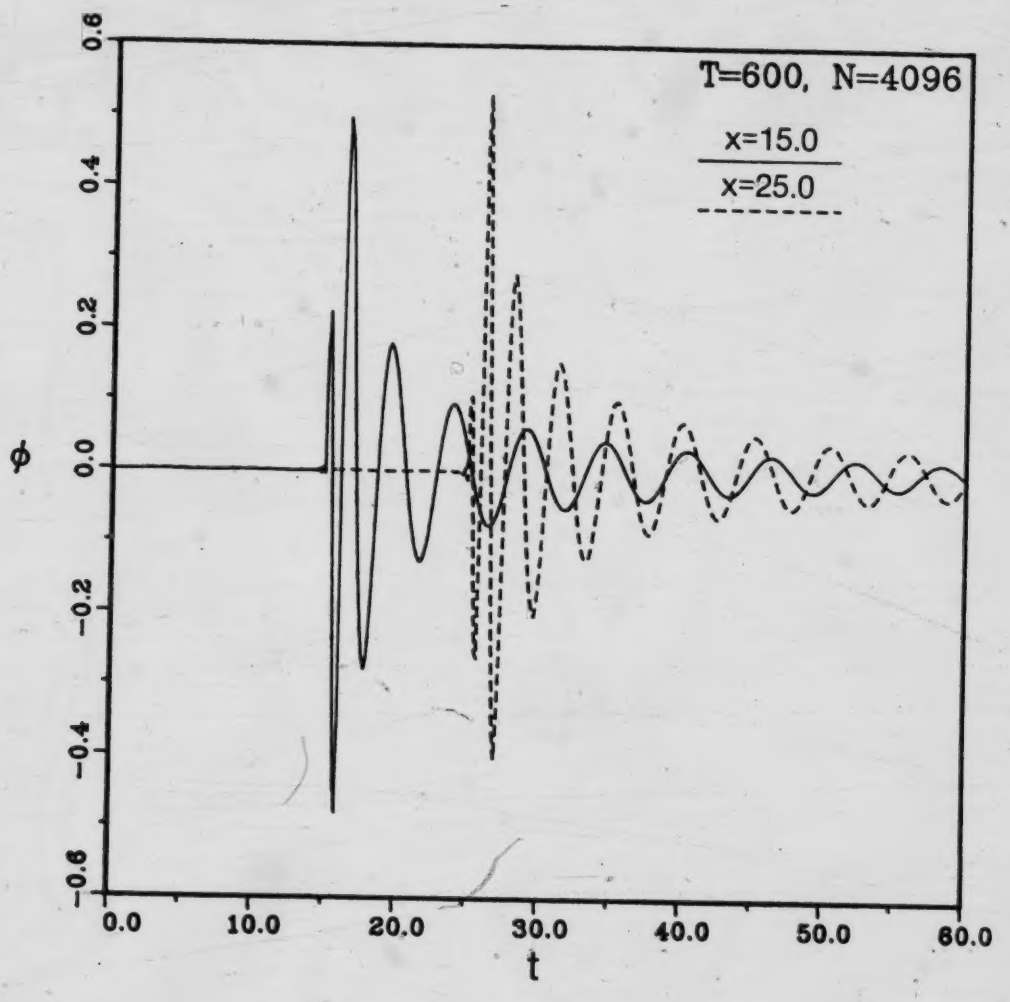

Figure 2.6 Solution of Klein-Gordon equation by FFT algorithm with quiescent initial conditions and boundary condition $\phi(0,t) = \sin \pi t \; H(t) \; H(1-t)$, T = 600, N = 4096.

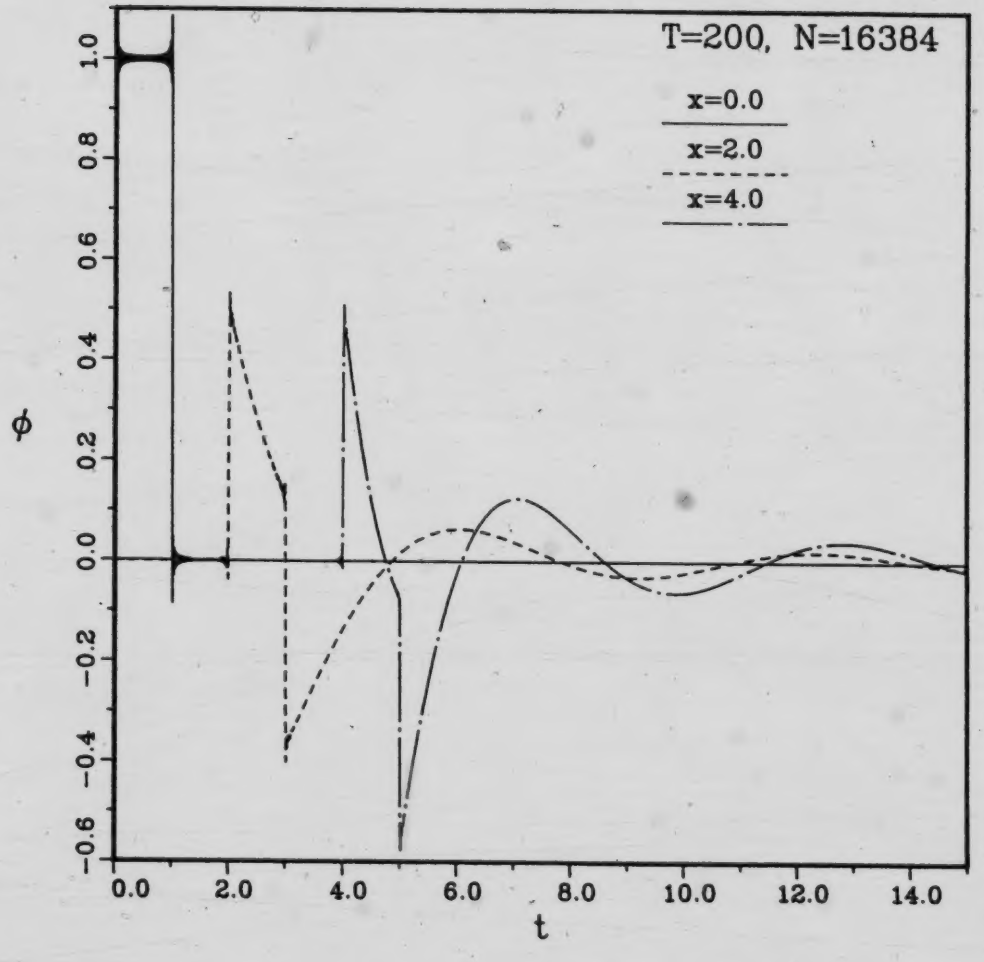

Figure 2.7 Solution of Klein-Gordon equation by FFT algorithm with quiescent initial conditions and boundary condition $\phi(0,t) = H(t)\ H(1-t)$, T = 200, and N = 16384.

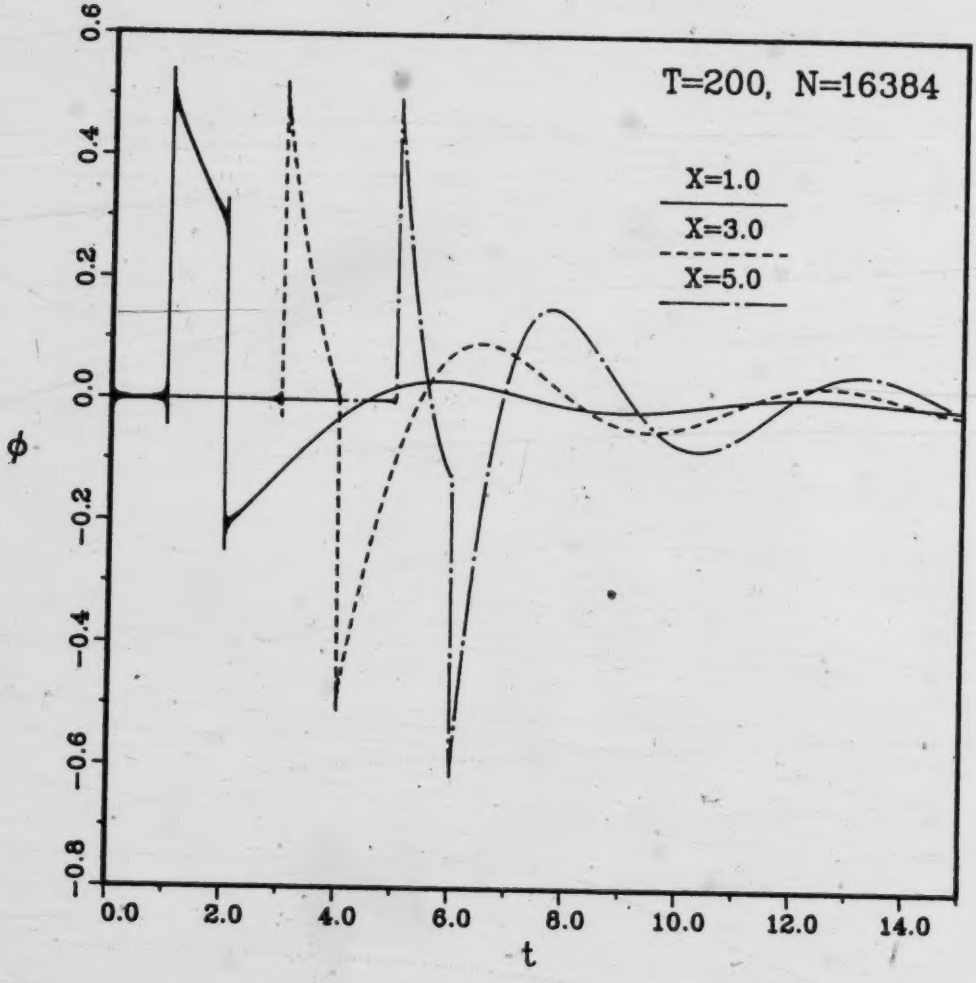

Figure 2.8 Solution of Klein-Gordon equation by FFT algorithm with quiescent initial conditions and boundary condition $\phi(0,t) = H(t)\,H(1-t)$, T = 200, and N = 16384.

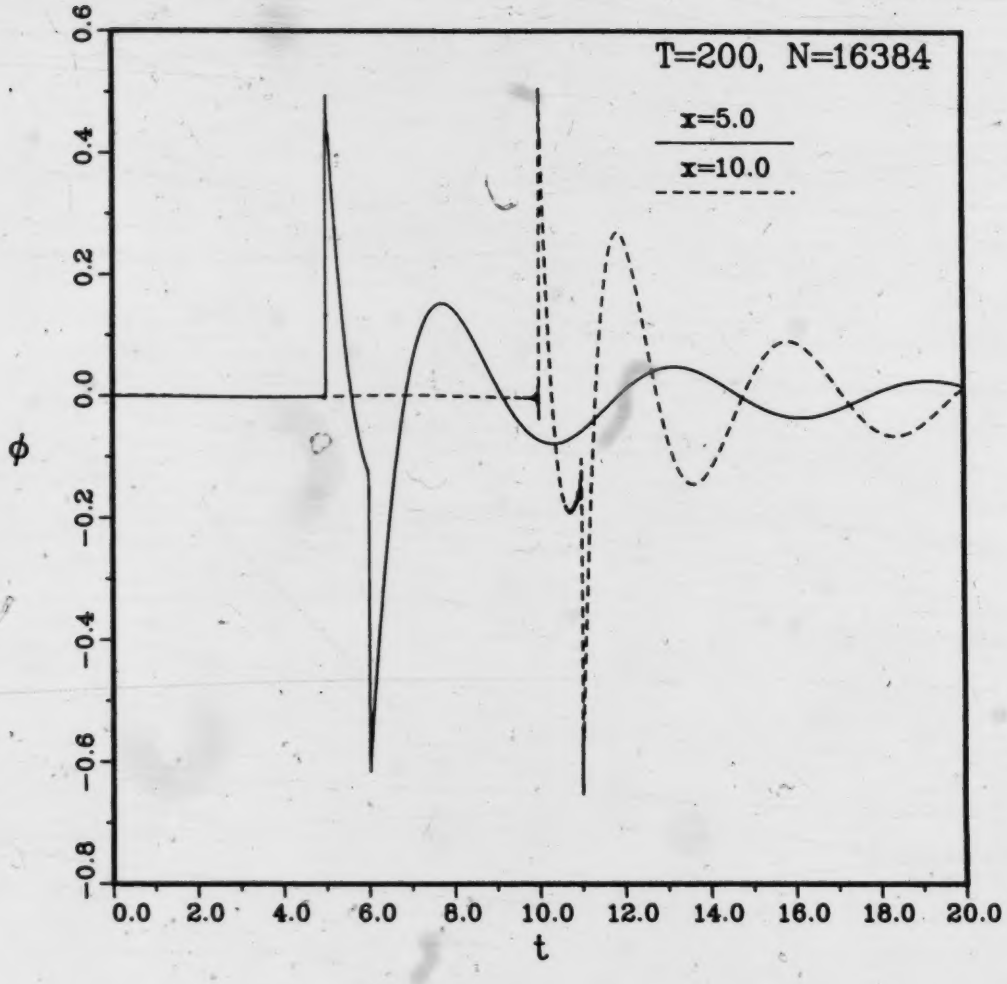

Figure 2.9 Solution of Klein-Gordon equation by FFT algorithm with quiescent initial conditions and boundary condition $\phi(0,t) = H(t)\,H(1-t)$, T = 200 and N = 16384.

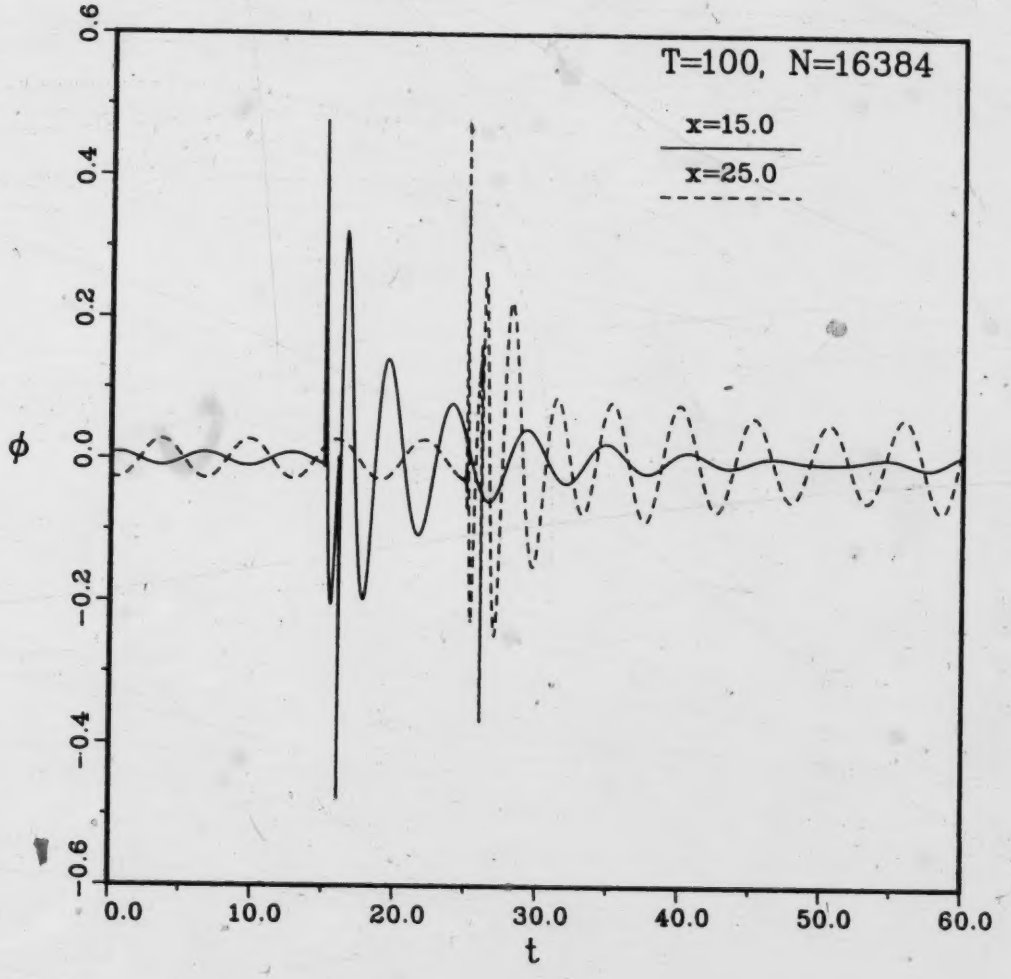

Figure 2.10 Solution of Klein-Gordon equation by FFT algorithm with quiescent initial conditions and boundary condition $\phi(0,t) = H(t)\,H(1-t)$, T = 100, and N = 16384. Aliasing is apparent.

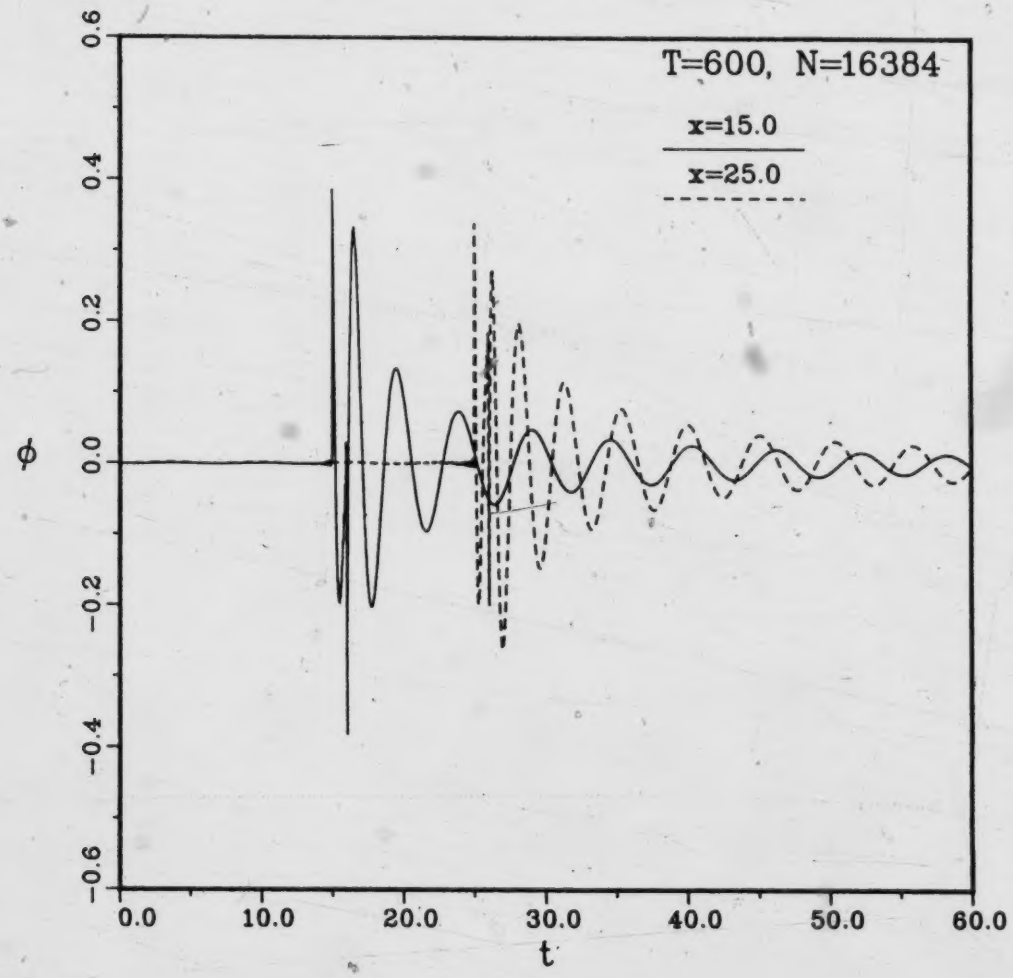

Figure 2.11 Solution of Klein-Gordon equation by FFT algorithm with quiescent initial conditions and boundary condition $\phi(0,t) = H(t)\,H(1-t)$, T = 600 and N = 16384.

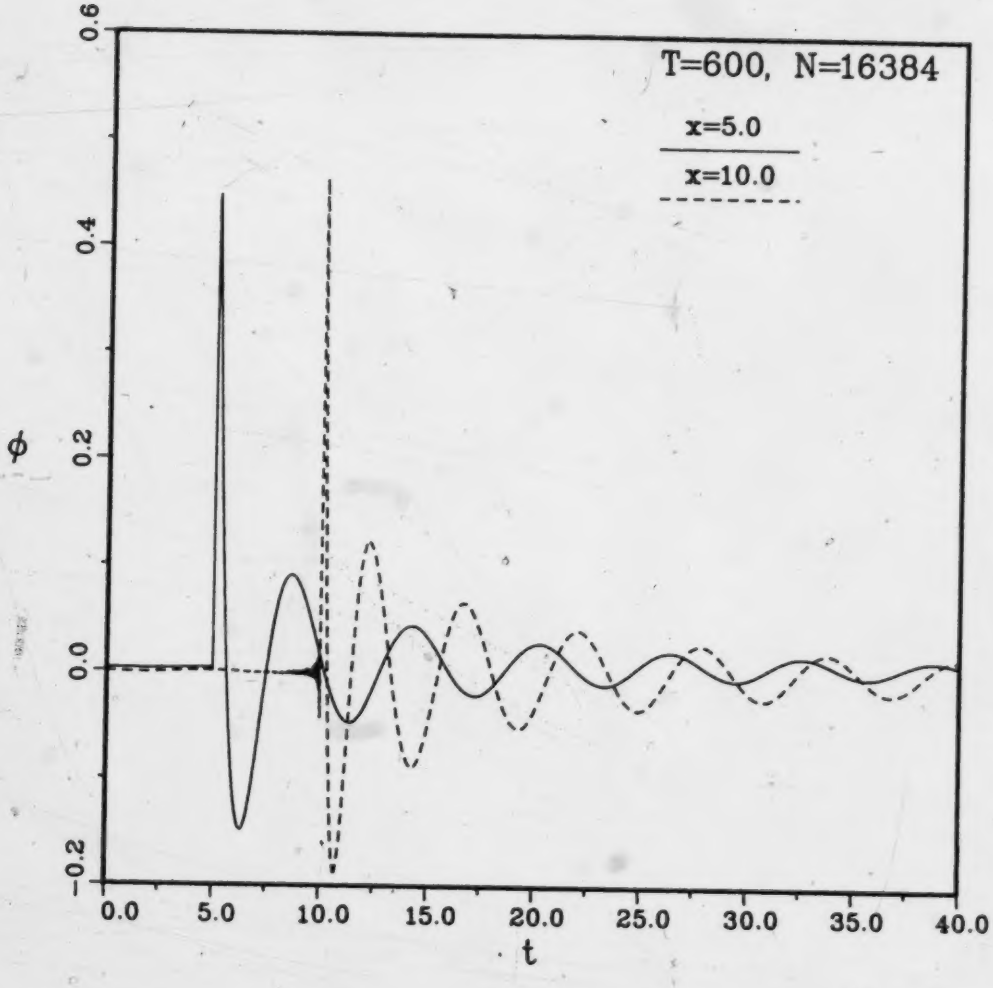

Figure 2.12 Solution of Klein-Gordon equation by FFT algorithm with quiescent initial conditions and boundary condition $\phi(0,t) = H(t)$, T = 600 and N = 16384.

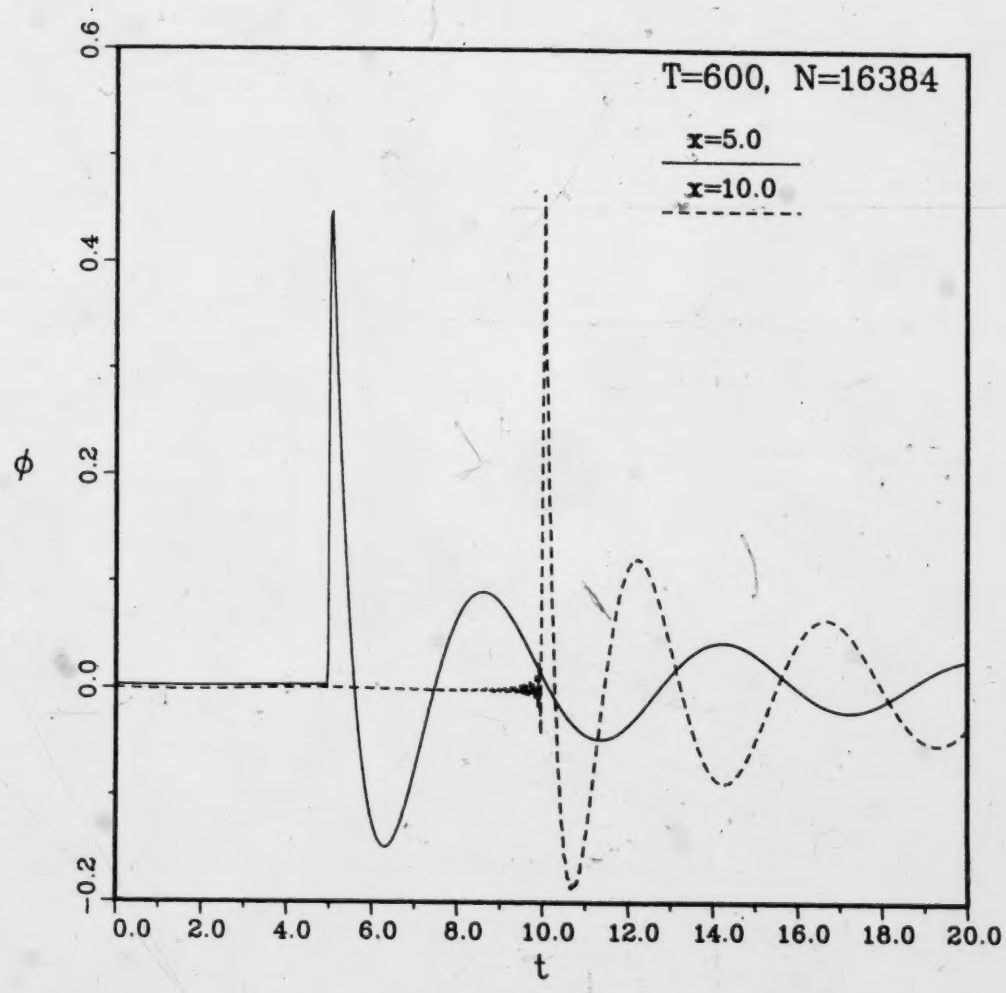

Figure 2.13 Solution of Klein-Gordon equation by FFT algorithm with quiescent initial conditions and boundary condition $\phi(0,t) = H(t)$, T = 600 and N = 16384.

Chapter III

Plane Wave Propagation in a Linear Viscoelastic Solid

3.1 Introduction

In this chapter, a modification of MacCormack's scheme (Lorimer, 1986) is applied to the one spatial dimension problem of plane wave propagation resulting from the sudden application to the surface of a linear viscoelastic solid half-space, of a spatially uniform stress, which may be a constant direction shearing stress or a normal stress. This problem has previously been considered in detail (Lorimer, 1986) but in this present study, the governing system of equations of the problem is reformulated so that solutions can be obtained from a simpler application of MacCormack's scheme than previously given, and the method of characteristics is also facilitated.

Viscoelastic solids with relaxation moduli of the form,

$$G(t) = E\left\{\alpha_o + \sum_{n=1}^{N} \alpha_n e^{-t/\tau_n}\right\} \tag{3.1}$$

are considered, where E is the appropriate impact modulus, τ_n are the relaxation times, and α_n are positive constants such that

$$\sum_{n=0}^{N} \alpha_n = 1 .$$

When N = 1, the standard model is obtained which is the simplest viscoelastic solid which exhibits an impact response.

MacCormack's scheme is applied to the governing equations with initial and boundary conditions specified. The reformulated system of

equations also facilitates the application of the method of characteristics for $N \geq 2$, and the numerical solutions obtained from MacCormack's scheme are compared to solutions obtained from the method of characteristics.

One purpose of this chapter is to demonstrate that the method of characteristics and MacCormack's scheme, suitably modified, are useful methods for obtaining solutions of linear viscoelastic plane wave propagation problems when $N \geq 2$. Most of these problems are almost intractable by transform methods.

This investigation is a preliminary to the application of MacCormack's scheme to problems of finite deformation in viscoelastic solids with suitable constitutive equations. MacCormack's scheme is a shock capturing technique and would be a useful technique for nonlinear problems where the position of the wavefront is not known a priori. The method of characteristics for nonlinear problems is often almost intractable as, in general, the characteristic curves are not straight lines and a shock front does not coincide with a characteristic.

The governing system of equations is derived, and the methods of solution are outlined. Numerical results are presented for $N = 1$ and $N = 2$.

3.2 Governing Equations

The governing system of partial differential equations for one dimensional plane wave propagation in the x direction in a linear viscoelastic material is well known and consists of the equation of motion,

$$\frac{\partial \sigma}{\partial x} - \rho \frac{\partial v}{\partial t} = 0, \tag{3.2}$$

the equation of compatibility,

$$\frac{\partial \epsilon}{\partial t} - \frac{\partial v}{\partial x} = 0, \tag{3.3}$$

and the differential form of the constitutive equation (3.1),

$$\sum_{n=0}^{N} p_n \frac{\partial^n \sigma}{\partial t^n} = \sum_{n=0}^{N} q_n \frac{\partial^n \epsilon}{\partial t^n}, \tag{3.4}$$

where ρ is the density, ϵ is the strain, v is the particle velocity and $p_N = 1$. The equivalence of equations (3.1) and (3.4) is subject to certain initial conditions (Christensen, 1982) which are satisfied in the present problem.

Solutions are obtained for N = 1, 2 and the corresponding differential forms of the constitutive equation are,

$$\frac{\partial \sigma}{\partial t} + \frac{\sigma}{\tau_1} = q_2 \left(\frac{\partial \epsilon}{\partial t} + \frac{\alpha_o \epsilon}{\tau_1} \right), \tag{3.5}$$

and

$$\frac{\partial^2 \sigma}{\partial t^2} + p_1 \frac{\partial \sigma}{\partial t} + p_o \sigma = q_2 \frac{\partial^2 \epsilon}{\partial t^2} + q_1 \frac{\partial \epsilon}{\partial t} + q_o \epsilon, \tag{3.6}$$

respectively, where

$$p_o = (\tau_1\tau_2)^{-1},\ p_1 = (\tau_1 + \tau_2)/\tau_1\tau_2,\ q_o = E\alpha_o/(\tau_1\tau_2),$$

$$q_1 = E\left[(\alpha_o + \alpha_1)\tau_1 + (\alpha_o + \alpha_2)\tau_2\right]/\tau_1\tau_2,\quad q_2 = E\ .$$

We consider N = 1 and N = 2, however extension of the theory to N > 2 is straightforward.

Equations (3.2), (3.3) and

$$\frac{\partial\sigma}{\partial t} + E\frac{\partial v}{\partial x} + \frac{\sigma}{\tau_1} - \frac{E}{\tau_1}\alpha_o\epsilon = 0, \tag{3.7}$$

for N = 1, and

$$\frac{\partial\dot{\sigma}}{\partial t} + q_1\frac{\partial v}{\partial x} + q_2\frac{\partial\dot{v}}{\partial x} + p_1\dot{\sigma} + p_o\sigma - q_o\epsilon = 0, \tag{3.8}$$

where $\dot{\sigma} = \partial\sigma/\partial t$ and $\dot{v} = \partial v/\partial t$, for N = 2, are a system of first order partial differential equations.

The transient response of a viscoelastic fluid with two relaxation times has been previously considered Glauz and Lee (1953) and the constitutive equation for this material can be written in the form of equation (3.6) with $q_o = 0$. However the material is instead represented by a four parameter spring-dashpot model consisting of a Kelvin element in series with a Maxwell element as shown in Figure (3.1). Another four parameter spring-dashpot model, shown in Figure (3.2), is also governed by equation (3.6) with $q_o = 0$. Solutions obtained by Glauz and Lee (1953) by the method of characteristics apply only to the particular model shown in Figure (3.1) and not to the general form for a four parameter fluid as given by equation (3.6) with $q_o = 0$.

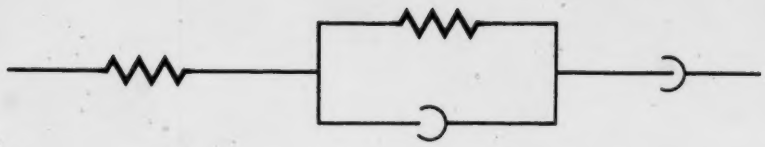

Figure 3.1 A second order viscoelastic fluid represented by a Kelvin element in series with a Maxwell element.

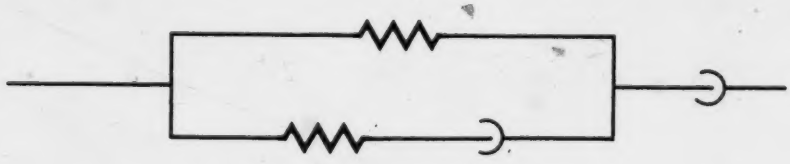

Figure 3.2 A second order viscoelastic fluid represented by a standard model in series with a dashpot.

The following nondimensional quantities are introduced,

$$\bar{x} = \frac{x}{T}\left[\frac{\rho}{E}\right]^{1/2}, \quad \bar{t} = \frac{t}{T}, \quad \bar{\tau}_1 = \frac{\tau_1}{T}, \quad \bar{\tau}_2 = \frac{\tau_2}{T},$$

$$\bar{v} = v\left[\frac{\rho}{E}\right]^{1/2}, \quad \bar{\sigma} = \frac{\sigma}{E}, \quad \dot{\bar{\sigma}} = \frac{\dot{\sigma}T}{E},$$

$$\bar{q}_o = q_o \frac{T^2}{E}, \quad \bar{q}_1 = q_1 \frac{T}{E}, \quad \bar{q}_2 = \frac{q_2}{E} = 1,$$

$$\bar{p}_o = p_o T^2, \quad \bar{p}_1 = p_1 T, \tag{3.9}$$

where

$$T = \frac{\alpha_1 \tau_1^2 + \alpha_2 \tau_2^2}{\alpha_1 \tau_1 + \alpha_2 \tau_2}$$

is the mean relaxation time (Pipkin, 1972). Henceforth, nondimensional quantities are used but the superposed bars are omitted.

The system of nondimensional governing equations can be written in matrix form and is,

$$\frac{\partial \underset{\sim}{u}}{\partial t} + \underset{\sim}{A}\frac{\partial \underset{\sim}{u}}{\partial x} + \underset{\sim}{b}(\underset{\sim}{u}) = \underset{\sim}{0} \tag{3.10a}$$

when N = 1 and

$$\frac{\partial \underset{\sim}{u}}{\partial t} + \underset{\sim}{A}\frac{\partial \underset{\sim}{u}}{\partial x} + \underset{\sim}{b}\left(\underset{\sim}{u}, \int_o^t \underset{\sim}{u}(\eta)\, d\eta\right) \tag{3.10b}$$

when N = 2.

The matrix $\underset{\sim}{A}$ is given by

$$(\underset{\sim}{A}) = \begin{Bmatrix} 0 & -1 & 0 \\ -1 & 0 & 0 \\ 0 & -1 & 0 \end{Bmatrix} \tag{3.11}$$

for all N, and $\underset{\sim}{u}$ and $\underset{\sim}{b}$ are given by

$$\underset{\sim}{u} = \begin{Bmatrix} \sigma \\ v \\ \epsilon \end{Bmatrix}, \quad \underset{\sim}{b} = \begin{Bmatrix} \sigma - a_o \epsilon \\ 0 \\ 0 \end{Bmatrix}, \tag{3.12}$$

when N = 1 and

$$\underset{\sim}{u} = \begin{Bmatrix} \dot{\sigma} \\ \dot{v} \\ \dot{\epsilon} \end{Bmatrix}, \quad \underset{\sim}{b} = \begin{Bmatrix} p_1\dot{\sigma} + p_o\sigma - q_1\dot{\epsilon} - q_o\epsilon \\ 0 \\ 0 \end{Bmatrix}, \tag{3.13}$$

when N = 2, and $(\dot{}) = \partial/\partial t$.

Matrices $\underset{\sim}{u}$ and $\underset{\sim}{b}$ involve partial time derivatives of σ, v, ϵ of order up to (N - 1) for all N. Numerical results are presented for N = 1 and N = 2; however, the methods described can be extended to consider N > 2.

The eigenvalues of $\underset{\sim}{A}$ are $\lambda = 0, \pm 1$ for all N. Nondimensional wave speeds are $\pm$ 1 and the corresponding characteristics in the (x,t) plane with slopes 0, +1, -1 are referred to as the ζ^o, ζ^+, ζ^- characteristics respectively.

Relations along the characteristics are (Whitham, 1973),

$$\underset{\sim}{\ell}_i^T \frac{d\underset{\sim}{u}}{dt} + \underset{\sim}{\ell}_i^T \underset{\sim}{b} = 0 \quad \text{on} \quad \frac{dx}{dt} = \lambda_i, \; i = 1, 2, 3 \tag{3.14}$$

where the superscript T denotes the transpose and $\underset{\sim}{\ell}_i$ are the left eigenvectors associated with λ_i and are defined by

$$\underset{\sim}{\ell}_i^T \underset{\sim}{A} = \lambda_i \underset{\sim}{\ell}_i^T, \quad i = 1, 2, 3 . \tag{3.15}$$

The left eigenvectors of $\underset{\sim}{A}$ are obtained from equation (3.15), so that

$$\begin{aligned}
&(1, 0, -1)\frac{d\underset{\sim}{u}}{dt} + (1, 0, -1)\underset{\sim}{b} = 0 \quad \text{on} \quad \frac{dx}{dt} = 0 , \\
&(1, -1, 0)\frac{d\underset{\sim}{u}}{dt} + (1, -1, 0)\underset{\sim}{b} = 0 \quad \text{on} \quad \frac{dx}{dt} = 1 , \\
&(1, 1, 0)\frac{d\underset{\sim}{u}}{dt} + (1, 1, 0)\underset{\sim}{b} = 0 \quad \text{on} \quad \frac{dx}{dt} = -1 ,
\end{aligned} \tag{3.16}$$

are obtained from equations (3.14) for all N.

Equations (3.16) give

$$\begin{aligned}
&\frac{d\sigma}{dt} - \frac{d\epsilon}{dt} + \sigma - \alpha_o\epsilon = 0 \quad \text{on} \quad \frac{dx}{dt} = 0 , \\
&\frac{d\sigma}{dt} - \frac{dv}{dt} + \sigma - \alpha_o\epsilon = 0 \quad \text{on} \quad \frac{dx}{dt} = 1 , \\
&\frac{d\sigma}{dt} + \frac{dv}{dt} + \sigma - \alpha_o\epsilon = 0 \quad \text{on} \quad \frac{dx}{dt} = -1 ,
\end{aligned} \tag{3.17}$$

when N = 1, and

$$\begin{aligned}
&\frac{d\dot{\sigma}}{dt} - \frac{d\dot{\epsilon}}{dt} + p_1\dot{\sigma} + p_o\sigma - q_1\dot{\epsilon} - q_o\epsilon = 0 \quad \text{on} \quad \frac{dx}{dt} = 0 , \\
&\frac{d\dot{\sigma}}{dt} - \frac{d\dot{v}}{dt} + p_1\dot{\sigma} + p_o\sigma - q_1\dot{\epsilon} - q_o\epsilon = 0 \quad \text{on} \quad \frac{dx}{dt} = 1 , \\
&\frac{d\dot{\sigma}}{dt} + \frac{d\dot{v}}{dt} + p_1\dot{\sigma} + p_o\sigma - q_1\dot{\epsilon} - q_o\epsilon = 0 \quad \text{on} \quad \frac{dx}{dt} = -1 ,
\end{aligned} \tag{3.18}$$

when N = 2.

Relations along the characteristics (ζ°, $\zeta+$, $\zeta-$) can be similarly obtained for $N > 2$.

Boundary-initial value problems for the interval $0 \leq x < \infty$, and quiescent initial conditions are considered. Solutions are obtained for the boundary conditions;

$$\sigma(0,t) = \sigma_o H(t) \tag{3.19}$$

and

$$\sigma(0,t) = \sigma_o \sin \pi t \; H(1-t)H(t) \tag{3.20}$$

where $H(\;)$ denotes the Heaviside unit function, and σ_o is constant.

3.3 Numerical Techniques

3.3.1 Application of MacCormack's Scheme

The predictor and corrector finite difference equations of MacCormack's scheme, modified to incorporate the matrix $\underset{\sim}{b}$ in equations (3.10), are

$$\overline{\underset{\sim}{u}_j^{n+1}} = \underset{\sim}{u}_j^n - \frac{\Delta t}{\Delta x}\left(\underset{\sim\sim}{A}\underset{\sim}{u}_{j+1}^n - \underset{\sim\sim}{A}\underset{\sim}{u}_j^n\right) - \Delta t\, \underset{\sim}{b}_j^n \tag{3.21}$$

$$\underset{\sim}{u}_j^{n+1} = \frac{1}{2}\left\{\underset{\sim}{u}_j^n + \overline{\underset{\sim}{u}_j^{n+1}} - \frac{\Delta t}{\Delta x}\left(\underset{\sim\sim}{A}\overline{\underset{\sim}{u}_j^{n+1}} - \underset{\sim\sim}{A}\overline{\underset{\sim}{u}_{j-1}^{n+1}}\right) - \Delta t\, \overline{\underset{\sim}{b}_j^{n+1}}\right\}$$

where $\underset{\sim}{u}_j^n$ and $\underset{\sim}{b}_j^n$ are the finite difference approximations to $\underset{\sim}{u}$ and $\underset{\sim}{b}$ respectively, at mesh point $j\Delta x$, $n\Delta t$.

When $N > 1$, the matrix $(\underset{\sim}{u}_j^n)$ consists of the $(N-1)^{th}$ partial time derivative of σ_j^n, v_j^n, ϵ_j^n, consequently additional relationships are

required to determine σ_j^n, v_j^n, and ϵ_j^n at each time step.

Along the ζ° characteristics,

$$\dot{\sigma} - \frac{d\sigma}{dt} = 0, \quad \dot{v} - \frac{dv}{dt} = 0, \quad \dot{\epsilon} - \frac{d\epsilon}{dt} = 0. \tag{3.22}$$

A first order finite difference scheme of equations (3.22) is,

$$\sigma_j^{n+1} = \Delta t\, \dot{\sigma}_j^n + \sigma_j^n, \; v_j^{n+1} = \Delta t\, \dot{v}_j^n + v_j^n, \; \epsilon_j^{n+1} = \Delta t\, \dot{\epsilon}_j^n + \epsilon_j^n. \tag{3.23}$$

When N = 2, equations (3.23) are used in addition to equations (3.21) to determine $\sigma_j{}^n$, $v_j{}^n$, $\epsilon_j{}^n$ at each time step. When N > 2, equations (3.21) are used along with (N - 1) successive numerical integrations and it may be necessary to implement a more elaborate numerical integration scheme than (3.23) to improve the accuracy.

In order to apply equations (3.21), $\sigma(0,t)$, $v(0,t)$, $\epsilon(0,t)$ are required for N = 1, and $\dot{\sigma}(0,t)$, $\dot{v}(0,t)$, $\dot{\epsilon}(0,t)$ are required for N = 2. Boundary conditions, equations (3.19) or (3.20), give $\sigma(0,t)$ and $\dot{\sigma}(0,t)$. The remaining dependent variables at x = 0 are obtained from a forward difference predictor and corrector finite difference scheme (Gottleib, 1978),

$$\overline{v_o^{n+1}} = v_o^n - \frac{\Delta t}{\Delta x}\left(-\sigma_1^n + \sigma_o^n\right),$$

$$v_o^{n+1} = \frac{1}{2}\left\{ v_o^n + \overline{v_o^{n+1}} - \frac{\Delta t}{\Delta x}\left[-\overline{\sigma_1^{n+1}} + \overline{\sigma_o^{n+1}}\right]\right\},$$

$$\overline{\epsilon_o^{n+1}} = \epsilon_o^n - \frac{\Delta t}{\Delta x}\left(-v_1^n + v_0^n\right),$$

$$\epsilon_o^{n+1} = \frac{1}{2}\left\{ \epsilon_o^n + \overline{\epsilon_o^{n+1}} - \frac{\Delta t}{\Delta x}\left[-v_1^{\overline{n+1}} + v_o^{\overline{n+1}}\right]\right\}, \qquad (3.24)$$

when N = 1, and,

$$\dot{v}_o^{\overline{n+1}} = \dot{v}_o^n - \frac{\Delta t}{\Delta x}\left(-\dot{\sigma}_1^n + \dot{\sigma}_0^n\right),$$

$$\dot{v}_o^{n+1} = \frac{1}{2}\left\{\dot{v}_o^n + \dot{v}_o^{\overline{n+1}} - \frac{\Delta t}{\Delta x}\left[-\dot{\sigma}_1^{\overline{n+1}} + \dot{\sigma}_o^{\overline{n+1}}\right]\right\},$$

$$\dot{\epsilon}_o^{\overline{n+1}} = \dot{\epsilon}_o^n - \frac{\Delta t}{\Delta x}\left(-\dot{v}_1^n + \dot{v}_o^n\right),$$

$$\dot{\epsilon}_o^{n+1} = \frac{1}{2}\left\{\dot{\epsilon}_o^n + \dot{\epsilon}_o^{\overline{n+1}} - \frac{\Delta t}{\Delta x}\left[-\dot{v}_1^{\overline{n+1}} + \dot{v}_o^{\overline{n+1}}\right]\right\}, \qquad (3.25)$$

when N = 2.

A stability analysis (Anderson, 1984) indicates $\nu \leq 1$ is a necessary condition for numerical stability of the finite difference scheme when $\underline{b} = 0$, where $\nu = \mu\Delta t/\Delta x$ is the Courant number and μ is the numerically greatest eigenvalue of $\underline{A}$. So far there is no stability analysis for the finite difference scheme when $\underline{b} \neq 0$, however as it was found previously (Lorimer, 1986) the scheme is unstable when $\nu = 1$, although with the system of equations considered, the instability is much weaker than that observed by Lorimer (1986). Satisfactory results were obtained with $\alpha_o = 0.9$, $\nu = 1.0$ and $\alpha_o = 0.1$, $\nu = 0.99$.

3.3.2. Method of Characteristics

The method of characteristics for linear problems where the position of the wavefront is known a priori and the shock front coincides with a characteristic is well known and can be found in any standard text on applied numerical analysis (Burden, 1978, Gerald, 1984).

The equations along the characteristics, equations (3.17) and (3.18), can be written in finite difference terms to a first order approximation as;

$$\sigma_j^{n+1} - \sigma_j^n - \left(\epsilon_j^{n+1} - \epsilon_j^n \right) + \Delta t \, (b_1)_j^n = 0 ,$$

$$\sigma_j^{n+1} - \sigma_{j-1}^n - \left(v_j^{n+1} - v_{j-1}^n \right) + \Delta t \, (b_1)_{j-1}^n = 0 ,$$

$$\sigma_j^{n+1} - \sigma_{j+1}^n + \left(v_j^{n+1} - v_{j+1}^n \right) + \Delta t \, (b_1)_{j+1}^n = 0 , \qquad (3.26)$$

where $(b_1)_j^n = \sigma_j^n - \alpha_o \epsilon_j^n$, when N = 1, and

$$\dot{\sigma}_j^{n+1} - \dot{\sigma}_j^n - \left(\dot{\epsilon}_j^{n+1} - \dot{\epsilon}_j^n \right) + \Delta t \, (b_1)_j^n = 0,$$

$$\dot{\sigma}_j^{n+1} - \dot{\sigma}_{j-1}^n - \left(\dot{v}_j^{n+1} - \dot{v}_{j-1}^n \right) + \Delta t \, (b_1)_{j-1}^n = 0,$$

$$\dot{\sigma}_j^{n+1} - \dot{\sigma}_{j+1}^n + \left(\dot{v}_j^{n+1} - \dot{v}_{j+1}^n \right) + \Delta t (b_1)_{j+1}^n = 0, \qquad (3.27)$$

where $(b_1)_j^n = p_1\dot{\sigma}_j^n + p_o\sigma_j^n - q_1\dot{\epsilon}_j^n - q_o\epsilon_j^n$, when N = 2.

An expression for the decay of a discontinuity at the wavefront can be obtained (Christensen, 1982). For boundary condition (3.19), the nondimensional form of the stress at the wavefront is,

$$\sigma(x,t)\Big|_{x = t^+} = \sigma_o \exp\,[(G'(0))/G(0))x] \tag{3.28}$$

where t^+ indicates the value behind the wavefront and G(0), G'(0) are obtained from equation (3.1). This gives the magnitude of a propagating discontinuity for any mechanical model. Also, from the discontinuity relations at the wavefront,

$$\sigma = -v, \quad \sigma = \epsilon, \quad \text{at} \quad x = t^+ . \tag{3.29}$$

Equations (3.28) and (3.29) can be incorporated into method of characteristics giving σ, v, ϵ at the wavefront and $\dot{\sigma}$, $\dot{v}$, $\dot{\epsilon}$ can also be obtained at the wavefront from a wavefront expansion. This would require a minor modification of the mesh used which is shown in Figure 3.3. When N = 1,2 it was found that it was not necessary to implement this technique, however, when N > 2, the wavefront expansion technique may be required to improve the accuracy at the wavefront.

Equations (3.23) are used in addition to equations (3.27) when N = 2. This procedure for N ≥ 2 seems to be new and is superior to that proposed by Glauz and Lee (1953) which involves a system of six equations for the four parameter fluid. The system of equations, given in matrix form by (3.10b) is treated as a system of first order linear

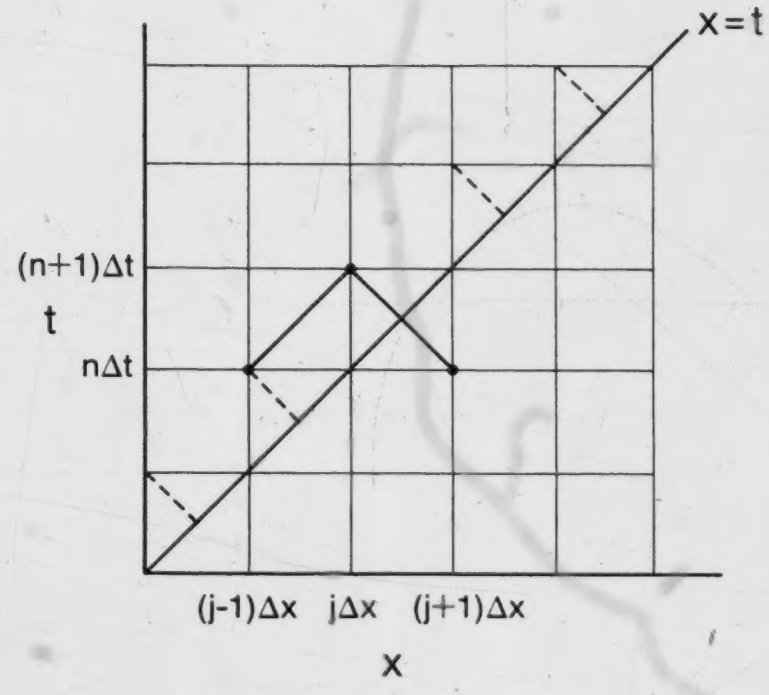

Figure 3.3 The solid lines represent the mesh used for the method of characteristics. If a wavefront expansion technique is incorporated at the wavefront x = t, the mesh would be modified at x = t as indicated by the dashed lines.

hyperbolic partial differential equations with dependent variables $\dot{\sigma}$, $\dot{v}$, $\dot{\epsilon}$ although the vector $\underline{b}$ is a function of σ and ϵ as well as $\dot{\sigma}$ and $\dot{\epsilon}$.

3.4 Numerical Results

Numerical results are presented graphically in Figures 3.4 to 3.18, for $\alpha_o = 0.1, 0.9, 1.0$, $\Delta x = 0.01$ and $\nu = 0.99, 1.0$.

Figures 3.4 to 3.11 are results obtained for boundary condition given by equation (3.19) for $N = 1$ and $N = 2$. When $N = 1$ and $\alpha_o = 1$, the material is perfectly elastic and the wave propagates without change in shape. The results shown in Figure 3.4 and 3.5 indicate no numerical dispersion when $\nu = 1.0$ and numerical dispersion when $\nu < 1$. This is similar to the results for $\alpha_o = 0.9$, $N = 1$ and $N = 2$, shown in Figures 3.6 to 3.9. There is numerical dispersion when $\nu < 1$, however, there is no indication of numerical instability for $N = 2$ at $x = 0$ (Figures 3.8 and 3.9) as was found in the previous study (Lorimer, 1986). It was found that when $\alpha = 0.1$, $\nu = 1.0$ the solution is unstable for $N = 1$, $N = 2$, while for $\nu < 1$ there is no evidence of numerical instability or numerical dispersion as indicated in Figures 3.10 and 3.11.

Using equation (3.28), the decay of the discontinuity can be computed and compared to values obtained by the finite difference scheme and method of characteristics. Table 3.1 compares σ at $x = t^+$ obtained from the numerical methods to the exact value given by equation (3.28) for $\alpha_o = 0.9$, $\nu = 1.0$, and $N = 2$. In the results presented, there is a very close agreement between exact values of

stress at the wavefront and the numerical values, consequently it was not necessary to implement a wavefront expansion technique to obtain $\dot{\sigma}$, $\dot{\epsilon}$, $\dot{v}$ at $x = t^+$. However, when $N > 2$, it may be necessary to employ this technique to improve the accuracy.

Table 3.1 Calculation of nondimensional stress at $x = t^+$ for $N = 2$, with $\sigma(0,t) = \sigma_o H(t)$, $\sigma_o = 1$, and quiescent initial conditions, for $\nu = 1.0$ (Refer to Figure 3.8)

Nondimensional Time	Exact Value	Numerical Value	
		MacCormack	Characteristics
	$\sigma_{x=t^+}$	$\sigma_{x=t^+}$	$\sigma_{x=t^+}$
1.50	.9104	.9116	.9106
3.00	.8288	.8268	.8287
4.51	.7545	.7543	.7544
6.01	.6868	.6881	.6864
7.51	.6253	.6276	.6251
9.01	.5692	.5669	.5694

Figures (3.12) to (3.18) are results obtained for boundary conditions given by equation (3.20) for $N = 1$ and $N = 2$. When $\alpha_o = 1$, 0.9, $\nu = 1.0$ there is no evidence of numerical dispersion for $N = 1$, $N = 2$ as indicated in Figures 3.12 to 3.14. For $\alpha_o = 0.1$, $N = 1$ and $N = 2$, there is evidence of weak numerical instability for $\nu = 1.0$, and no numerical instability for $\nu = 0.99$ as indicated by Figures 3.15 to 3.18.

In all of the examples which did not exhibit numerical dispersion or numerical instability, there is very close agreement between the finite difference scheme and method of characteristics.

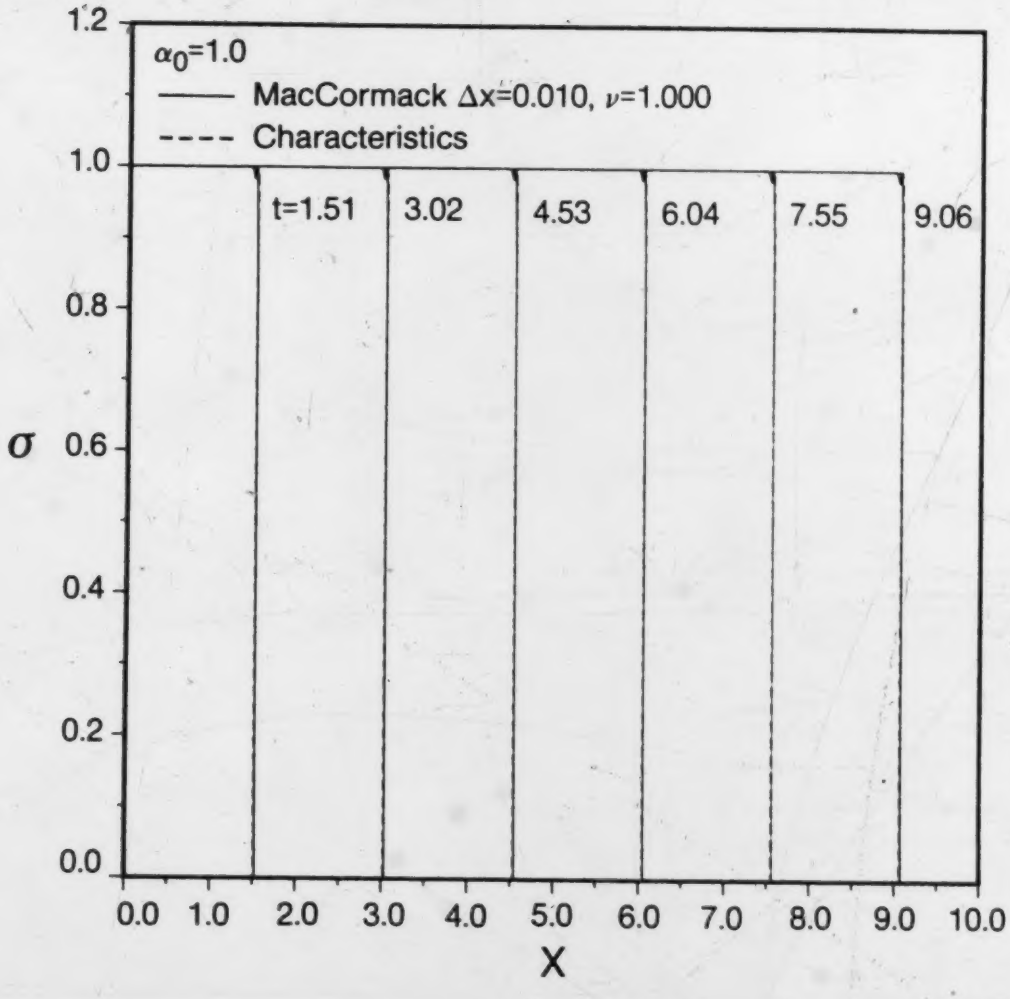

Figure 3.4 Standard Model α_o = 1.0 - Nondimensional σ versus nondimensional x for $\sigma(0,t) = \sigma_o H(t)$, with σ_o = 1 and ν = 1.0.

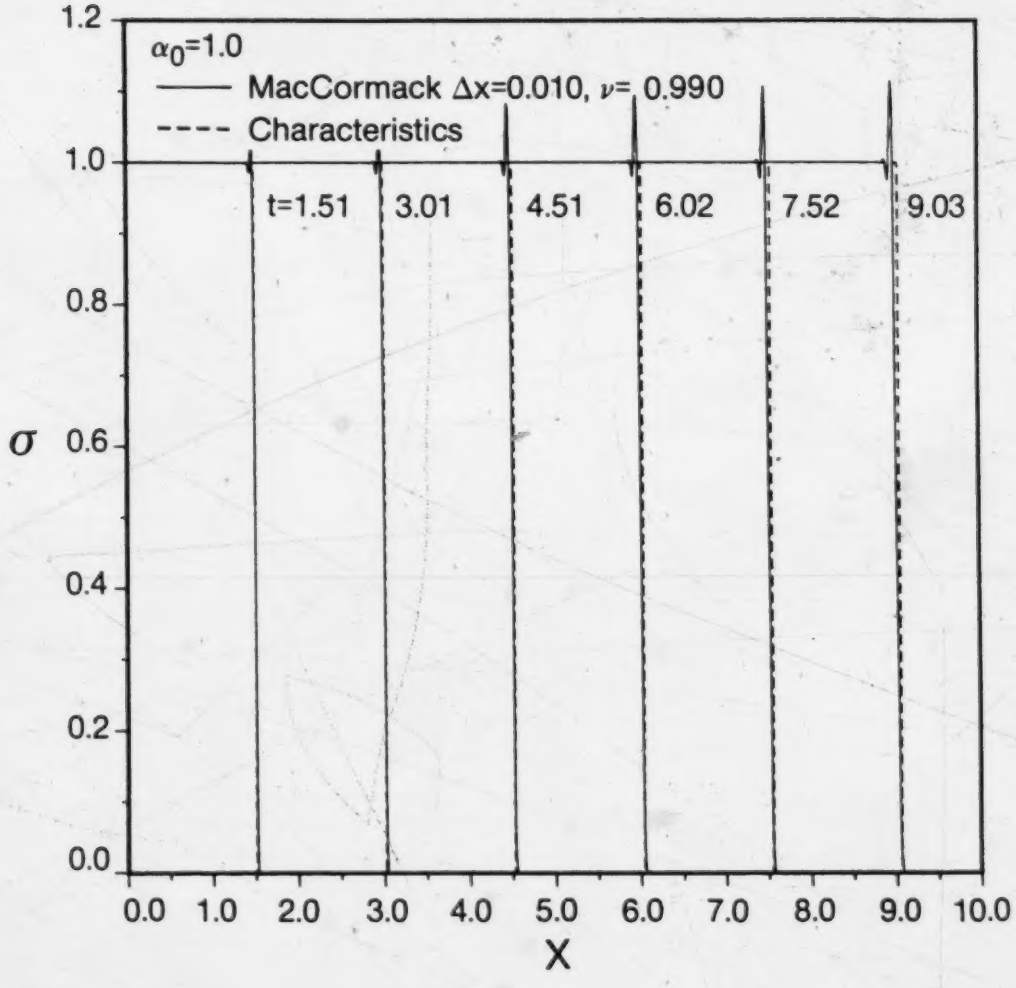

Figure 3.5 Standard Model α_o = 1.0 - Nondimensional σ versus nondimensional x for $\sigma(0,t) = \sigma_o H(t)$, with σ_o = 1 and ν = 0.99.

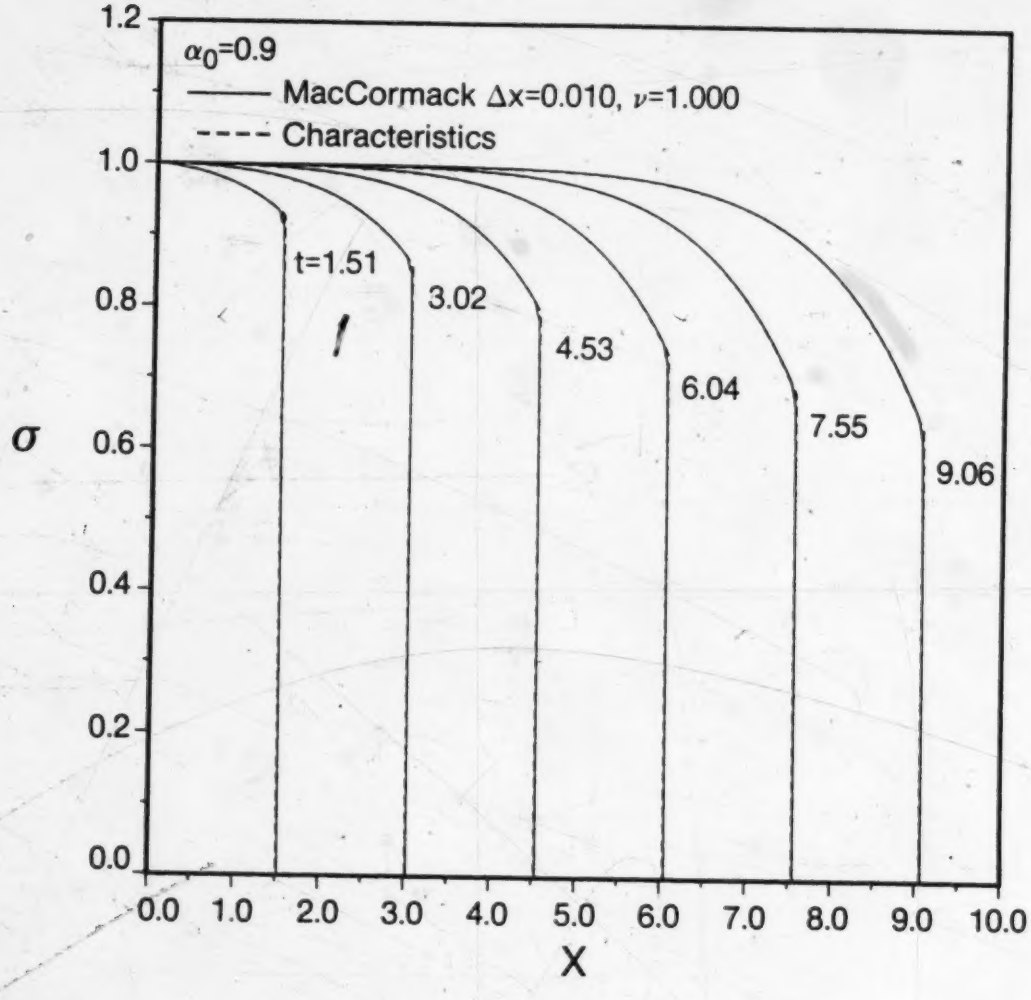

Figure 3.6 Standard Model α_o = 0.9 - Nondimensional σ versus nondimensional x for $\sigma(0,t) = \sigma_o H(t)$, with σ_o = 1 and ν = 1.

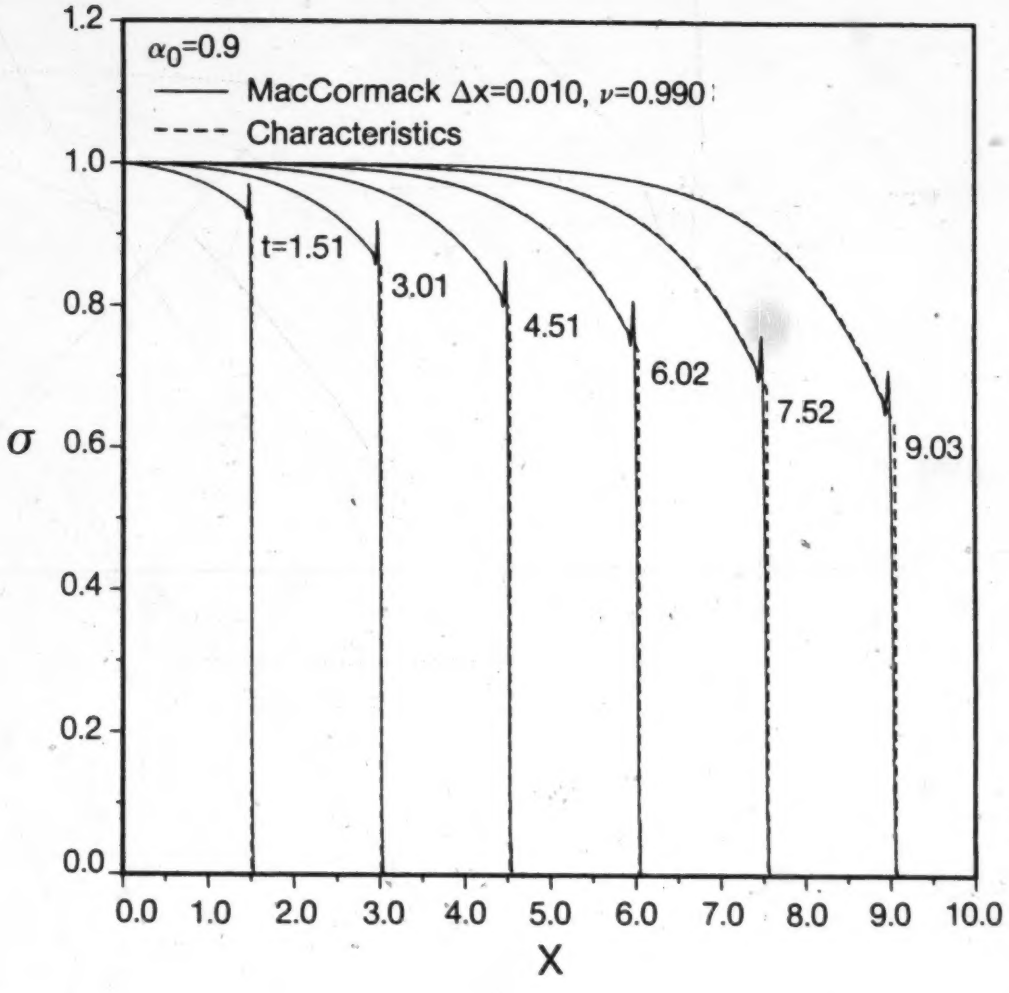

Figure 3.7 Standard Model α_o = 0.9 - Nondimensional σ versus nondimensional x for $\sigma(0,t) = \sigma_o H(t)$, with σ_o = 1 and ν = 0.99.

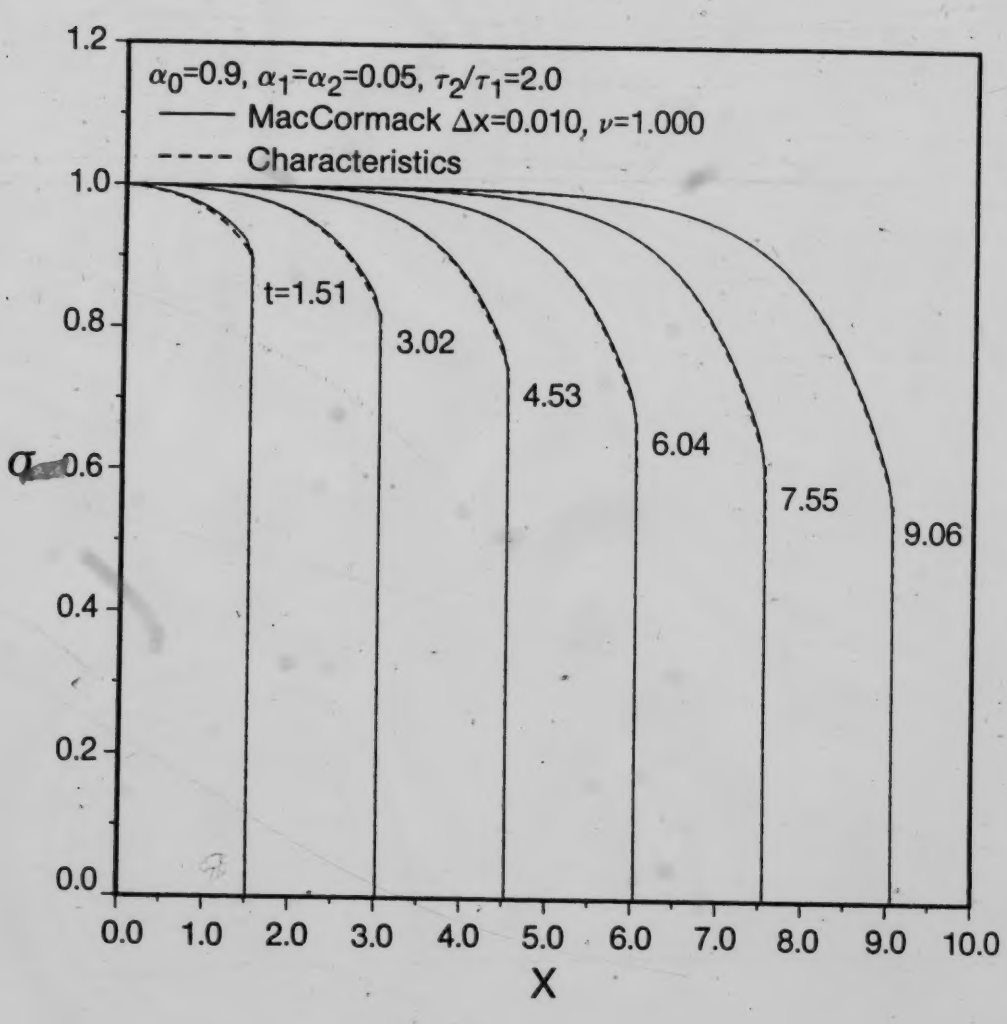

Figure 3.8 Extended Model (N = 2) α_o = 0.9 - Nondimensional σ versus nondimensional x for $\sigma(0,t) = \sigma_o H(t)$, with σ_o = 1 and ν = 1.0.

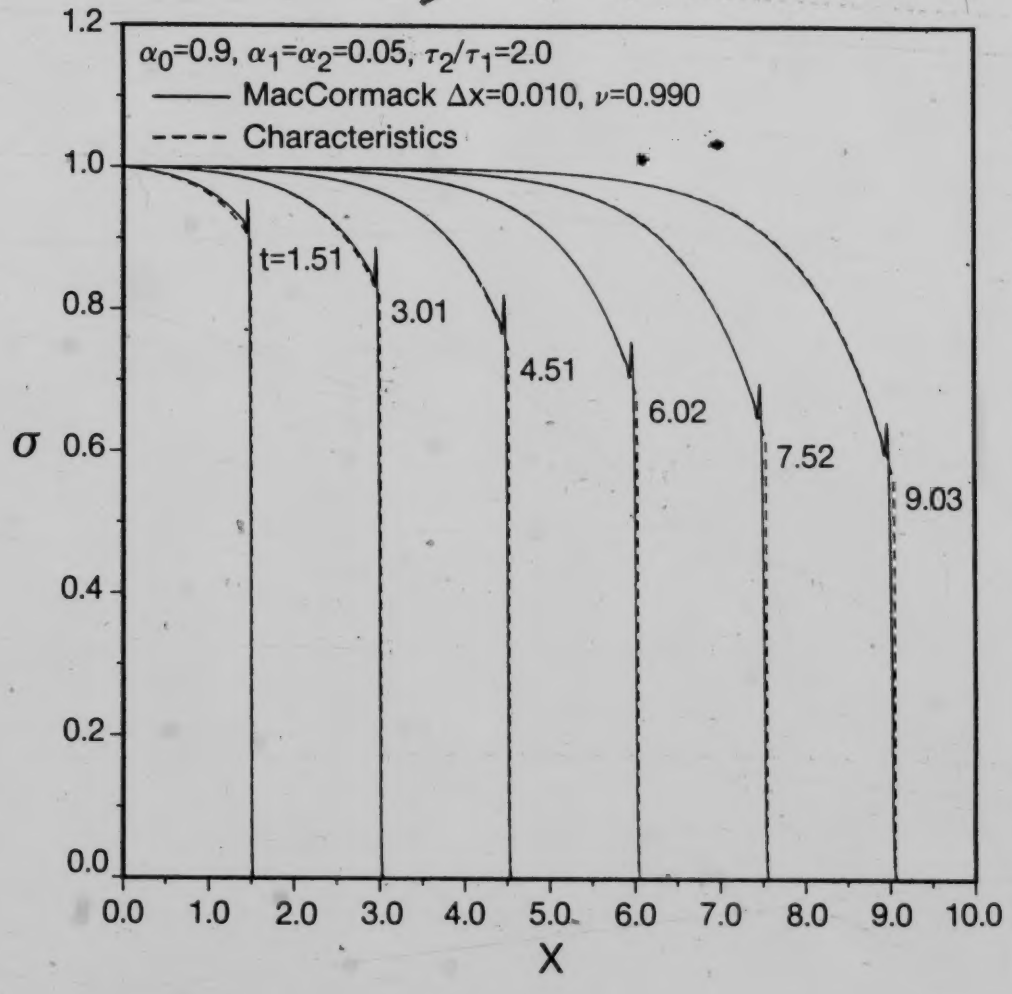

Figure 3.9 Extended Model (N = 2) α_o = 0.9 - Nondimensional σ versus nondimensional x for $\sigma(0,t) = \sigma_o H(t)$, with σ_o = 1 and ν = 0.99.

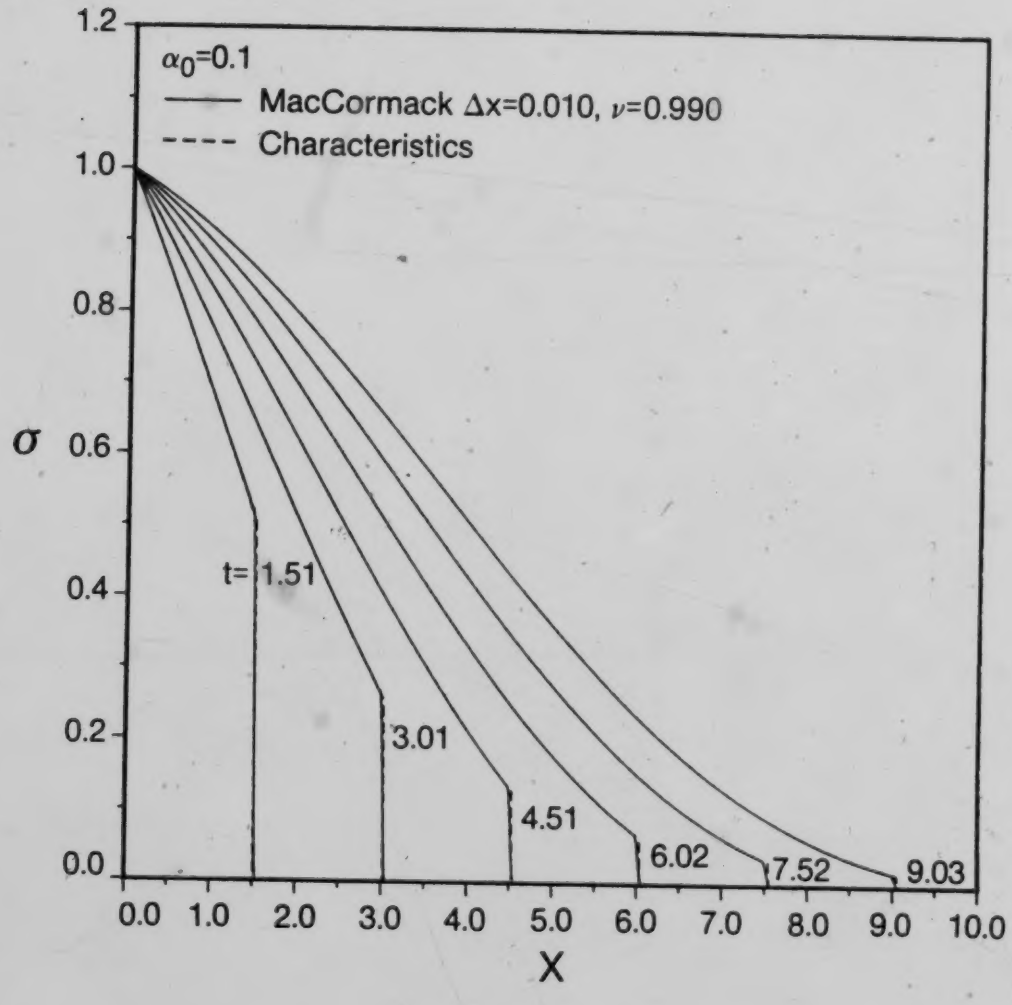

Figure 3.10 Standard Model - α_o = 0.1 - Nondimensinal σ versus nondimensional x for $\sigma(0,t) = \sigma_o$ H(t), with σ_o = 1, ν = 1.

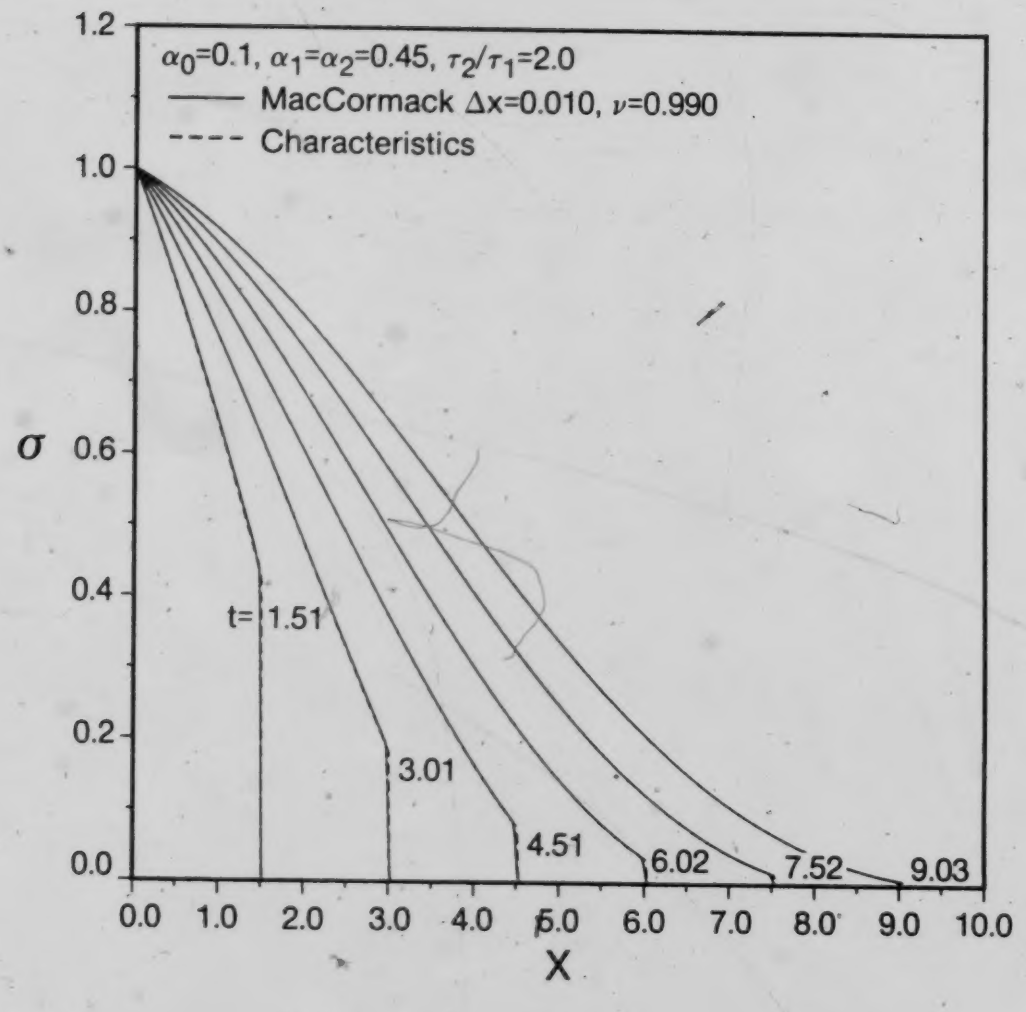

Figure 3.11 Extended Model (N = 2) α_o = 0.1 - Nondimensional σ versus nondimensional x for $\sigma(0,t) = \sigma_o H(t)$, with σ_o = 1 and ν = 0.99.

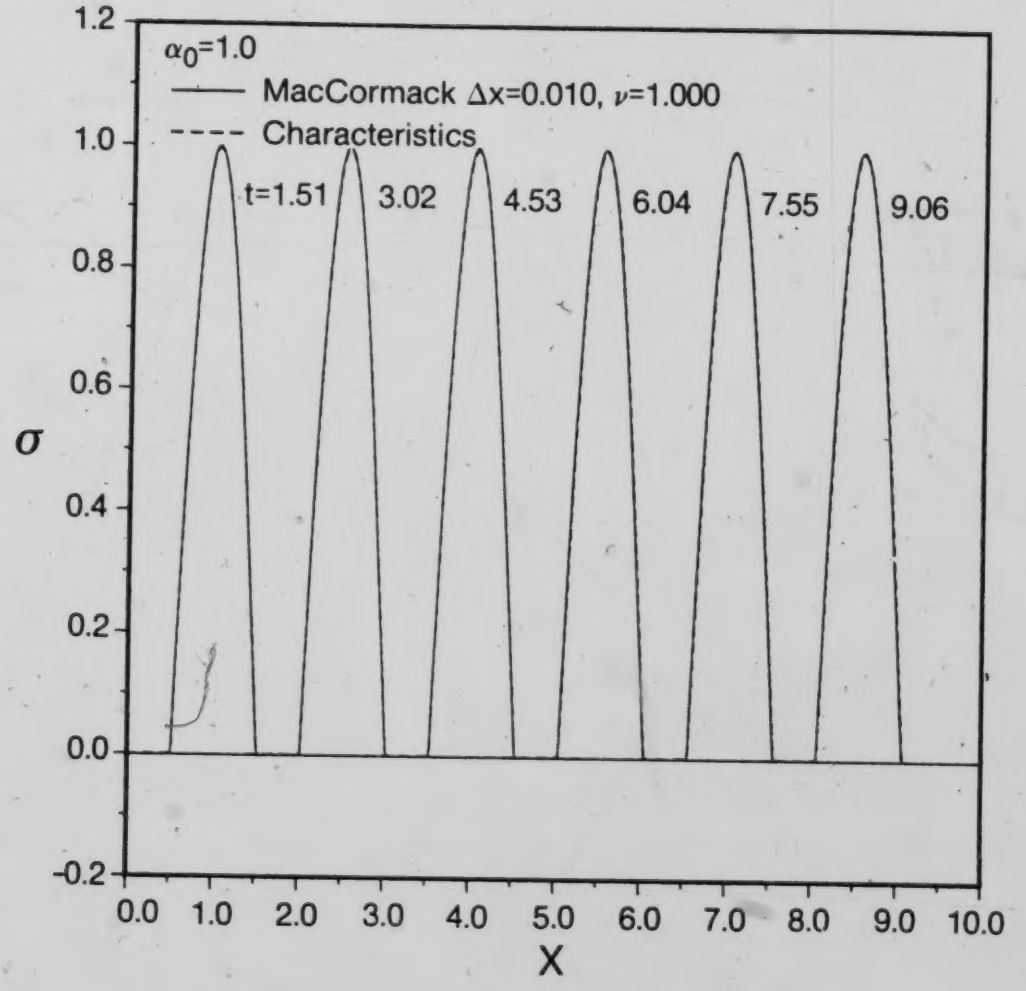

Figure 3.12 Standard Model α_o = 1.0 - Nondimensional σ versus nondimensional x for $\sigma(0,t) = \sigma_o \sin \pi t\ H(t)\ H(1-t)$, with σ_o = 1 and ν = 1.0.

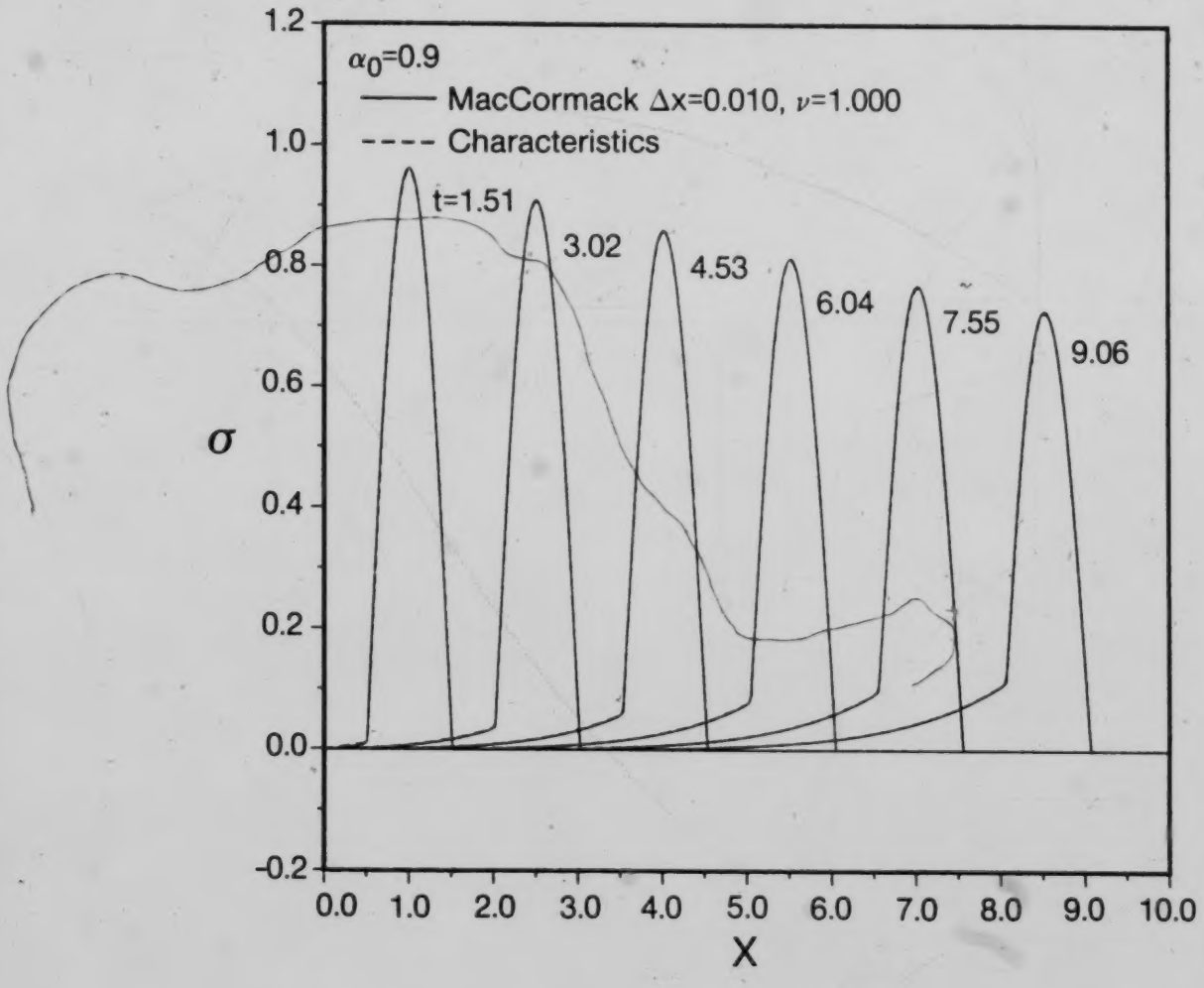

Figure 3.13 Standard Model α_o = 0.9 - Nondimensional σ versus nondimensional x for $\sigma(0,t) = \sigma_o \sin \pi t\ H(t)\ H(1-t)$, with σ_o = 1 and ν = 1.0.

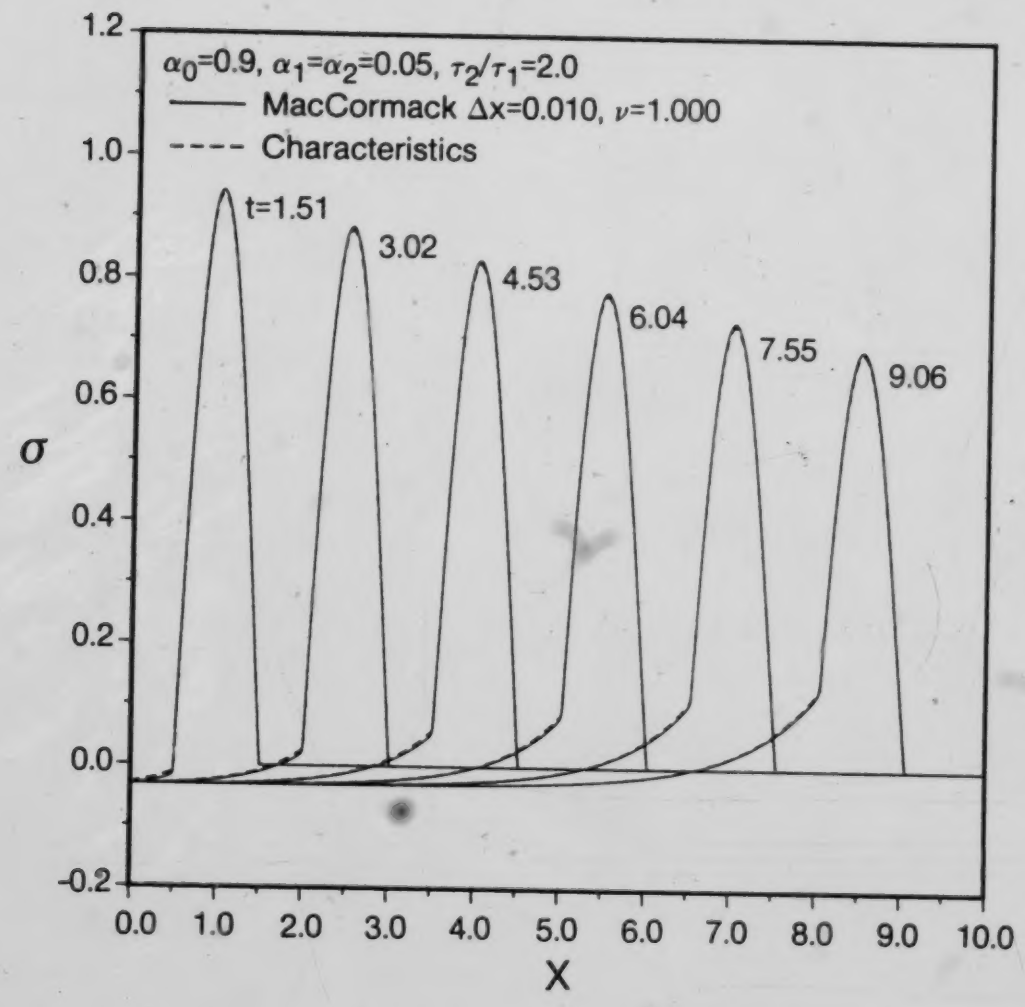

Figure 3.14 Extended Model (N = 2) α_o = 0.9 - Nondimensional σ versus nondimensional x for $\sigma(0,t) = \sigma_o \sin \pi t\ H(t)\ H(1-t)$, with σ_o = 1 and ν = 1.0.

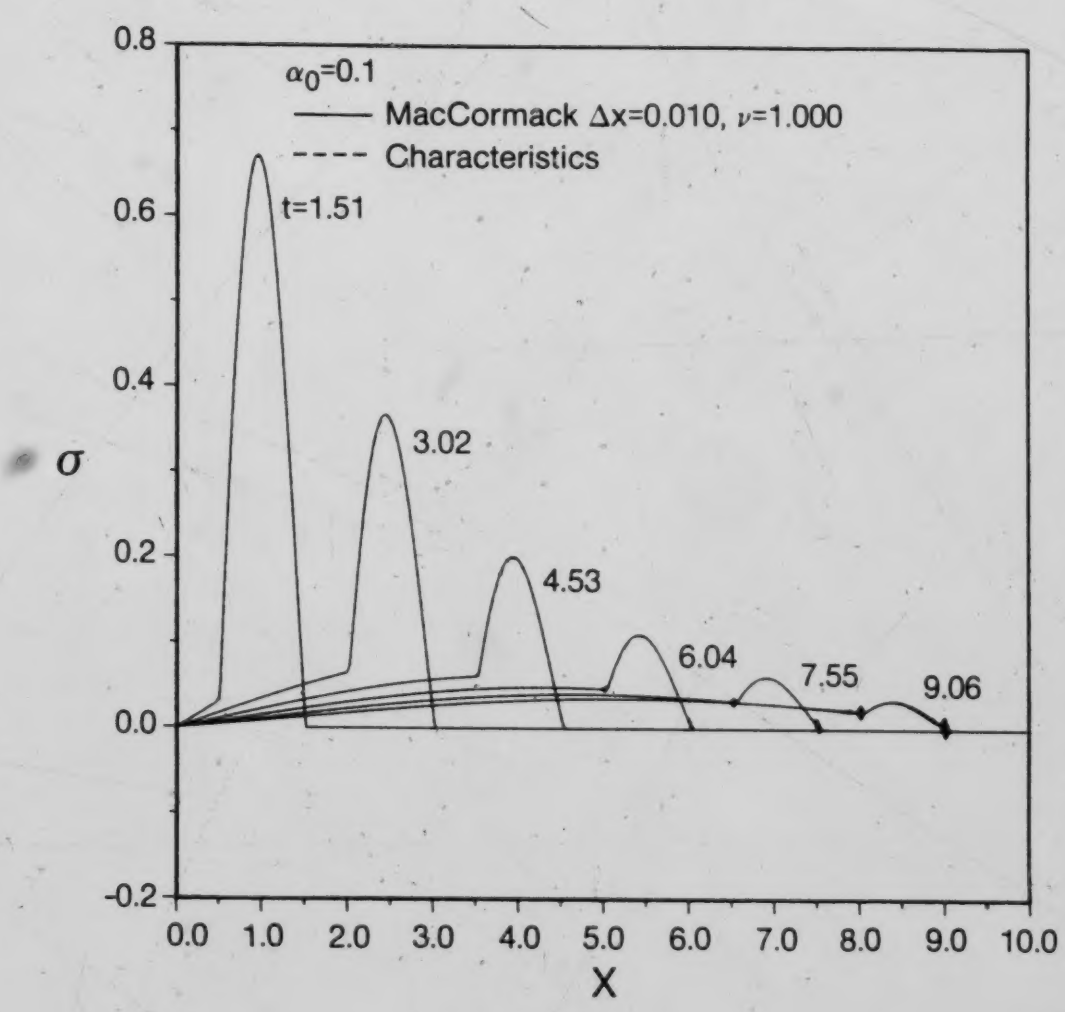

Figure 3.15 Standard Model α_o = 0.1 - Nondimensional σ versus nondimensional x for $\sigma(0,t) = \sigma_o \sin \pi t\ H(t)\ H(1-t)$, with σ_o = 1 and ν = 1.0.

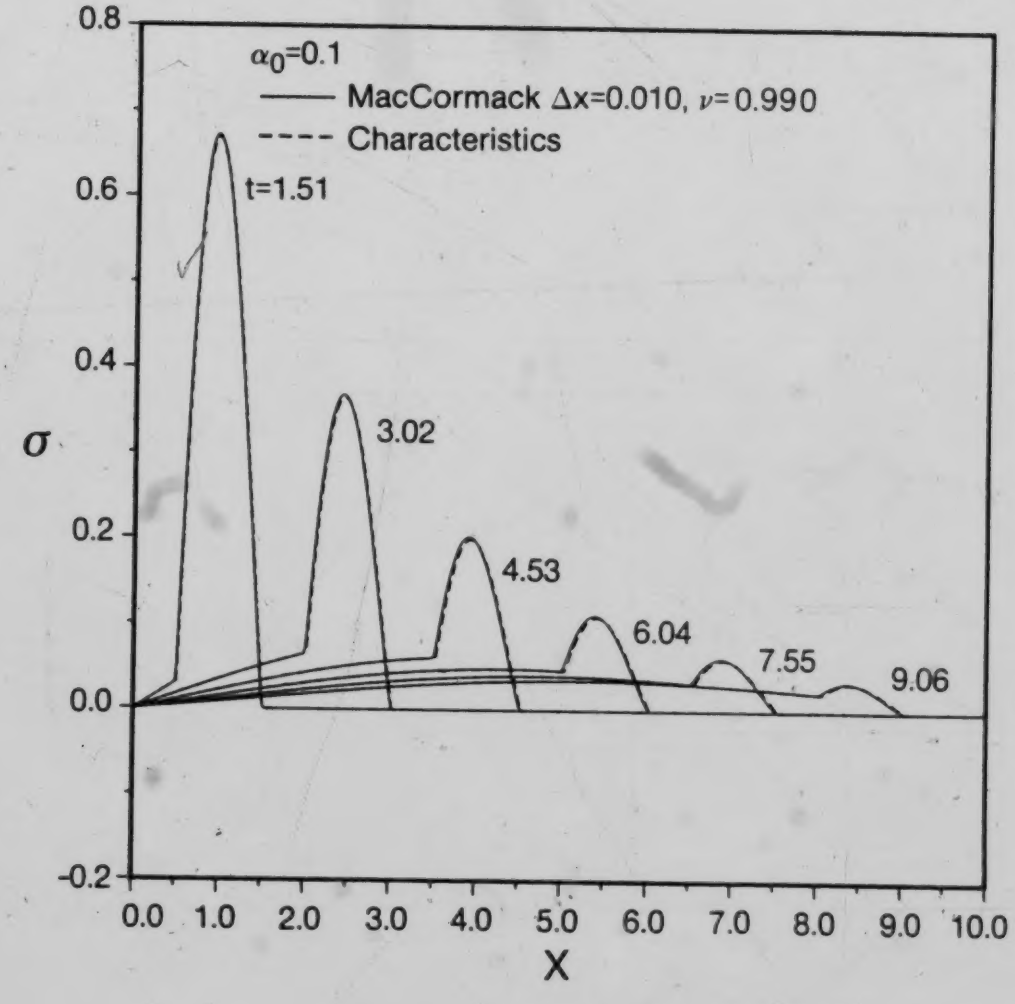

Figure 3.16 Standard Model α_o = 0.1 - Nondimensional σ versus nondimensional x for $\sigma(0,t) = \sigma_o \sin \pi t\ H(t)\ H(1-t)$, with σ_o = 1 and ν = 0.99.

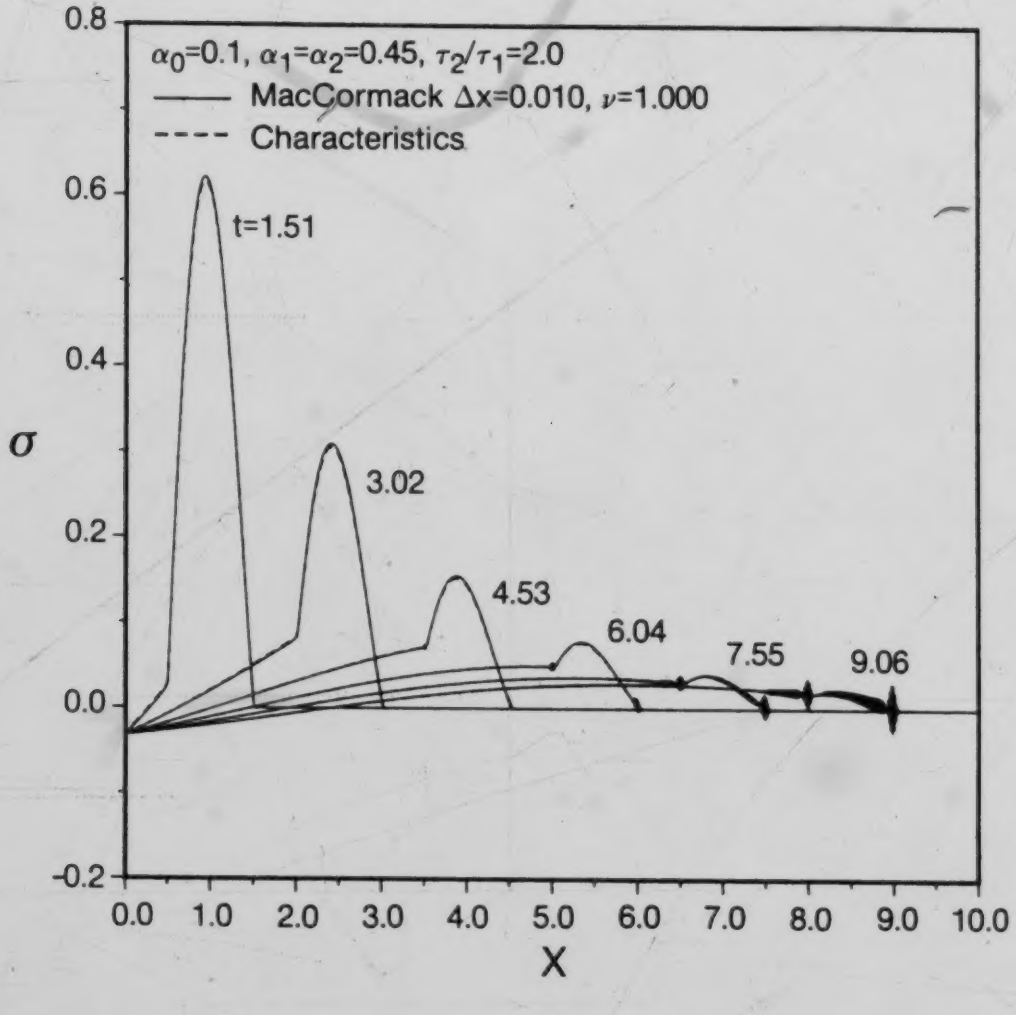

Figure 3.17 Extended Model (N = 2) α_o = 0.1 - Nondimensional σ versus nondimensional x for $\sigma(0,t) = \sigma_o \sin \pi t\, H(t)\, H(1-t)$, with σ_o = 1 and ν = 1.0.

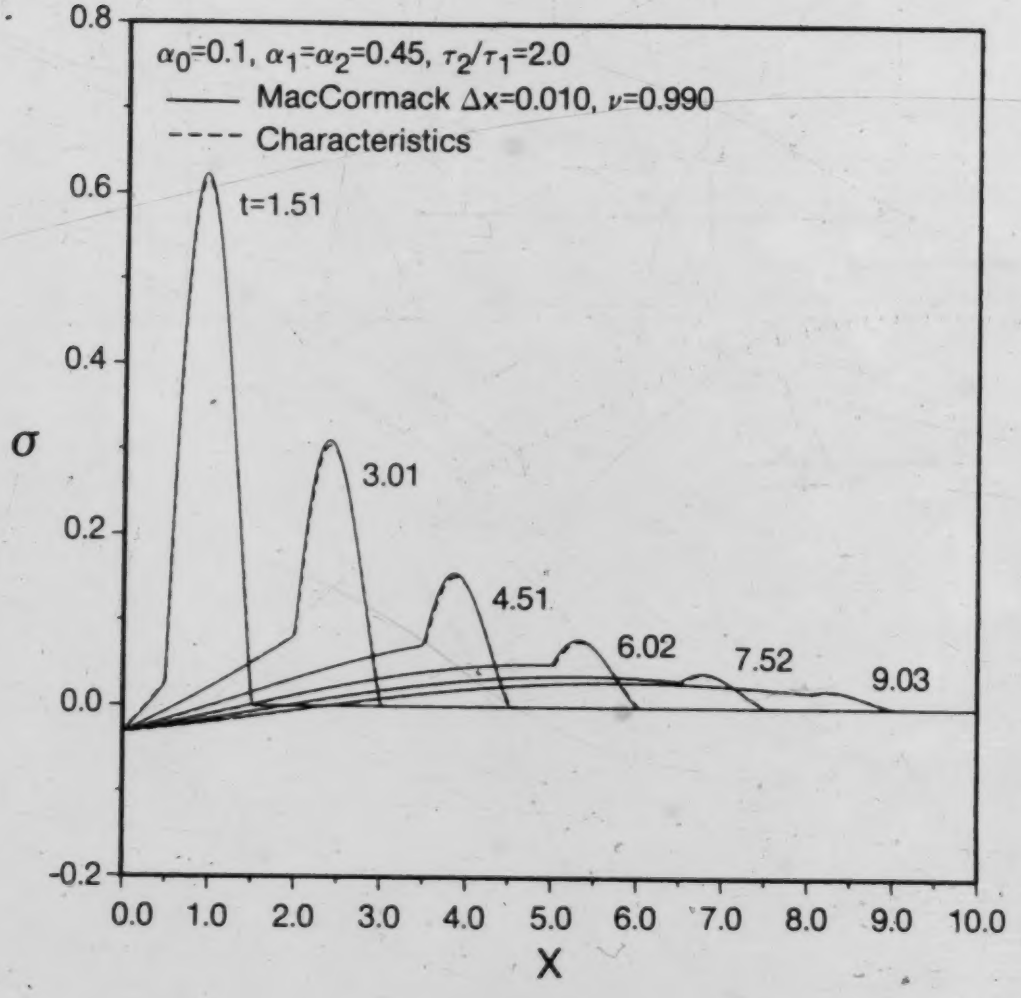

Figure 3.18 Extended Model (N = 2) α_o = 0.1 - Nondimensional σ versus nondimensional x for $\sigma(0,t) = \sigma_o \sin\pi t\ H(t)\ H(1-t)$, with σ_o = 1 and ν = 0.99.

Chapter IV

Thermomechanics of Hyperelastic Solids

4.1 Constitutive Assumptions

The preceding chapters dealt with linear problems, in the remaining chapters we consider problems of finite deformations of an isotropic hyperelastic solid. A hyperelastic solid is an elastic solid for which a stored energy function exists, that is, the solid is capable of storing elastic energy.

We consider particular cases of a class of isothermal strain energy functions for isotropic hyperelastic solids, which can be expressed in the form,

$$W(\lambda_1, \lambda_2, \lambda_3) = \mu f(\lambda_1, \lambda_2, \lambda_3) + k\, g(J) \tag{4.1}$$

where λ_1, λ_2, λ_3 are the principal stretches, $J = \lambda_1\lambda_2\lambda_3$ and μ and k are the isothermal shear and bulk moduli respectively, for infinitesimal deformation from the natural reference state at temperature T_o. The function f is symmetric in λ_1, λ_2, λ_3 and is zero when $\lambda_1 = \lambda_2 = \lambda_3$ and the function g satisfies the conditions,

$$g(1) = g'(1) = 0 \quad \text{and} \quad g''(1) = 1 \,. \tag{4.2}$$

Justification for the form (4.1) for rubber-like materials is given by Chadwick and Creasy (1984).

It has been shown by Ogden (1982) that results of hydrostatic compression tests for rubber-like materials are in close agreement with the relation

$$\frac{q}{k} = \frac{1}{9}\left(J^{-10} - J^{-1}\right) , \tag{4.3}$$

where q is the hydrostatic pressure. Since

$$\frac{q}{k} = -\frac{dg}{dJ} , \tag{4.4}$$

for hydrostatic compression, equation (4.3) implies that,

$$g = \frac{1}{9}\left(\frac{J^{-9}}{9} + \ell n\, J - \frac{1}{9}\right) . \tag{4.5}$$

Equation (4.5) may not be valid for finite positive volume strain, however if positive volume strains are such that $(J-1) \ll 1$, equation (4.5) is a realistic expression for g(J) since a Taylor series expansion gives

$$g = \frac{1}{2}(J-1)^2 + 0\left((J-1)^3\right) . \tag{4.6}$$

Equation (4.1) is for a compressible solid and we later consider the limiting case of an incompressible solid, since the assumption of incompressibility is realistic for the problems which we consider in the following chapters. These problems involve finite deformation of a solid rubber-like material with $\mu/k \ll 1$ and the hydrostatic part of the Cauchy stress tensor is negligible compared with k.

A compressible generalization of a three term strain energy function due to Ogden is

$$W = \sum_{i=1}^{3} \frac{\mu_i}{a_i}\left(\lambda_1^{a_i} + \lambda_2^{a_i} + \lambda_3^{a_i} - 3\,J^{a_i/3}\right) + kg(J) , \tag{4.7}$$

where $\sum_{i-1}^{3} \mu_i a_i = 2\mu$, and W is the strain energy per unit volume in the reference state.

The incompressible limit of (4.7) is,

$$W = \sum_{i-1}^{3} \frac{\mu_i}{a_i} \left(\lambda_1^{a_i} + \lambda_2^{a_i} + \lambda_3^{a_i} - 3 \right), \tag{4.8}$$

which was proposed by Ogden (1972). The compressible generalization (4.7) was proposed by Chadwick and Creasy (1984).

A special case of equation (4.7) with $\mu_3 = 0$, is a compressible generalization,

$$W = \frac{\mu}{2} \left\{ \alpha(\lambda_1^2 + \lambda_2^2 + \lambda_3^2 - 3\, J^{2/3}) + (1-\alpha)(\lambda_1^{-2} + \lambda_2^{-2} + \lambda_3^{-2} - 3\, J^{-2/3}) \right\} + kg(J) \tag{4.9}$$

where $0 \le \alpha \le 1$, of the Mooney-Rivlin strain energy function. The incompressible limit of (4.9) is,

$$W = \frac{\mu}{2} \left\{ \alpha(\lambda_1^2 + \lambda_2^2 + \lambda_3^2 - 3) + (1-\alpha)(\lambda_1^{-2} + \lambda_2^{-2} + \lambda_3^{-2} - 3) \right\}. \tag{4.10}$$

When $\alpha = 1$, the Neo-Hookean strain energy function is recovered from (4.10).

A fundamental equation of state for an isotropic hyperelastic solid is given by the Helmholtz free energy function as a function of deformation and temperature,

$$A = \hat{A}\,(\lambda_1,\ \lambda_2,\ \lambda_3,\ T)\ . \tag{4.11}$$

An alternative fundamental equation of state for an isotropic hyperelastic solid is given by the internal energy as a function of deformation and entropy,

$$U = \hat{U}\,(\lambda_1,\ \lambda_2,\ \lambda_3,\ S)\ . \tag{4.12}$$

The strain energy function at reference temperature T_o is related to A by

$$W(\lambda_1,\ \lambda_2,\ \lambda_3) = \rho_o A(\lambda_1,\ \lambda_2,\ \lambda_3,\ T_o)\ , \tag{4.13}$$

where ρ_o is the density in the reference configuration. The strain energy W is per unit volume of the reference state, and A is per unit mass.

In the following chapters, problems involving simple tension of an incompressible hyperelastic string are considered. The stretch in the direction of the tensile force is λ, and transverse stretches are $\lambda_2 = 1/\sqrt{\lambda}$, $\lambda_3 = 1/\sqrt{\lambda}$. The simple tension forms of the strain energy functions (4.8) and (4.10) are,

$$W = \sum_{i=1}^{3} \frac{\mu_i}{a_i}\left[\lambda^{a_i} + 2\lambda^{-a_i/2} - 3\right]\ , \tag{4.14}$$

and

$$W = \frac{\mu}{2}\left\{\alpha\,(\lambda^2 + \frac{2}{\lambda} - 3) + (1 - \alpha)(\lambda^{-2} + 2\lambda - 3)\right\}\ , \tag{4.15}$$

respectively. Ogden (1977) has shown that the relation,

$$P = \sum_{i=1}^{3} \mu_i \left(\lambda^{a_i - 1} - \lambda^{-a_i/2 - 1} \right) , \tag{4.16}$$

obtained from

$$P = \frac{dW}{d\lambda} (\lambda) \tag{4.17}$$

and (4.14) gives a close fit with experimental data for isothermal simple tension of certain rubbers up to stretches of about 7 when the μ_i/μ and a_i take the values,

$$\begin{aligned} \mu_1/\mu &= 1.491, \quad \mu_2/\mu = 0.003, \quad \mu_3/\mu = -0.0237, \\ a_1 &= 1.3, \quad a_2 = 5.0, \quad a_3 = -2.0. \end{aligned} \tag{4.18}$$

The corresponding relation for (4.15) is

$$P = \mu(\alpha + (1-\alpha)\lambda^{-1})(\lambda - 1/\lambda^2) , \tag{4.19}$$

which, with $\alpha = 0.6$, gives a close fit with simple tension experimental data for λ up to about 3.5. Relation (4.16) and (4.18) and relation (4.19) with $\alpha = 0.6$ are shown graphically in Figure 4.1.

4.2 Mechanical Incompressibility

The problems considered in the following chapters involve rapid deformation which is assumed to be adiabatic since rubber-like materials are relatively poor conductors of heat. Strain energy functions such as those given in the previous section are generally

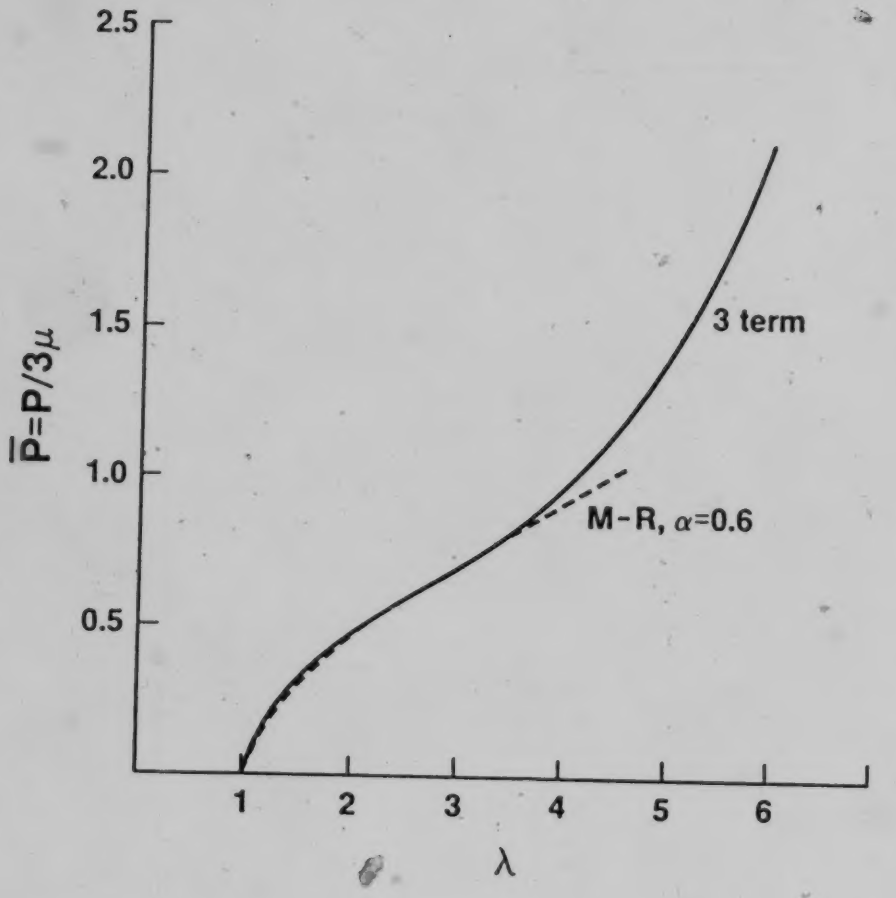

Figure 4.1 Isothermal nominal stress-stretch relation for Ogden's 3 term strain energy function with parameters (4.18), and Mooney-Rivlin strain energy function with $\alpha = 0.6$.

taken to be for isothermal deformation. It is desirable to investigate the error involved in considering an isothermal stress-stretch relationship rather than an adiabatic relation.

The problems considered in the following chapters are for a mechanically incompressible solid. It can be shown that if the solid is mechanically incompressible then any deformation must be isochoric, that is the coefficient of thermal expansion is zero (Ogden, Private Communication).

4.3 Strictly Entropic Elasticity

The internal energy U is related to the Helmholtz free energy by

$$U = A + TS \ . \tag{4.20}$$

For our present purpose it is convenient to express U as a function of deformation and temperature,

$$U = \hat{U}\ (\lambda_1,\ \lambda_2,\ \lambda_3,\ T) \tag{4.21}$$

which is not a fundamental equation of state. In order to consider the thermodynamic effects we consider a material whose internal energy is expressible as the sum of a function of J and a function of T so that

$$U = U_1(J) + U_2(T) \ . \tag{4.22}$$

This decomposition has been discussed in detail by Chadwick (1974) and such a material is described as strictly entropic for isochoric deformation. Changes in internal energy during isochoric deformation depend only on the temperature changes and not on the distortion. If equation (4.22) is valid it can be shown that the specific heat C at a

constant deformation is a function of the temperature only, and if $|T-T_o|/T_o \ll 1$, the temperature dependence can be neglected. For the small temperature changes which occur in the problems considered, C is assumed to be constant.

It follows from theory in Chadwick (1974) that,

$$A = \frac{W}{\rho_o}\frac{T}{T_o} - \frac{\alpha\, kh(J)(T-T_o)}{\rho_o} + C\,(T-T_o) - CT\,\ell n\,\frac{T}{T_o}\,, \tag{4.23}$$

where h is a response function such that $h(1) = 0$ and $h'(1) = 1$, which for $|J-1| \ll 1$ is approximated by $J-1$. The entropy is given by,

$$S = -\frac{\partial A}{\partial T} = -\left\{\frac{W}{\rho_o T_o} - \frac{\alpha kh(J)}{\rho_o} - C\,\ell n\,\frac{T}{T_o}\right\}. \tag{4.24}$$

For isentropic[1] deformation from the reference state, it follows from equation (4.24) that

$$\frac{W}{\rho_o T_o} - \frac{\alpha kh(J)}{\rho_o} = C\,\ell n\,\frac{T}{T_o}\,,$$

or

$$T - T_o = T_o\left\{\exp\left[\beta\left(\frac{W}{\mu} - \frac{\alpha\, T_o h(J)}{\eta}\right)\right] - 1\right\}, \tag{4.25}$$

where $\beta = \mu/(\rho_o C T_o)$ and $\eta = \mu/k$. A typical value of the non-dimensional quantity β for rubber-like solids is $\beta = 10^{-3}$ (Chadwick, 1974).

---

[1]The term isentropic is taken to mean reversible adiabatic. An adiabatic deformation of an elastic solid is isentropic except where shocks occur.

As the limit of incompressibility is approached, that is as $\mu/k \to 0$ with μ held constant, $h \to 0$ and $\alpha T_o/\eta$ is bounded, that is $\alpha T_o = O(\eta)$, so that for an incompressible solid,

$$A = \frac{W}{\rho_o}\frac{T}{T_o} + C(T - T_o) - CT\,\ell n\,\frac{T}{T_o}\,, \tag{4.26}$$

$$S = \frac{-W}{\rho_o T_o} + C\ell n\,\frac{T}{T_o}\,. \tag{4.27}$$

For isentropic deformation from the reference state,

$$T - T_o = T_o\left\{\exp\left[\beta\,\frac{W}{\mu}\right] - 1\right\}. \tag{4.28}$$

It follows from equations (4.20), (4.27) and (4.28) that a fundamental equation of state for an incompressible strictly entropic elastic solid is

$$\hat{U} = CT_o\left\{\exp\left[\frac{S}{C} + \beta\frac{W}{\mu}\right] - 1\right\}. \tag{4.29}$$

For the problem of simple tension of an incompressible hyperelastic string, which is considered in the following chapters, the strain energy function is given as a function of λ, so that

$$\hat{W}(\lambda) = W(\lambda,\ 1/\sqrt{\lambda},\ 1/\sqrt{\lambda}),$$

where λ is the stretch in the direction of the tension. The nominal stress is given by

$$P = \frac{\partial \hat{W}}{\partial \lambda} = \rho_o\,\frac{\partial A}{\partial \lambda}\,(\lambda, T_o)\,, \tag{4.30}$$

for isothermal stretch from the reference state, also

$$P(\lambda,S) = \rho_o \frac{\partial \hat{U}}{\partial \lambda}(\lambda,S) , \tag{4.31}$$

$$P(\lambda,T) = \rho_o \frac{\partial \hat{A}}{\partial \lambda}(\lambda,T) , \tag{4.32}$$

where $W(\lambda_1, \lambda_2, \lambda_3)$ is replaced by $\hat{W}(\lambda)$ in equations (4.26) and (4.29). Therefore, when non-isothermal simple tension of an incompressible solid which exhibits strictly entropic elasticity is considered, (4.30) should be replaced by

$$P(\lambda,T) = \frac{T}{T_o} \frac{d\hat{W}}{d\lambda} , \tag{4.33}$$

or equivalently by,

$$\hat{P}(\lambda,S) = \frac{d\hat{W}}{d\lambda} \exp\left(\frac{S}{C} + \beta \frac{\hat{W}}{\mu} \right) . \tag{4.34}$$

The entropy is taken as zero in the reference state so that for isentropic deformation from the reference state,

$$\hat{P}(\lambda,0) = \frac{d\hat{W}}{d\lambda} \exp\left(\beta \frac{\hat{W}}{\mu} \right) . \tag{4.35}$$

The error resulting from adopting the isothermal relation (4.17) instead of the adiabatic relation (4.35) for a strictly entropic material is investigated in Chapter V. Also, when a jump in λ occurs across a shock, the deformation is piecewise isentropic with a jump in entropy across the shock, if the adiabatic relation is adopted. According to equation (4.34) this results in a change in the isentropic P,λ relation as the shock passes. The error resulting from neglect of

the effect of the entropy jump on the P,λ relation is also investigated in Chapter V.

4.4 Modified Entropic and Peizotropic Elasticity

Chadwick and Creasy (1984) proposed a modified entropic elastic model, where the internal energy function is divisible into two parts, so that for simple tension,

$$\tilde{U} = U_1(\lambda) + U_2(T) \quad . \tag{4.36}$$

In the strictly entropic model proposed by Chadwick (1974), which was discussed in the previous section, the dependence of U_1 on the deformation is through J.

The specific heat at a constant deformation is defined as,

$$C = \left(\frac{\partial \tilde{U}}{\partial T}\right)_{\lambda} = \frac{dU_2}{dT} = \phi(T) \quad , \tag{4.37}$$

also

$$C(T) = T \left(\frac{\partial S}{\partial T}\right)_{\lambda} \quad . \tag{4.38}$$

Equations (4.37) and (4.38) imply that the specific entropy is divisible into two parts,

$$S(\lambda,T) = S_1(\lambda) + S_2(T) \quad . \tag{4.39}$$

A simplified form of the free energy function for a modified entropic elastic material given by Chadwick and Creasy (1984) is,

$$A(\lambda,T) = \frac{\mu}{\rho_o}\left\{ f(\lambda)\,\frac{T}{T_o} - \gamma\, f(\lambda)\left[\frac{T}{T_o} - 1\right]\right\}$$

$$+ \frac{k}{\rho_o}\, g(J)\,\frac{T}{T_o} - \alpha\, k\,\frac{h(J)}{\rho_o}\,(T-T_o) + A_2(T)\,, \qquad (4.40)$$

where $0 \le \gamma \le 1$, $f(\lambda)$ is the response function appearing in (4.1), and,

$$A_2(T) = C(T - T_o) - CT\,\ell n\,\frac{T}{T_o}\,. \qquad (4.41)$$

The limit of (4.40) for incompressible materials can be obtained by the procedure outlined in the previous section, and is

$$A(\lambda,T) = \frac{\mu}{\rho_o}\left\{ f(\lambda)\,\frac{T}{T_o} - \gamma\, f(\lambda)\left[\frac{T}{T_o} - 1\right]\right\} + A_2(T)\,. \qquad (4.42)$$

The internal energy and entropy are,

$$U(\lambda,T) = \frac{\gamma\hat{W}}{\rho_o} + C(T - T_o)\,, \qquad (4.43)$$

and

$$S(\lambda,T) = -(1 - \gamma)\frac{\hat{W}}{\rho_o T_o} + C\ell n\,\frac{T}{T_o}\,, \qquad (4.44)$$

respectively.

When $\gamma = 0$, the strictly entropic material is recovered and the internal energy and entropy are,

$$U(\lambda,T) = C(T - T_o) \ , \quad S(\lambda,T) = \frac{-\hat{W}}{\rho_o T_o} + C \ \ell n \frac{T}{T_o} \ , \tag{4.45}$$

respectively, and $U = U(T)$. Equations (4.45) are identical to results obtained in the previous section which were derived based on the strictly entropic model proposed by Chadwick (1974).

When $\gamma = 1$, a piezotropic material is recovered and the internal energy and entropy are,

$$\hat{U}(\lambda,T) = \frac{\hat{W}}{\rho_o} + C(T - T_o) \ , \tag{4.46}$$

$$S(\lambda,T) = C\ell n \frac{T}{T_o} \ , \tag{4.47}$$

and, $S = S(T)$. A fundamental equation of state for a piezotropic material can be obtained from (4.46) and (4.47) and is,

$$\hat{U}(\lambda,S) = \frac{\hat{W}}{\rho_o} + \frac{1}{3\beta}\left(\exp \frac{S}{C} - 1\right) \ . \tag{4.48}$$

For a piezotropic material, $S = S(T)$, consequently an isentropic deformation is identical to an isothermal deformation. From (4.31) and (4.48),

$$P(\lambda,S) = \rho_o \frac{\partial \hat{U}}{\partial \lambda} = \frac{\partial \hat{W}}{\partial \lambda} \ , \tag{4.49}$$

and the adiabatic stress-stretch relation is identical to the isothermal stress-stretch relation. Therefore, by using an isothermal stress-stretch relation we are solving the problem for a piezotropic

material. Mechanical and thermal effects are completely uncoupled for a piezotropic material.

The Gaussian statistical theory of rubber elasticity predicts strictly entropic elasticity (Treloar, 1975). However experimental data presented by Chadwick and Creasy (1984) indicate that a modified entropic model with a value of γ in equation (4.40) approximately 0.85 is more realistic for most rubbers.

Chapter V

Finite Amplitude Wave Propagation in a Stretched Hyperelastic String

5.1 Governing Equations

We consider plane motion of a hyperelastic string and obtain the conservation form of the system of Lagrangian governing equations and the corresponding form with dependent variables u, v, λ, and θ, where u and v are the x_1 and x_2 components, respectively, of the particle velocity and θ is the angle the tangent to the string makes with the x_1 axis of the rectangular Cartesian coordinate system $0x_2$. The dependent variables for the system of equations derived by Beatty and Haddow (1985) are τ, ν, λ and θ where τ and ν are the tangential and normal components, respectively, of the particle velocity, however, these dependent variables, or combinations of them, are not convenient for determination of a system in conservation form. To apply numerical techniques, it is desirable to have the equations in conservation form.

We consider a perfectly flexible uniform hyperelastic string whose reference configuration is taken as the unstressed natural configuration at temperature T_o and occupies an interval of the x_1 axis. The x_1 coordinate of a particle in the reference configuration is denoted by X and at time t the particle is at place $\underline{x} = \underline{x}(X,t)$.

The problem geometry is illustrated in Figure 5.1. If $s(X,t)$ denotes the arc length, measured from a fixed point $\underline{x} = \underline{x}(X_o,t)$, in the deformed configuration, the stretch is given by

$$\lambda(X,t) = \frac{\partial s}{\partial X} , \tag{5.1}$$

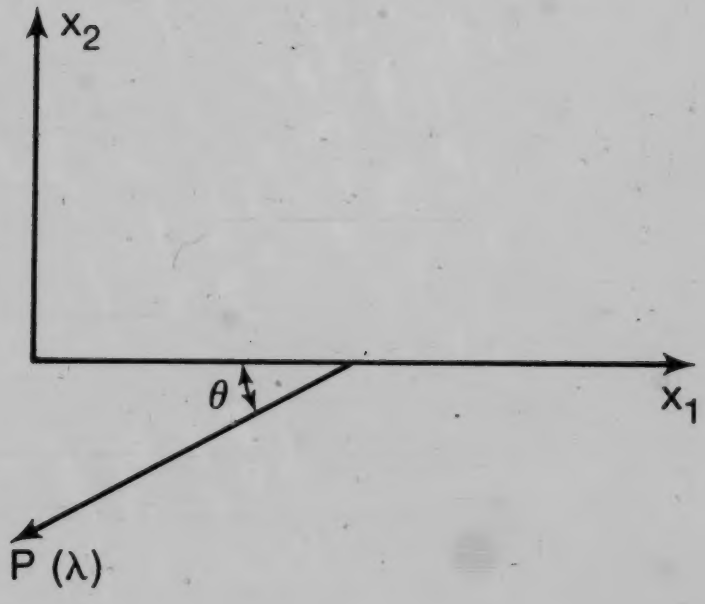

Figure 5.1 Problem geometry

and it follows that

$$\frac{\partial(\lambda\cos\theta)}{\partial t} = \frac{\partial u}{\partial X}\ ,\quad \frac{\partial(\lambda\sin\theta)}{\partial t} = \frac{\partial v}{\partial X}\ , \tag{5.2}$$

where $\theta = \theta(X,t)$.

The string is assumed to be perfectly flexible consequently the direction of the tensile force P per unit cross sectional area of the string in the reference configuration, is tangential to the string. We are adopting the isentropic approximation and P is expressed as a function of λ only. The non-zero components S_{11}, S_{12} of the nominal stress tensor[1] are given by

$$S_{11} = P(\lambda)\cos\theta, \quad \text{and } S_{12} = P(\lambda)\sin\theta\ .$$

Consequently the Lagrangian equations of motion, with body forces neglected are,

$$\frac{\partial\ (P(\lambda)\cos\theta/\rho_o)}{\partial X} = \frac{\partial u}{\partial t}\ ,\quad \frac{\partial(P(\lambda)\sin\theta/\rho_o)}{\partial X} = \frac{\partial v}{\partial t}\ . \tag{5.3}$$

The system of equations (5.2) and (5.3) is in conservation form and may be expressed in matrix notation as

$$\frac{\partial \underset{\sim}{G}}{\partial t} + \frac{\partial \underset{\sim}{H}\ (G)}{\partial X} = \underset{\sim}{0}\ , \tag{5.4}$$

---

[1]Here the nominal stress is the transpose of the first Piola-Kirchhoff Stress.

where $\underset{\sim}{G} = (\lambda\cos\theta,\ \lambda\sin\theta, u, v)^T$, $\underset{\sim}{H} = -(u, v,\ P\cos\theta/\rho_o,\ P\sin\theta/\rho_o)^T$ and a superposed T denotes the transpose. A convenient non-conservation form obtained from equation (5.4) is

$$\frac{\partial \underset{\sim}{G}}{\partial t} + \underset{\sim}{B}\,\frac{\partial \underset{\sim}{G}}{\partial X} = \underset{\sim}{0} \tag{5.5}$$

where the matrix $\underset{\sim}{B} = \partial\underset{\sim}{H}(G)/\partial\underset{\sim}{G}$ is,

$$(\underset{\sim}{B}) = \begin{Bmatrix} 0 & 0 & -1 & 0 \\ 0 & 0 & 0 & -1 \\ -c_{11} & -c_{12} & 0 & 0 \\ -c_{21} & c_{22} & 0 & 0 \end{Bmatrix}, \tag{5.6}$$

$$c_{11} = \left(\frac{1}{\rho_o}\frac{dP}{d\lambda}\cos^2\theta + \frac{P}{\rho_o\lambda}\sin^2\theta \right),$$

$$c_{22} = \left(\frac{1}{\rho_o}\frac{dP}{d\lambda}\sin^2\theta + \frac{P}{\rho_o\lambda}\cos^2\theta \right),$$

$$c_{12} = c_{21} = \left(\frac{1}{\rho_o}\frac{dP}{d\lambda} - \frac{P}{\rho_o\lambda} \right)\sin\theta\cos\theta .$$

The eigenvalues of $\underset{\sim}{B}$ are $\pm c_L$ and $\pm c_T$ where

$$c_L^2 = \frac{1}{\rho_o}\frac{dP}{d\lambda}, \quad c_T^2 = \frac{P}{\rho_o\lambda} . \tag{5.7}$$

If the adiabatic approximation is adopted P varies with λ only, in regions of the (X,t) plane which are shock free.

System (5.5) is strictly hyperbolic if $c_L^2 > 0$, $c_T^2 > 0$, and $c_L \neq c_T$. If the system is strictly hyperbolic there are four distinct families of characteristics with slopes $\pm c_L$ and $\pm c_T$ in the (X,t) plane,

so that λ and θ are propagated with Lagrangian wave speeds c_L and c_T, respectively, along these characteristics. The terms longitudinal and transverse wave speeds are used to describe c_L and c_T, respectively. For the strain energy functions considered in this study, $c_L^2 > 0$ and $c_T^2 > 0$ for all $\lambda > 1$, however, $c_L = c_T$ for isolated values of $\lambda > 1$.

Relations along the characteristics are obtained from

$$\underset{\sim}{\ell}^T \frac{d\underset{\sim}{G}}{dt} = \underset{\sim}{0} \quad \text{on} \quad \frac{dX}{dt} = \alpha \ ,$$

where $\alpha = \pm c_L, \pm c_T$ and $\underset{\sim}{\ell}$ is the corresponding left eigenvector of $\underset{\sim}{B}$, this gives

$$\frac{d}{dt}(\lambda\cos\theta) - \frac{(c_{11} - \alpha^2)}{c_{21}} \frac{d}{dt}(\lambda\sin\theta) - \frac{1}{\alpha}\frac{du}{dt} + \frac{(c_{11} - \alpha^2)}{\alpha\, c_{12}} \frac{dv}{dt} = 0$$

$$\text{on} \quad \frac{dx}{dt} = \alpha \ ,$$

or

$$c_L \frac{d\lambda}{dt} - \cos\theta \frac{du}{dt} - \sin\theta \frac{dv}{dt} = 0 \quad \text{on} \quad \frac{dX}{dt} = c_L \ ,$$

$$c_L \frac{d\lambda}{dt} + \cos\theta \frac{du}{dt} + \sin\theta \frac{dv}{dt} = 0 \quad \text{on} \quad \frac{dX}{dt} = -c_L \ , \tag{5.8}$$

$$c_T\lambda \frac{d\theta}{dt} + \sin\theta \frac{du}{dt} - \cos\theta \frac{dv}{dt} = 0 \quad \text{on} \quad \frac{dX}{dt} = c_T \ ,$$

$$c_T\lambda \frac{d\theta}{dt} - \sin\theta \frac{du}{dt} + \cos\theta \frac{dv}{dt} = 0 \quad \text{on} \quad \frac{dX}{dt} = -c_T \ .$$

The use of these relations when there is interaction between the c_L and c_T characteristics is almost intractable. Collins (1967) does

present some solutions for the analogous problem of propagation of transverse waves in an incompressible elastic material when there is interaction, however he makes considerable approximations which are not applicable for the string problem.

A further conservation equation, the equation of conservation of energy, can be obtained from (5.2) and (5.3) and the relation (4.38)

$$P(\lambda,S) = \rho_o \frac{\partial U}{\partial \lambda} ,$$

where $U(\lambda,S)$ is the internal energy per unit mass and S is the specific entropy. With the adiabatic approximation this equation becomes,

$$\frac{\partial}{\partial t}\left\{ \rho_o \frac{(u^2 + v^2)}{2} + \rho_o U \right\} - \frac{\partial}{\partial X}\left\{ P(u\cos\theta + v\sin\theta) \right\} = 0 . \qquad (5.9)$$

If we adopt the isentropic approximation, (5.9) is not required.

5.2 Discontinuity Relations

Jump relations for discontinuities are given by Beatty and Haddow (1985). In this section these jump relations are considered in a different way and in more detail. We use the term shock to denote a discontinuity of either λ or θ.

Since system (5.4) is in conservation form the jump relations across a shock are given by,

$$V[\underline{G}] = [\underline{H}] \qquad (5.10)$$

where the square brackets indicate the jump across the shock, of the enclosed quantity, and V is the Lagrangian shock velocity. Two expressions for V^2,

$$V^2 = [c_T^2 \lambda\cos\theta]/[\lambda\cos\theta], \quad V^2 = [c_T^2 \lambda\sin\theta]/[\lambda\sin\theta] ,$$

can be obtained from (5.10). These are compatible if and only if, either

$$\frac{(\lambda\sin\theta)^+}{(\lambda\cos\theta)^+} = \frac{(\lambda\sin\theta)^-}{(\lambda\cos\theta)^-} \quad \text{or} \quad [c_T^2] = 0 , \tag{5.11}$$

where the superscripts + and - indicate values ahead of, and behind the shock, respectively. It may be deduced from (5.11) that, across a shock, there are three possibilities $\theta^+ = \theta^-$ and $[c_T^2] \neq 0$, $\theta^+ = \theta^- \pm \pi$ and $[c_T^2] \neq 0$, $\theta^+ \neq \theta^-$ and $[c_T^2] = 0$. For the present problem, the possibility $\theta^+ = \theta^- \pm \pi$ is not physically admissible so that a discontinuity with both c_T^2 and θ discontinuous is not possible. In general $[c_T^2] = 0$ implies that $[\lambda] = 0$, however, if $c_L(\lambda_c) = c_T(\lambda_c)$ for $\lambda = \lambda_c$, there is a set, Ω, of pairs of values of λ, where

$$\Omega = \{(\lambda',\lambda'') \mid 1 \leq \lambda' < \lambda_c < \lambda'', \; c_T(\lambda') = c_T(\lambda'')\}.$$

If there is a jump in λ and $(\lambda^+,\lambda^-)\in\Omega$, a jump in θ is possible across the jump in λ. Otherwise a jump in θ cannot occur across a jump in λ and vice-versa. If $[c_T^2] \neq 0$, there are two possible shock velocities, V_L and V_T, the velocities of propagation of discontinuities of λ and θ, respectively. It then follows from (5.10) that there are two sets of discontinuity relationships,

$$V_L[\lambda]\cos\theta = -[u] , \qquad V_L[\lambda]\sin\theta = -[v] , \tag{5.12}$$

$$V_L[u] = -[P]\cos\theta/\rho_o , \qquad V_L[v] = -[P]\sin\theta/\rho_o , \tag{5.13}$$

and

$$V_T\lambda[\cos\theta] = -[u] , \qquad V_T\lambda[\sin\theta] = -[v] , \tag{5.14}$$

$$V_T[u] = -P[\cos\theta]/\rho_o , \qquad V_T[v] = -P[\sin\theta]/\rho_o . \tag{5.15}$$

It follows from equations (5.12) and (5.13) that

$$V_L = \pm \left\{ \frac{[P]}{\rho_o[\lambda]} \right\}^{1/2} , \tag{5.16}$$

and from equations (5.14) and (5.15) that

$$V_T = \pm \left\{ \frac{P}{\rho_o \lambda} \right\}^{1/2} . \tag{5.17}$$

Comparison of $(5.7)_2$ and (5.17) shows that $V_T = \pm c_T$ consequently a discontinuity of θ is propagated along a characteristic.

A further jump relation,

$$V \left[\rho_o \frac{(u^2 + v^2)}{2} + \rho_o U \right] = -\left[P(u\cos\theta + v\sin\theta) \right] \tag{5.18}$$

is obtained from (5.9). Since a discontinuity with both λ and θ discontinuous is not possible when $[c_T^2] \neq 0$, and U does not depend explicitly on θ, (5.18) gives

$$V_T \left[\rho_o \frac{(u^2 + v^2)}{2} \right] = -\left[P(u\cos\theta + v\sin\theta) \right] , \tag{5.19}$$

across a jump in θ and with V replaced by V_L holds across a jump in λ. If the isentropic approximation is adopted, and an isothermal stress-stretch relation used, (5.18) with $\rho_o U$ replaced by W is not satisfied across a jump in λ.

When $[c_T^2] = 0$ and $[\lambda] \neq 0$, $[\theta] \neq 0$, then $V_L = V_T = V$ and there is only one set of discontinuity relations,

$$V[\lambda\cos\theta] = -[u] \ , \ V[\lambda\sin\theta] = -[v] \ , \tag{5.20}$$

$$V[u] = -[P\cos\theta]/\rho_o \ , \ V[v] = -[P\sin\theta]/\rho_o \ , \tag{5.21}$$

where $V = \pm \left(\frac{P^+}{\rho_o \lambda^+}\right)^{1/2} = \pm \left(\frac{P^-}{\rho_o \lambda^-}\right)^{1/2}$.

5.3 Exceptional Condition and Genuine Non-Linearity

For the string problem considered in this chapter there are, in general four families of characteristics with slopes $\pm c_L$ and $\pm c_T$. We will describe these families of characteristics as the $c_L^{\pm}$ and $c_T^{\pm}$ characteristic fields, respectively.

According to Jeffrey (1976) a characteristic field is genuinely nonlinear if $\nabla_{\underline{G}} c \cdot \underline{r} \neq 0$, where, for the string problem, $\nabla_{\underline{G}} c$ is the row vector

$$\left\{\frac{\partial c}{\partial(\lambda\cos\theta)} \ , \ \frac{\partial c}{\partial(\lambda\sin\theta)} \ , \ \frac{\partial c}{\partial u} \ , \ \frac{\partial c}{\partial v}\right\} \ ,$$

c is the eigenvalue and $\underline{r}$ is the right eigenvector corresponding to the characteristic field. If $\nabla_{\underline{G}} c \cdot \underline{r} = 0$, the characteristic field is said to be exceptional, that is not genuinely nonlinear.

It can be shown for the string problem that

$$\nabla_{\underline{G}} c_T \cdot \underline{r}_T^+ - \nabla_{\underline{G}} c_T \cdot \underline{r}_T^- = 0,$$

and

$$\nabla_{\underline{G}} c_L \cdot \underline{r}_L^+ \neq 0, \quad -\nabla_{\underline{G}} c_L \cdot \underline{r}_L^- \neq 0,$$

where $\underline{r}_T^{\pm}$ and $\underline{r}_L^{\pm}$ are the right eigenvectors corresponding to $\pm c_T$ and $\pm c_L$ respectively. It follows the $c_L^{\pm}$ are genuinely nonlinear and the $c_T^{\pm}$ characteristic fields are not genuinely nonlinear. This means a discontinuity of θ can propagate along a characteristic and a smooth solution for θ cannot evolve into a discontinuous solution. Also an initial discontinuity of θ propagates as a discontinuity.

5.4 Similarity Solutions

Similarity solutions, valid until the first reflection, can be obtained where the dependent variables are functions of $Z = X/t$. Introducing the independent variable Z into the governing system of partial differential equations in non-conservation form (5.5), a system of ordinary differential equations,

$$(\underline{B} - Z\underline{I}) \frac{d\underline{G}}{dZ} = 0 \tag{5.22}$$

where $\underline{G}$ is given below (5.4) and $\underline{B}$ is given by (5.6), and $\underline{I}$ is the identity matrix, is then obtained. A non trivial solution to system (5.22) exists, if and only if $Z = \pm c_T$ or $Z = \pm c_L$.

Solutions satisfying (5.22) and the jump relations consist of centered simple waves and/or shocks. Since $|V_T| = c_T$ and a discontinuity of θ propagates along a characteristic, it follows from the discussion in section 5.4 that the initial discontinuity of θ at X=0 cannot result in a centered simple wave but propagates as a discontinuity.

5.5 Solutions

First we consider the special case with $\theta = 0$ and $v = 0$, $\forall(X,t)\epsilon\{(X,t):0 \le X \le L,\ t > 0\}$, that is simple tension of a string which occupies the interval [0,L] of the x_1 axis, in the undeformed natural reference state at temperature T_o. It is fixed at $X = L$ and is subjected to an initial tensile force, at $X = 0$ as shown in Figure 5.2 so that the x_1 coordinate of a particle is given by,

$$x_1 = L - \lambda_o(L - X) ,$$

where $\lambda_o \ge 1$. Initial conditions are

$$u(X,0) = 0, \quad \lambda(X,0) = \lambda_o , \tag{5.23}$$

and boundary conditions are

$$P(0,t) = P_f H(t) + P_o H(-t), \quad u(L,t) = 0 , \tag{5.24}$$

where $P_o = \tilde{P}(\lambda_o)$ and $P_f(\lambda_f) \ge 0$, which means the tensile force at $X = 0$ is suddenly changed from P_o to P_f.

Similarity solutions which are valid until the first reflection occurs at $X = L$, are readily obtained.

It follows that the governing system of partial differential equations (5.4) is reduced to a system of two equations,

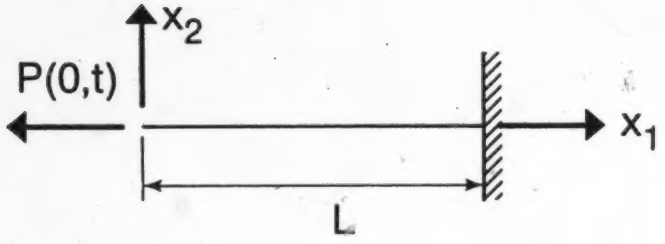

Figure 5.2 Problem geometry of simple tension problem.

$$\frac{\partial \lambda}{\partial t} - \frac{\partial u}{\partial X} = 0,$$

$$\frac{\partial u}{\partial t} - \frac{\partial (P(\lambda)/\rho_o)}{\partial X} = 0 . \tag{5.25}$$

If the system (5.25) is hyperbolic the problem involves the propagation of longitudinal waves only, and there are two distinct families of characteristics with slopes $\pm c_L$ in the (X,t) plane. It then follows from equations (5.8) the relations along the characteristics are

$$u - \int_{\lambda_o}^{\lambda} c_L(\eta)d\eta = \text{const} \quad \text{on } \frac{dX}{dt} = c_L,$$

$$u + \int_{\lambda_o}^{\lambda} c_L(\eta)d\eta = \text{const} \quad \text{on } \frac{dX}{dt} = -c_L. \tag{5.26}$$

Similarity solutions, valid until the first reflection can be obtained as outlined in section 5.4, however for this problem the system of four ordinary differential equations (5.22) has been reduced to a system of two equations, where

$$\underset{\sim}{G} = (\lambda, u)^T ,$$

and

$$\underset{\sim}{B} = \begin{Bmatrix} 0 & -1 \\ \frac{-1}{\rho_o}\frac{\partial P(\lambda)}{\partial \lambda} & 0 \end{Bmatrix} .$$

The jump relations across a longitudinal shock follow from (5.12), (5.13) and (5.18),

$$V_L[\lambda] = -[u] , \qquad V_L[u] = -[P]/\rho_o , \tag{5.27}$$

$$V_L\left[\rho_o \frac{u^2}{2} + \rho_o U \right] = -[Pu] , \tag{5.28}$$

since $\theta = 0$ and $v = 0$.

It is convenient to introduce the following non-dimensionalization scheme, which is adopted in what follows in this chapter,

$$\bar{P} = \frac{P}{3\mu} , \ \bar{\underline{q}} = \frac{\underline{q}}{c_o} , \ \bar{X} = \frac{X}{L} , \ \bar{t} = \frac{c_o t}{L} , \ \bar{U} = \frac{\rho_o U}{3\mu} , \ \bar{W} = \frac{W}{3\mu} , \ \bar{S} = \frac{S}{C} , \tag{5.29}$$

where $\underline{q} = (u, c_L, V_L)^T$, $c_o = c(1) = (3\mu/\rho_o)^{1/2}$ is the wave speed for infinitesimal amplitude longitudinal waves propagating into an undeformed region. Henceforth we use non-dimensional variables given by (5.29) but omit the bars. We now present two solutions for loading of a string and later consider an unloading problem in connection with thermodynamic considerations and also in connection with a reflection problem. Isothermal stress-stretch relations are used for the first two problems and the error involved in using these relations is investigated for the unloading problem.

5.5.1 Mooney-Rivlin String

The non-dimensional longitudinal wave speed obtained from $(5.7)_1$ and the isothermal stress-stretch relation (4.19) is,

$$c_L = \left\{ \frac{1}{3} \left[\alpha \left[1 + \frac{2}{\lambda^3} \right] + 3(1-\alpha)\lambda^{-4} \right] \right\}^{1/2} . \tag{5.30}$$

Also from equation (4.19) it can be shown that $d^2P/d\lambda^2 < 0$ for $0 \le \alpha \le 1$, consequently no shock involving a discontinuity of λ is initiated at $X = 0$, $t = 0$ if $P_f > P_o$ which is the case we now consider.

The solution obtained consists of the solutions in three regions of the (X,t) plane and are bounded by characteristics as shown in Figure 5.3. The solution is valid until the first reflection. Region 1 is the undisturbed region of uniform state ahead of the wave front which propagates with speed $c_L(\lambda_o)$; region 2 represents a centered simple wave, and region 3 is a region of uniform state. The solution satisfying (5.25), the discontinuity relations (5.27) and the initial and boundary data (5.23) and (5.24) is as follows:

$$\begin{aligned}
&\text{Region 1:} \quad \frac{X}{t} \ge c_L(\lambda_o); \\
&\qquad \lambda = \lambda_o, \; u = 0 . \\
&\text{Region 2:} \quad c_L(\lambda_o) \ge \frac{X}{t} \ge c_L(\lambda_f); \\
&\qquad \frac{X}{t} = c_L(\lambda), \quad u = -\int_{\lambda_o}^{\lambda} c_L(\eta)\,d\eta . \\
&\text{Region 3:} \quad c_L(\lambda_f) > \frac{X}{t} \ge 0; \\
&\qquad \lambda = \lambda_f, \quad u = -\int_{\lambda_o}^{\lambda_f} c_L(\lambda)\,d\lambda ,
\end{aligned} \tag{5.31}$$

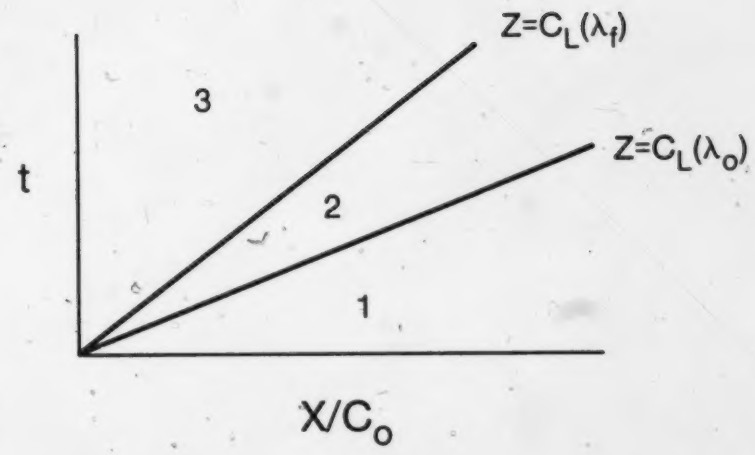

Figure 5.3 Similarity solution for simple tension loading problem when $P_f > P_o$, valid for Mooney-Rivlin strain energy function, and 3 term strain energy function when $\lambda_i > \lambda_f > \lambda_o \geq 1$. The solution is valid for $tc_L(\lambda_o) \leq 1$.

where λ_f is the final stretch obtained from boundary condition $(5.24)_1$ and the constitutive relation (4.19). Equations (5.31) may be obtained from equations (5.5) - (5.9) in Beatty and Haddow (1985) when $\theta = \phi = 0$. The above solution is valid for $tc_L(\lambda_o) \leq 1$.

5.5.2 Three Term Strain Energy Function

The nondimensional longitudinal wave speed obtained from $(5.7)_1$ and the isothermal stress-stretch relation (4.16) is,

$$c_L = \left\{ \sum_{i=1}^{3} \frac{\mu_i}{3\mu} \left[\left(a_i - 1 \right) \lambda^{a_i - 2} + \left(\frac{a_i}{2} + 1 \right) \lambda^{-a_i/2 - 2} \right] \right\}^{1/2}, \tag{5.32}$$

where the a_i and μ_i are given by (4.18).

Solutions for $\lambda_i > \lambda_f > \lambda_o \geq 1$, where λ_i is the stretch at the inflection point as shown in Figure 5.4, are of the same form as those presented for the Mooney-Rivlin string.

The solution in the (X,t) plane is shown in Figure 5.5, for $\lambda_f > \lambda_i$ and $\lambda_T > \lambda_o \geq 1$, where λ_T is the point of tangency of the tangent which passes through λ_f as shown in Figure 5.4. This solution consists of three regions;

Region 1: $\frac{X}{t} \geq c_L(\lambda_o)$;

$$\lambda = \lambda_o \ , \ u = 0. \tag{5.33}$$

Region 2: $c_L(\lambda_o) \geq \frac{X}{t} \geq c_L(\lambda_T)$;

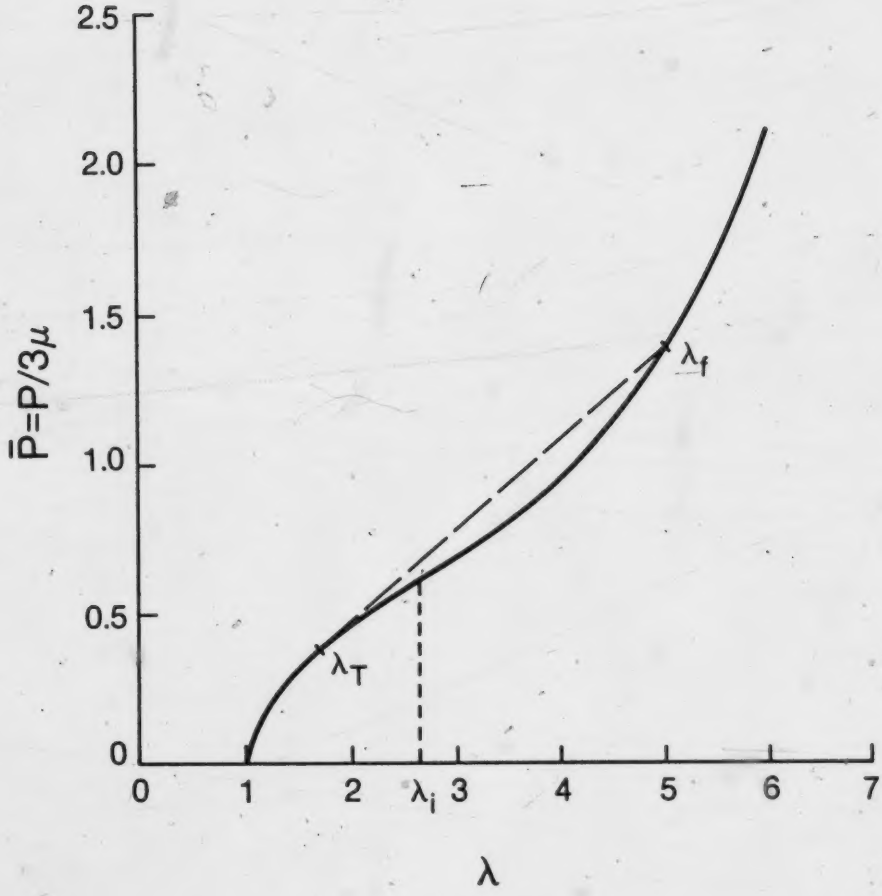

Figure 5.4 Isothermal stress-stretch relation for Ogden's 3 term strain energy function with parameters (4.18).

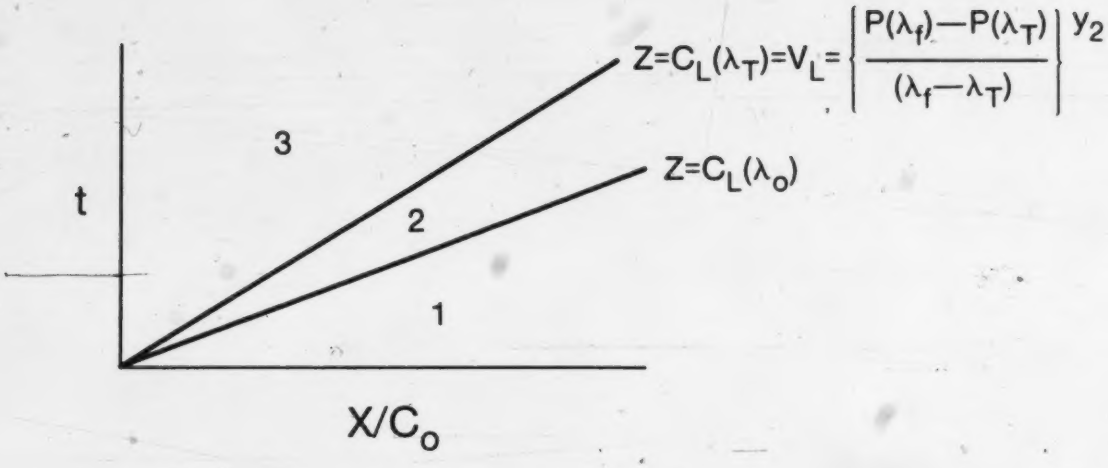

Figure 5.5 Similarity solution for simple tension loading problem when $P_f > P_o$, valid for 3 term strain energy function when $\lambda_f > \lambda_i$ and $\lambda_T > \lambda_o \geq 1$. Solution is valid for $tc_L(\lambda_o) \leq 1$.

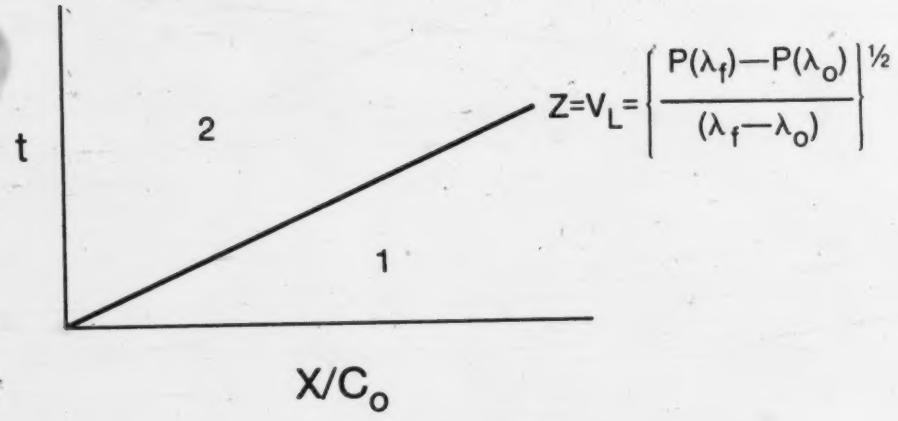

Figure 5.6 Similarity solution for simple tension loading problem when $P_f > P_o$, valid 3 term strain energy function when $\lambda_f > \lambda_i$ and $\lambda_o \geq \lambda_T \geq 1$. Solution is valid for $tV_L \leq 1$.

$$\frac{X}{t} = c_L(\lambda), \quad u = -\int_{\lambda_o}^{\lambda} c_L(\eta)d\eta \ .$$

Region 3: $c_L(\lambda_T) < \frac{X}{t} \geq 0$;

$$\lambda = \lambda_f \ , \quad u = u_f \ .$$

In Figure 5.5, $Z = V_L = c_L(\lambda_T)$ is both a characteristic and a longitudinal shock, where

$$V_L = \left[\frac{(P(\lambda_f) - P(\lambda_T))}{(\lambda_f - \lambda_T)} \right]^{1/2} \ . \tag{5.34}$$

The final stretch λ_f is obtained from boundary condition $(5.24)_1$ and the constitutive relation (4.16). The above solution is valid for $tc_L(\lambda_o) \leq 1$.

A longitudinal shock involving a discontinuity in λ is initiated at $X = 0$, $t = 0$, when $\lambda_f > \lambda_i$ and $\lambda_o \geq \lambda_T \geq 1$. The solution in the (X,t) plane is shown in Figure 5.6, and consists of two regions of constant state separated by the shock $Z = V_L$, where

$$V_L = \left[\frac{(P(\lambda_f) - P(\lambda_o))}{(\lambda_f - \lambda_o)} \right]^{1/2} \ . \tag{5.35}$$

The final stretch λ_f is obtained from boundary condition $(5.24)_1$ and the constitutive relation (4.16), and u_f is obtained from (5.35) and $(5.27)_1$.

The similarity solution is valid for $t\,V_L \le 1$, however the solution after the first reflection can easily be found and is indicated in Figure 5.7. After reflection, there is a reflected shock and the stretch after reflection is λ_3 and $\lambda_3 > \lambda_2 = \lambda_f$. The incident and reflected shock velocities at X = L are denoted by $V_L^{(i)}$ and $V_L^{(r)}$ respectively. It follows from the jump relations (5.27) that,

$$V_L^{(i)} = \left\{ \frac{P(\lambda_1) - P(\lambda_2)}{\lambda_1 - \lambda_2} \right\}^{1/2}, \quad V_L^{(r)} = -\left\{ \frac{P(\lambda_3) - P(\lambda_2)}{\lambda_3 - \lambda_2} \right\}^{1/2}; \tag{5.36}$$

$$u_2 = -V_L^{(i)}(\lambda_2 - \lambda_1) = V_L^{(r)}(\lambda_3 - \lambda_2) \tag{5.37}$$

since $u_1 = u_3 = 0$. Equations $(5.36)_2$ and $(5.27)_2$ give

$$u_2 = \left\{ \frac{P(\lambda_3) - P(\lambda_2)}{\lambda_3 - \lambda_2} \right\}^{1/2} [\lambda_3 - \lambda_2]. \tag{5.38}$$

If λ_1 and λ_2 are known, u_2 is obtained from $(5.36)_1$ and $(5.37)_1$ and λ_3 is obtained numerically from (5.38). The solution obtained is valid for $t \le 1/V_L^{(i)} - 1/V_L^{(r)}$.

An unloading wave occurs when the reflected shock reaches X = 0 at $t = 1/V_L^{(i)} - 1/V_L^{(r)}$, resulting in a centered fan of characteristics.

5.6 Estimate of Validity of the Thermodynamic Approximations

In section 5.5, similarity solutions are obtained using isothermal stress-stretch relations rather than those for adiabatic deformations, also the effect of the jump in entropy across a shock on the

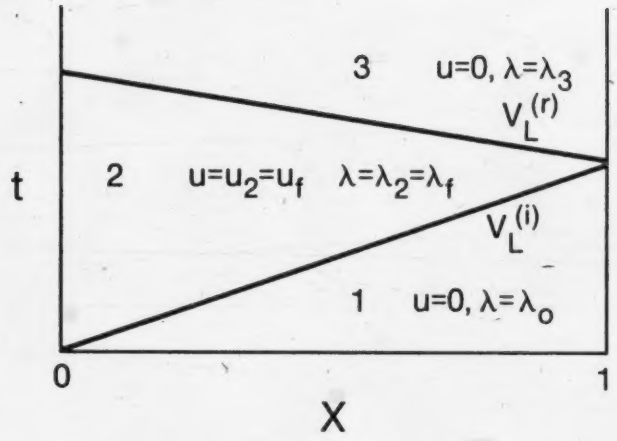

Figure 5.7 Solution with reflection for simple tension loading problem when $P_f > P_o$, valid for 3 term strain energy function when $\lambda_f > \lambda_i$ and $\lambda_o \geq \lambda_T \geq 1$. Solution is valid for $0 \leq t \leq 1/V_L^{(i)} - 1/V_L^{(r)}$.

constitutive relationships is neglected. The errors resulting from these approximations are evaluated for unloading of a Mooney-Rivlin string with $\alpha = 0.6$. The boundary conditions are given by (5.24) with $P_o > P_f$ so that $\lambda_f < \lambda_o$, and results are obtained for $\lambda_o = 1$, $\lambda_f = 3.5$, that is the tension force at $X = 0$ is suddenly removed. The similarity solution, valid until the first reflection, is considered and it is convenient in this discussion to denote the initial and final stretches by λ_1 and λ_2, respectively, rather than λ_o and λ_f, and for other variables the subscripts 1 and 2 denote the initial and final values, respectively. Since $d^2P/d\lambda^2 < 0$, an unloading shock is initiated at $X = 0$, $t = 0$. The entropy jump and corresponding temperature decrease across the shock, are calculated for strictly entropic and piezotropic materials which are the two limiting cases of modified entropic elasticity, as described in Chapter IV.

5.6.1 Strictly Entropic Material

The constitutive relation,

$$P = \frac{1}{3}\left(\alpha + (1 - \alpha)\lambda^{-1}\right)\left(\lambda - \lambda^{-2}\right) \exp\left(S + 3\beta W\right) , \qquad (5.39)$$

for a strictly entropic material is obtained from (4.34) and (4.15), and the internal energy (4.29) is,

$$U(\lambda,S) = \frac{1}{3\beta}\left(\exp(S + 3\beta W) - 1\right) , \qquad (5.40)$$

and $\tilde{U}(1,T_o) = 0$, where T_o is the temperature in the undeformed configuration.

The jump relations across the shock are from (5.27), (5.28),

$$V_L[\lambda] = -[u], \quad V_L[u] = -[P] , \tag{5.41}$$

$$V_L\left[\frac{u^2}{2} + U\right] = -[Pu] . \tag{5.42}$$

We will first assume that the string is stretched isothermally from its undeformed configuration to the initial stretch $\lambda_1 = 3.5$ and then released. Since, for an entropic material, the internal energy can be expressed as a function of temperature alone, it follows that $U_1 = 0$. Also, for an isothermal deformation to an initial stretch λ_1,

$$P_1 = \frac{1}{3}\left\{\alpha + (1-\alpha)\,\bar{\lambda}_1^{1}\,(\lambda_1 - \bar{\lambda}_1^{2})\right\} . \tag{5.43}$$

From jump relations (5.41) and (5.42),

$$V_L(\lambda_1 - 1) = u_2 , \quad U_2 = \frac{-u_2^2}{2} ,$$

since $\lambda_2 = 1$ ($P_2 = 0$), and $u_1 = 0$, so that

$$U_2 = \frac{-V_L^2}{2}\,(\lambda_1 - 1)^2, \tag{5.44}$$

where

$$V_L = \left\{\frac{P_1}{(\lambda_1 - 1)}\right\}^{1/2} . \tag{5.45}$$

The internal energy U_2 is obtained from (5.43), (5.44) and (5.45).

Also, from (5.40),

$$U_2 = \frac{1}{3\beta}\{\exp(S_2 + 3\beta W(\lambda_2)) - 1\},$$

and therefore solving for S_2,

$$S_2 = \ell n(3\beta U_2 + 1). \tag{5.46}$$

Also since $U_1 = 0$,

$$S_1 = -3\beta W(\lambda_1). \tag{5.47}$$

The entropy jump across the shock obtained from (5.46) and (5.47) with $\beta = 10^{-3}$, is $S_2 - S_1 = 7.0597 \times 10^{-4}$.

The temperature T_2, obtained from the relation $T = \partial U/\partial S(\lambda, S)$ and (5.40) is

$$T_2 = T_o \exp(S_2),$$

and therefore the corresponding temperature decrease across the shock is,

$$T_2 - T_o = T_o\{\exp(S_2) - 1\} = -0.894\ ^\circ K,$$

if we take $T_o = 293^\circ K$.

Next, we will assume that the string is stretched adiabatically from its undeformed configuration to the initial stretch $\lambda_1 = 3.5$, and then released. The stress corresponding to the stretch λ_1 is,

$$P_1 = \frac{1}{3}\{\alpha + (1-\alpha)\lambda_1^{-1}\}(\lambda_1 - \lambda_1^{-2})\exp(3\beta\,\bar{W}(\lambda_1)). \tag{5.48}$$

The internal energy at the initial stretch λ_1 is non-zero, and is,

$$U_1 = \frac{1}{3\beta} [\exp (3\beta W(\lambda_1) - 1] \ . \tag{5.49}$$

The jump relations (5.41) and (5.42) are then

$$V_L(\lambda_1 - 1) = u_2 \ , \quad \frac{u_2^2}{2} + U_2 = U_1 . \tag{5.50}$$

The velocity u_2 is obtained from (5.48), (5.45) and $(5.50)_1$, allowing U_2 to be obtained from (5.49) and $(5.50)_2$. The entropy S_2 at the final stretch λ_2 is then obtained from (5.46), and the entropy jump across the shock again obtained for $\beta = 10^{-3}$, is

$$S_2 = \ell n \ (3\beta \ U_2 + 1) = 7.0597 \times 10^{-4} \ ,$$

since $S_1 = 0$.

5.6.2 Piezotropic Material

The internal energy of an incompressible piezotropic material is (4.48),

$$U(\lambda,S) = W(\lambda) + \frac{1}{3\beta} (\exp S - 1) \ , \tag{5.51}$$

where $U(1,T_o) = 0$.

For a piezotropic material, the results are the same regardless if the string is stretched isothermally or adiabatically to the initial stretch λ_1 and then released. At the initial stretch λ_1, $U_1 = W(\lambda_1)$ and from the jump relation $(5.50)_2$,

$$U_2 - U_1 - \frac{u_2^2}{2} = W(\lambda_1) - \frac{u_2^2}{2} ,$$

where u_2^2 is obtained from (5.48), (5.45) and $(5.50)_1$. The internal energy evaluated at the stretch λ_2 is,

$$U_2 = \frac{1}{3\beta} (\exp S_2 - 1) ,$$

since $W(\lambda_2) = 0$. It follows that the entropy jump across the shock is,

$$S_2 = \ell n(3\beta U_2 + 1) = 0.00071 ,$$

for $\beta = 10^{-3}$, since $S_1 = 0$. The corresponding temperature increase is,

$$T - T_o = 0.208218 \ ^\circ K ,$$

if we take $T_o = 293^\circ K$.

It is interesting to note that for the strictly entropic material the temperature decreases upon unloading, while for the piezotropic material the temperature increases upon unloading.

It is evident from the analysis in this section that the thermodynamic effects are small, however it is interesting to consider some further numerical results for the unloading problem just considered. In Table 5.1 the values of $c_L(\lambda_1)$ and $c_L(1)$ are given for the various cases along with the values of $c_L^*(1)$ where $c_L^*(1)$ denotes the wave speed when the entropy jump across the shock is neglected, that is for the isentropic approximation.

Table 5.1 Comparison of wave speeds for strictly entropic and piezotropic cases.

Strictly entropic - isothermal stretch to λ_1

$$c_L(\lambda_1) = 0.4626, \quad c_L(1) = 0.9985, \quad c_L^*(1) = 0.9981$$

Strictly entropic - adiabatic stretch to λ_1

$$c_L(\lambda_1) = 0.4635, \quad c_L(1) = 1.00035, \quad c_L^*(1) = 1.0$$

Piezotropic

$$c_L(\lambda_1) = 0.4604, \quad c_L(1) = 1, \quad c_L^*(1) = 1$$

In Table (5.2) a comparison of some results for the strictly entropic case with adiabatic stretch to λ_1 and for piezotropic case is given.

Table 5.2 Comparison of results for strictly entropic and piezotropic cases. Adiabatic stretch to λ_1.

Strictly Entropic	Piezotropic
$P_1 = 0.8170$	0.8139
$V_L = 0.5717$	0.5706
$u_2 = 1.4291$	1.4264

Use of the piezotropic model is equivalent to considering a purely mechanical theory and using the isothermal stress stretch relation. There is no difficulty in principle in using the adiabatic stress stretch relation along with the isentropic approximation or even with

the adiabatic approximation with the effect on the stress-stretch relation of the entropy jump across the shock taken into account. However the above results indicate the additional complication is not justified for the range of stretch in the problems considered in this thesis. Consequently the results presented henceforth make use of the isothermal stress-stretch relation. Justification for the neglect of heat conduction, that is for the use of the adiabatic approximation, is strictly intuitive, namely that rubberlike materials are relatively poor conductors of heat and the example just considered indicates that temperature gradients are likely to be very small for the problems considered.

5.7 Reflection Problem for Unloaded String

The unloading problem considered in the previous section is extended to consider reflection at $X = L$, however for the reflection problem we take $\lambda_1 > \lambda_2 > 1$, that is the unloading at $X = 0$ is not complete. The solution of this problem is used in the next chapter to interpret certain experimental results and is of the same form as was discussed for the loading problem which is indicated in Figure 5.7. After reflection there is a reflected shock and the stretch after reflection is λ_3 and $\lambda_3 < \lambda_2$. The incident and reflected shock velocities at $X = L$ are denoted by $V_L^{(i)}$ and $V_L^{(r)}$ respectively. A purely mechanical theory is now adopted and it follows from the jump relations (5.39) that,

$$V_L^{(i)} = -\left\{\frac{P(\lambda_1) - P(\lambda_2)}{\lambda_1 - \lambda_2}\right\}^{1/2}, \quad V_L^{(r)} = -\left\{\frac{P(\lambda_3) - P(\lambda_2)}{\lambda_3 - \lambda_2}\right\}^{1/2}, \tag{5.52}$$

$$u_2 = -V_L^{(i)}(\lambda_2 - \lambda_1) - V_L^{(r)}(\lambda_3 - \lambda_2) \tag{5.53}$$

since $u_1 = u_3 = 0$. Equations $(5.50)_2$ and $(5.51)_2$ give

$$u_2 = \left\{\frac{P(\lambda_3) - P(\lambda_2)}{\lambda_3 - \lambda_2}\right\}^{1/2} \left(\lambda_3 - \lambda_2\right) . \tag{5.54}$$

If λ_1 and λ_2 are known, u_2 is obtained from $(5.49)_1$ and $(5.50)_1$ and λ_3 is obtained numerically from (5.51). If the value of λ_3 obtained is less than 1, no longitudinal reflected wave is possible since the string is assumed to be perfectly flexible.

5.8 Application of Godunov's Method

The similarity solutions presented for the simple tension problems are valid until the first reflection occurs at a fixed end. Only for special cases such as the loading and unloading problems discussed in previous sections is it possible to determine exact solutions after the first reflection. In general, the method of characteristics seems to be unattractive after the first reflection consequently it is desirable to investigate other numerical methods. Numerical techniques would also be a useful alternative for problems with boundary conditions that do not give rise to similarity or simple wave solutions.

Godunov's method (Sod, 1985) was developed for problems in gas dynamics. In Godunov's method, the exact solutions to a sequence of

local Riemann problems is used to obtain a first order accurate upwind finite difference method that is monotonicity preserving.

Consider the conservation form (5.25) of the governing partial differential equations, for the simple tension problem, in terms of the non-dimensional quantities defined by (5.29),

$$\frac{\partial \underset{\sim}{G}}{\partial t} + \frac{\partial \underset{\sim}{H}(G)}{\partial X} = 0 \ , \tag{5.55}$$

where $\underset{\sim}{G} = (\lambda, u)^T$, and $\underset{\sim}{H} = -(u, P(\lambda))^T$. In Godunov's method the initial conditions are considered to be piecewise constant functions of X,

$$\underset{\sim}{G}^n(X) = \underset{\sim}{G}_j^n, \quad X \epsilon \ I_j^{1/2} \ , \tag{5.56}$$

where $I_j^{1/2} = [(j - 1/2)\Delta X, (j + 1/2)\Delta X]$. On each interval $I_j = [j\Delta X, (j+1)\Delta X]$, equations (5.55), (5.56) define a sequence of local Riemann problems, and the similarity solution for the Riemann problem on the interval I_j, is denoted by

$$\underset{\sim}{G}_{j+1/2}^n = \underset{\sim}{R}(0, \underset{\sim}{G}_j^n, \underset{\sim}{G}_{j+1}^n) \ , \quad X \epsilon I_j .$$

If the CFL condition, $\nu < 1$ where $\nu = \mu \, \Delta t/\Delta X$ is the Courant number and μ the numerically greatest eigenvalue of $\underset{\sim}{B}$ is satisfied, then the waves generated by the individual Riemann problems will not interact. Because of the nonlinearity, μ changes at each time step; consequently, it is necessary to adjust Δt at each time step.

Solutions are presented for the neo-Hookean strain energy function, and individual Riemann problems are somewhat analogous to the

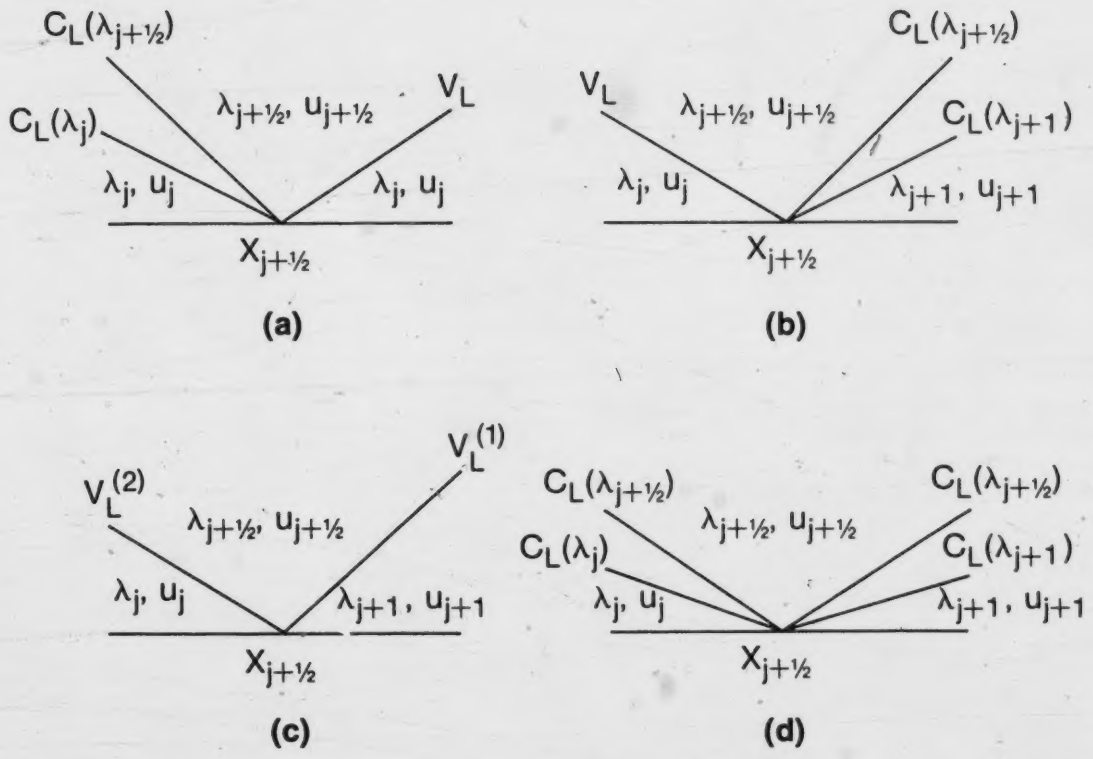

Figure 5.8 The possible similarity solutions for simple tension problem of a neo-Hookean strain energy function string.

shock tube problem described by Whitham (1974). For the problem considered, there are four possible similarity solutions on each interval I_j, as shown in Figure (5.8).

The solution shown in Figure (5.8)a occurs when $\lambda_{j+1}^n > \lambda_j^n$, and consists of a centered fan and shock. The solution $\underset{\sim}{G}_{j+1/2}^n$ is obtained from the following system of non-linear equations,

$$u_{j+1/2} - \int_{\lambda_j^n}^{\lambda_{j+1/2}^n} c_L(\lambda)\, d\lambda + u_j^n = 0 , \tag{5.57}$$

$$V_L\left(\lambda_{j+1/2}^n - \lambda_{j+1}^n\right) - \left(u_{j+1/2}^n - u_{j+1}^n\right) = 0 , \tag{5.58}$$

$$V_L\left(u_{j+1/2}^n - u_{j+1}^n\right) - \left(p_{j+1/2}^n - p_{j+1}^n\right) = 0 , \tag{5.59}$$

where (5.57) applies in the centered fan, and (5.58) and (5.59) are the jump relations across the longitudinal shock, V_L. For the above solution to be admissible, the entropy condition must be satisfied, which requires that

$$c_L\left(\lambda_{j+1/2}^n\right) > V_L > c_L\left(\lambda_{j+1}^n\right) . \tag{5.60}$$

When $\lambda_{j+1}^n < \lambda_j^n$, the mirror image of the above solution occurs, as shown in Figure (5.8)b. When the entropy condition (5.60) fails for solutions shown in Figures (5.8)a or (5.8)b, then one of the remaining two solutions shown in Figures (5.8)c and (5.8)d are possible and $\underset{\sim}{G}_{j+1/2}^n$ is obtained in a similar manner as outlined above.

The solution is advanced to the next time step by,

$$\underset{\sim}{G}_j^{n+1} = \underset{\sim}{G}_j^n - \frac{\Delta t}{\Delta X}\left(\underset{\sim}{H}_{j+1/2}^n - \underset{\sim}{H}_{j-1/2}^n\right), \tag{5.61}$$

where $\underset{\sim}{G}_{j+1/2}^n = \underset{\sim}{R}(0, \underset{\sim}{G}_j^n, \underset{\sim}{G}_{j+1}^n)$ and $\underset{\sim}{H}_{j+1/2}^n = \underset{\sim}{H}(\underset{\sim}{G}_{j+1/2}^n)$.

Results are presented for a neo-Hookean material with initial conditions,

$$\begin{aligned} u(X,0) &= 0, \\ \lambda(X,0) &= 1, \quad -2 \le X \le -0.5 \quad \text{and} \quad 0.5 \le X \le 2, \\ &= (1 + \cos 2\pi X), \quad -0.5 \le X \le 0.5, \end{aligned} \tag{5.62}$$

and the string is fixed at $X = \pm 2$. Initial conditions (5.62) are not physically realistic and are used as a numerical example only. Until the first reflection occurs at the fixed ends, the numerical solution can be compared to D'Alembert's solution of the classical wave equation.

Godunov's method was developed for initial value problems, and to apply the boundary conditions at $X = \pm 2$, the method of images is used.

Numerical results are shown in Figures 5.9 to 5.11. In Figure 5.9, results are shown before the first reflection occurs. The wave separates according to the classical wave equation, however due to the nonlinearity the wave changes shape as it propagates. The wave steepens behind the direction of propagation. Figures 5.10, 5.11 are results for times after the first reflection occurs. The tensile wave reflects as a tensile wave from the fixed ends and propagates towards the centre of the string. Again, the wave is observed to steepen behind the direction of propagation. For the results presented, the scheme was found to be numerically stable when $\nu = 1$.

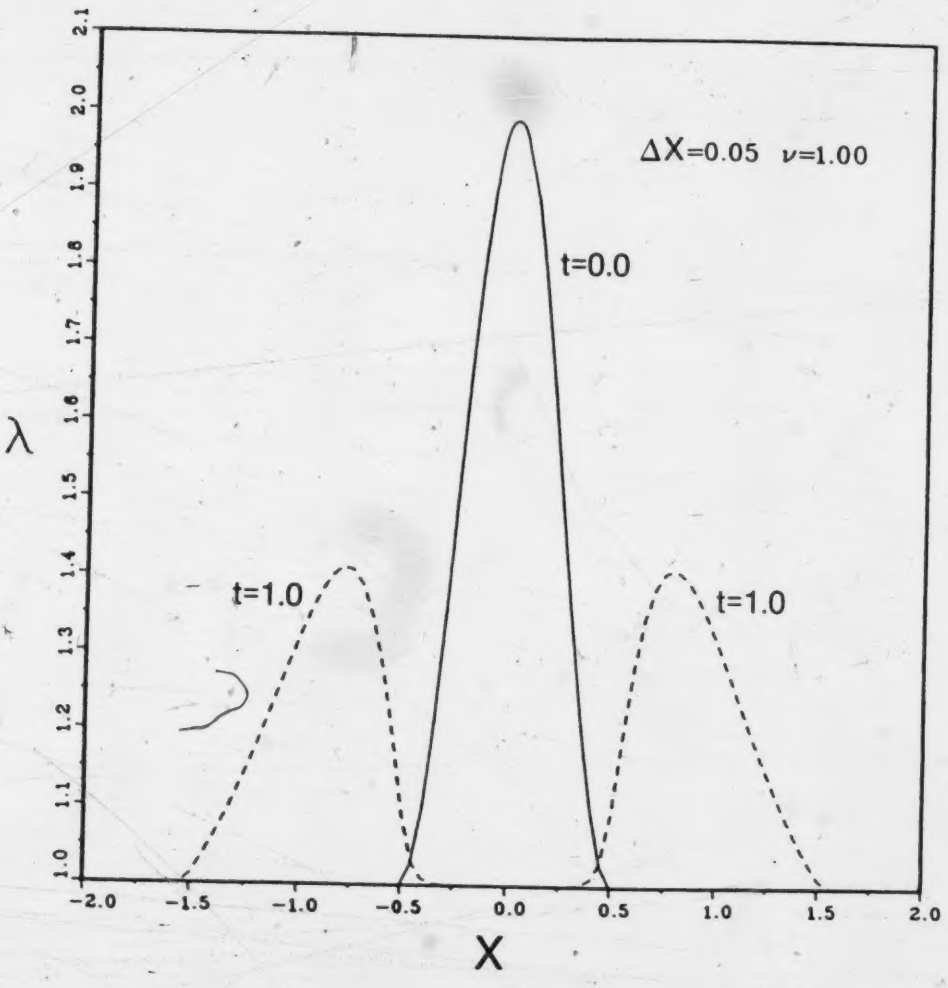

Figure 5.9 Godunov's method applied to the simple tension problem of a neo-Hookean string, with initial conditions $u(X,0) = 0$, $\lambda(X,0) = 1 + \cos 2\pi X$, and boundary conditions $u(-2,t) = u(2,t) = 0$.

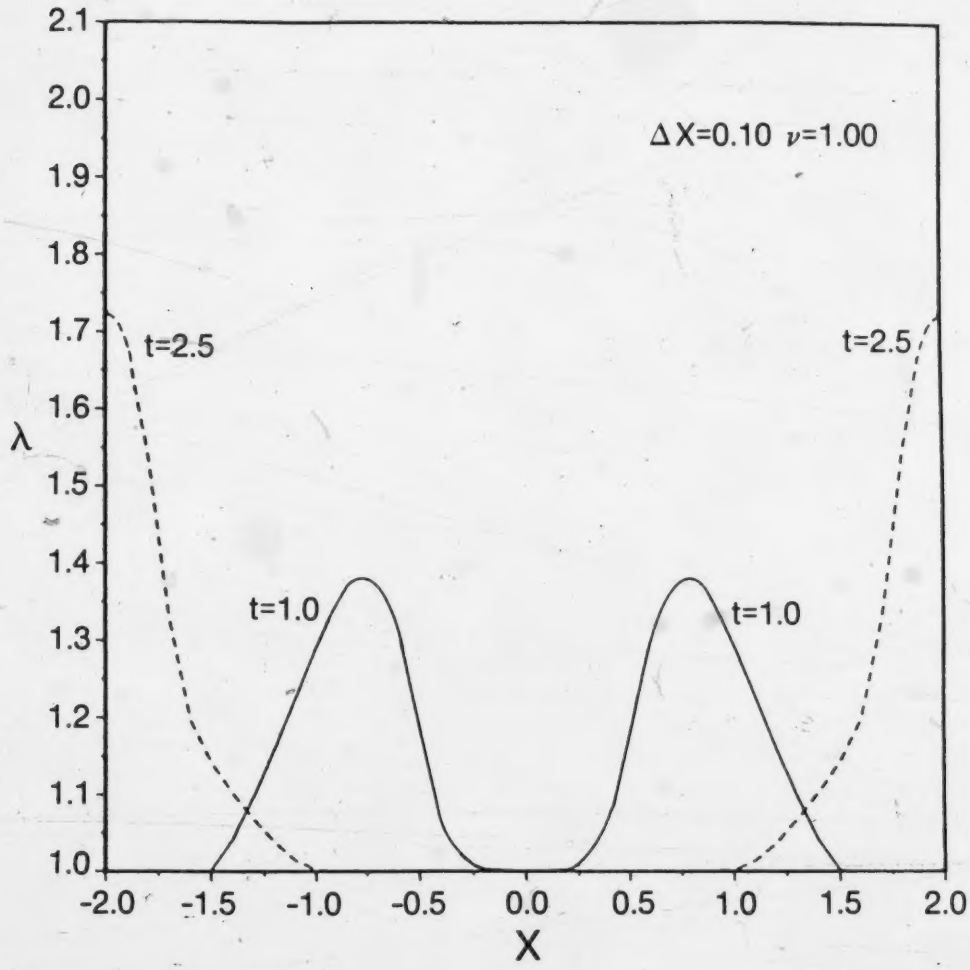

Figure 5.10 Godunov's method applied to simple tension problems of a neo-Hookean string, with initial conditions $u(X,0)=0$, $\lambda(X,0) = 1 + \cos 2\pi X$, and boundary conditions $u(-2,t) = u(2,t) = 0$.

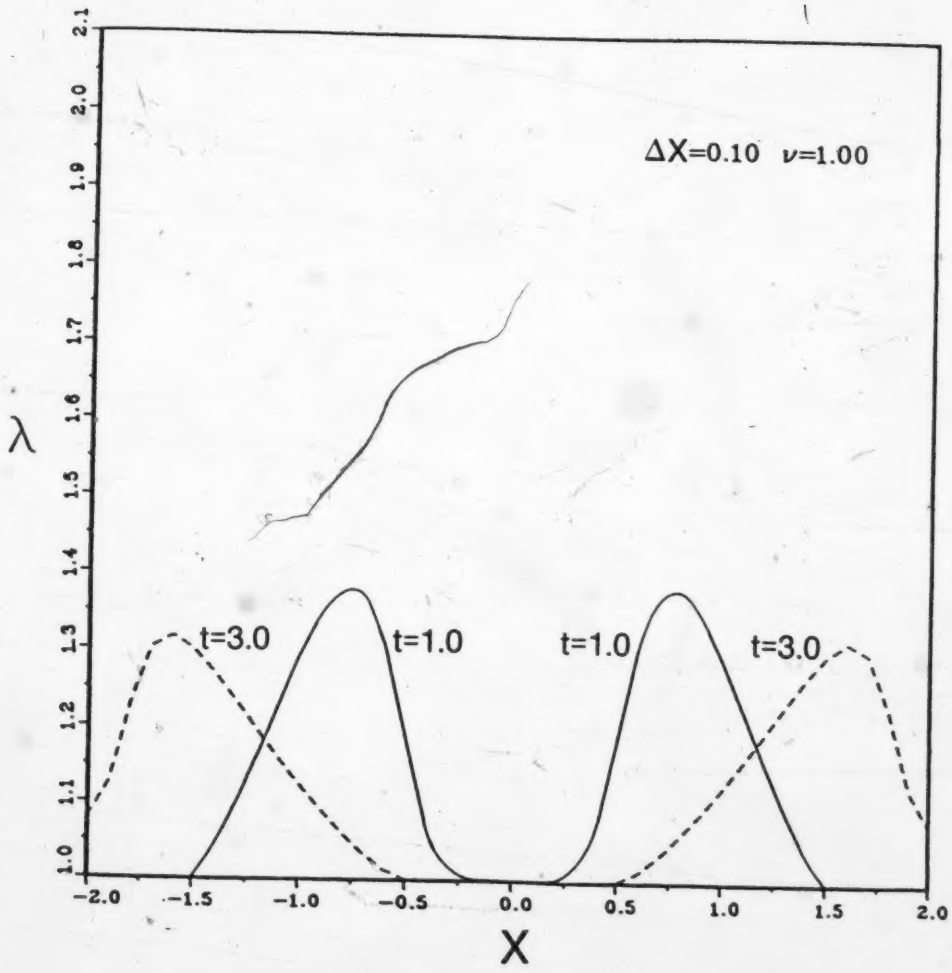

Figure 5.11 Godunov's method applied to simple tension problems of a neo-Hookean string, with initial conditions $u(X,0) = 0$, $\lambda(X,0) = 1 + \cos 2\pi X$, and boundary conditions $u(-2,t) = u(2,t) = 0$.

Chapter VI

Transverse Impact and Plucked String Problems

In this chapter, the governing equations for the finite deformation plane motion of a stretched hyperelastic string which were derived in Chapter V, are used to investigate the wave propagation which results when a prestretched string is suddenly subjected to a transverse impact and when a symmetrically plucked string is suddenly released. Similarity solutions, which are valid until the first reflection occurs at a fixed end, are presented.

The analogies of wave propagation in a stretched hyperelastic string to propagation of transverse waves in an incompressible elastic half-space (Collins, 1966), and to propagation of a line polarized transverse wave in a compressible hyperelastic half space (Davison, 1966), are also discussed.

6.1 Transverse Impact Problem

The problem geometry is shown in Figure 6.1. The string is subjected to an initial stretch $\lambda_o = \ell_o/L \geq 1$, where L is the unstretched natural length, and the ends of the string are fixed at $x_1 = \pm\ell_o$. The initial conditions are $\lambda = \lambda_o$, and $u = v = 0$, and at time $t = 0$ the particle $X = 0$ is given a constant normal velocity in the negative x_2 direction. After impact it is assumed that the subsequent deformed shape of the string is symmetrical about the x_2 axis, consequently only the part $X \epsilon [0,L]$ is considered, and the boundary condition is,

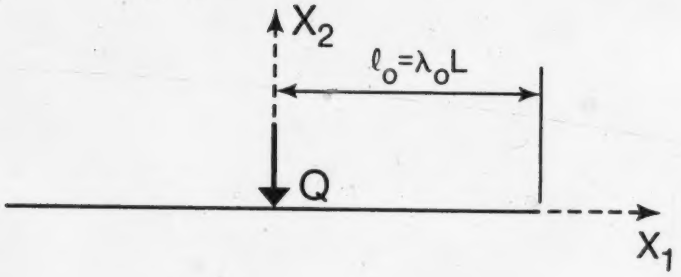

Figure 6.1 Problem geometry of transverse impact problem.

$$u(0,t) = 0, \quad v(0,t) = -QH(t) , \tag{6.1}$$

where Q is constant and H(t) is the unit step function.

Similarity solutions are presented for isothermal stress-stretch relations obtained from the Mooney-Rivlin ($\alpha = 0.6$) and Ogden's 3 term (with parameters given by (4.18)) strain energy functions which were discussed in detail in Chapter IV. The similarity solutions are valid until the first reflection occurs at X = L. In this chapter dimensional variables are used.

6.1.1 Mooney-Rivlin String

The isothermal stress-stretch relation obtained from the Mooney-Rivlin strain energy function is,

$$P = \frac{dW}{d\lambda} = \mu\,(\alpha + (1-\alpha)\lambda^{-1})(\lambda - 1/\lambda^2) , \tag{6.2}$$

and the wave speeds c_L and c_T are,

$$c_L = \left\{\frac{1}{\rho_o}\frac{dP}{d\lambda}\right\}^{1/2} = \left\{\frac{\mu}{\rho_o}\left[\alpha\left(1 + \frac{2}{\lambda^3}\right) + 3(1-\alpha)\lambda^{-4}\right]\right\}^{1/2} , \tag{6.3}$$

$$c_T = |V_T| = \left\{\frac{1}{\rho_o}\frac{P}{\lambda}\right\}^{1/2} = \left\{\frac{\mu}{\rho_o}\left[\alpha + \frac{(1-\alpha)}{\lambda}\right]\left(1 - \frac{1}{\lambda^3}\right)\right\}^{1/2} , \tag{6.4}$$

respectively. For the similarity solutions we note that V_T is positive for propagation in x_1 direction.

Since $|V_T| = c_T$ and a discontinuity of θ propagates along a characteristic it may be deduced that an initial discontinuity of θ at

$X = 0$ cannot result in a centered simple wave but propagates as a discontinuity.

The relation between the non-dimensional nominal stress, $\bar{P} = P/3\mu$, and λ with $\alpha = 0.6$ is shown in Figure 6.2. It follows from (6.3) and (6.4) that $c_L > c_T$ if $\lambda < \lambda c_1$ and $c_L < c_T$ if $\lambda > \lambda c_1$, where $\lambda c_1 = 2.4733$ for $\alpha = 0.6$. When $\lambda = \lambda c_1$, $c_L = c_T$.

First we present a solution which is valid if $\lambda_f < \lambda c_1$, where λ_f is the maximum stretch after impact. This solution is also valid for the neo-Hookean strain energy function, when $\alpha = 1.0$. Referring to the (X,t) plane shown in Figure 6.3a, the similarity solution is:

$$
\begin{aligned}
&\text{Region 1:} \quad X/t \geq c_L(\lambda_o); \\
&\qquad\qquad \lambda = \lambda_o, \ \theta = u = v = 0. \qquad (6.5)\\
&\text{Region 2:} \quad c_L(\lambda_o) \geq X/t \geq (c_L(\lambda_f); \\
&\qquad\qquad X/t = c_L(\lambda), \quad \theta = v = 0, \quad u = -I(\lambda). \\
&\text{Region 3:} \quad c_L(\lambda_f) \geq X/t > c_T(\lambda_f); \\
&\qquad\qquad \lambda = \lambda_f, \quad \theta = v = 0, \quad u = -I(\lambda_f). \\
&\text{Region 4:} \quad c_T(\lambda_f) > X/t \geq 0; \\
&\qquad\qquad \lambda = \lambda_f, \quad \theta = \theta_f, \quad u = 0, \ v = -Q,
\end{aligned}
$$

where

$$
I(\lambda) = \int_{\lambda_o}^{\lambda} c_L(\eta)\,d\eta \ . \qquad (6.6)
$$

The corresponding deformed shape of the string at an arbitrary time t is shown in Figure 6.3b. Equations (6.5) also follow from equations (5.5) - (5.8) in Beatty and Haddow (1985) when $\phi = 90°$.

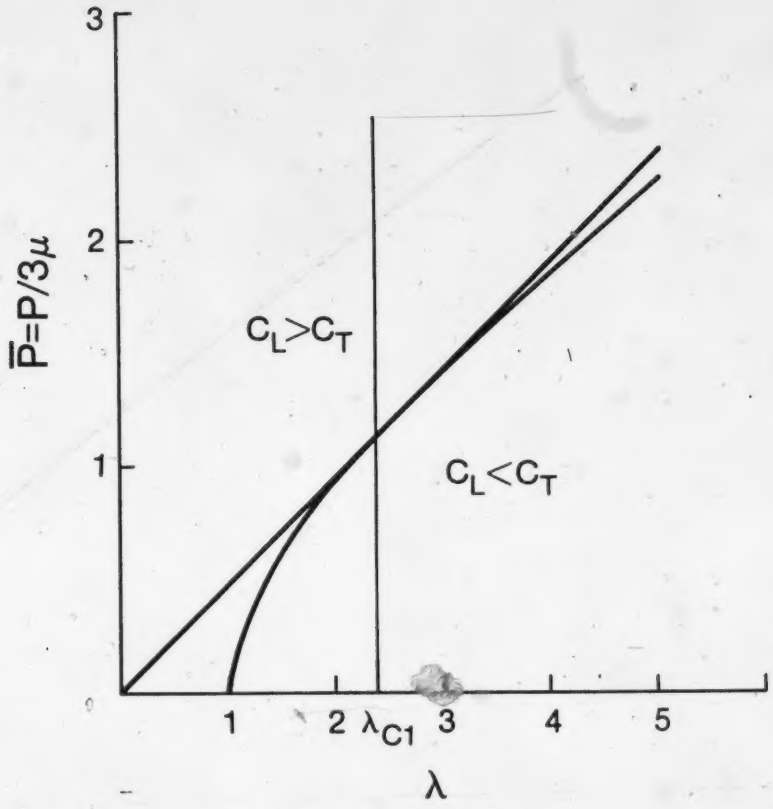

Figure 6.2 Isothermal stress-stretch relation for Mooney-Rivlin material with $\alpha = 0.6$.

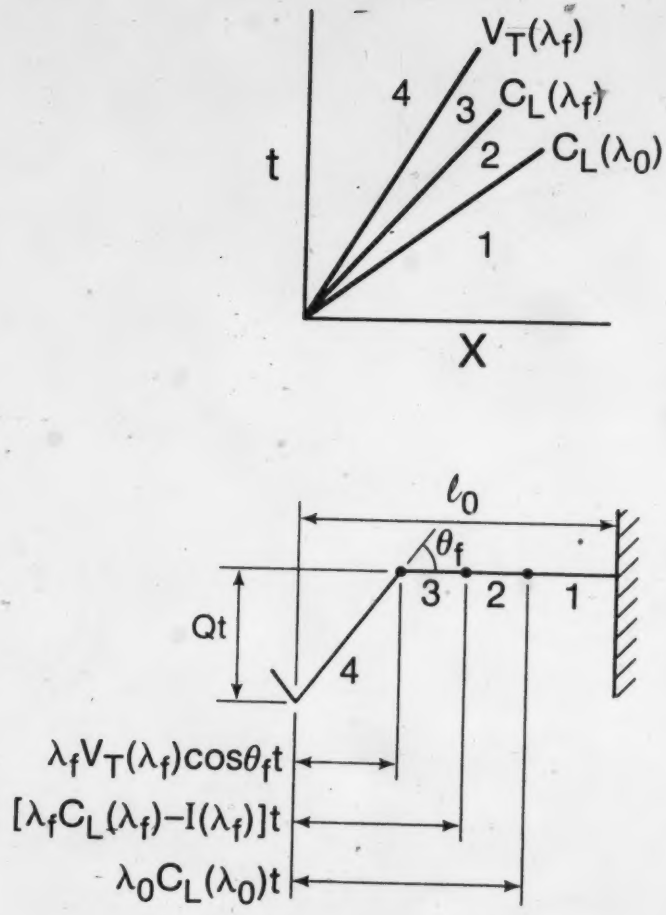

Figure 6.3 Transverse Impact Problem - Solution valid for Mooney-Rivlin string if $\lambda_f < \lambda_{c1}$.

This solution satisfies the system of ordinary differential equations (5.18), the jump relations (5.12), (5.13) and the entropy condition across the shocks. The entropy condition is satisfied if the shock speed is less than or equal to the wave speed behind and greater than or equal to the wave speed ahead of the shock. It should be noted that the jump in entropy across a transverse shock is zero and the transverse wave speeds behind and ahead of the shock are equal to the shock speed. It may be deduced from the jump relations (5.12) and (5.13) that,

$$Q^2 = I(\lambda_f)\{2\lambda_f c_T(\lambda_f) - I(\lambda_f)\}, \quad \sin\theta_f = Q/(\lambda_f V_T(\lambda_f)) , \tag{6.7}$$

and it follows that $\lambda_f < \lambda c_1$ if

$$Q^2 < I(\lambda_{c1})\{2\lambda_{c1} c_T(\lambda_{c1}) - I(\lambda_{c1})\} . \tag{6.8}$$

Equation (6.7) is equivalent to equation (5.12) in Beatty and Haddow (1985) when $\phi = \pi/2$. If λ_o and Q are given, λ_f and θ_f can be obtained from (6.7) and the solution completed. The region of validity obtained from (6.8) in the (Q,λ_o) plane is shown in Figure 6.4.

The solution valid if $\lambda_o < \lambda c_1$ and $\lambda_f > \lambda c_1$, is indicated in Figure 6.5, and consists of the following regions:

Region 1: $X/t \geq c_L(\lambda_o)$;

$\lambda = \lambda_o, \quad \theta = u = v = 0.$

Region 2: $c_L(\lambda_o) \geq X/t > c_L(\lambda_{c1}) = V_T(\lambda_{c1})$

$X/t = c_L(\lambda), \quad \theta = v = 0, \quad u = -I(\lambda).$

Region 3: $V_T(\lambda_{c1}) = c_L(\lambda_{c1}) > X/t \geq c_L(\lambda_f)$; (6.9)

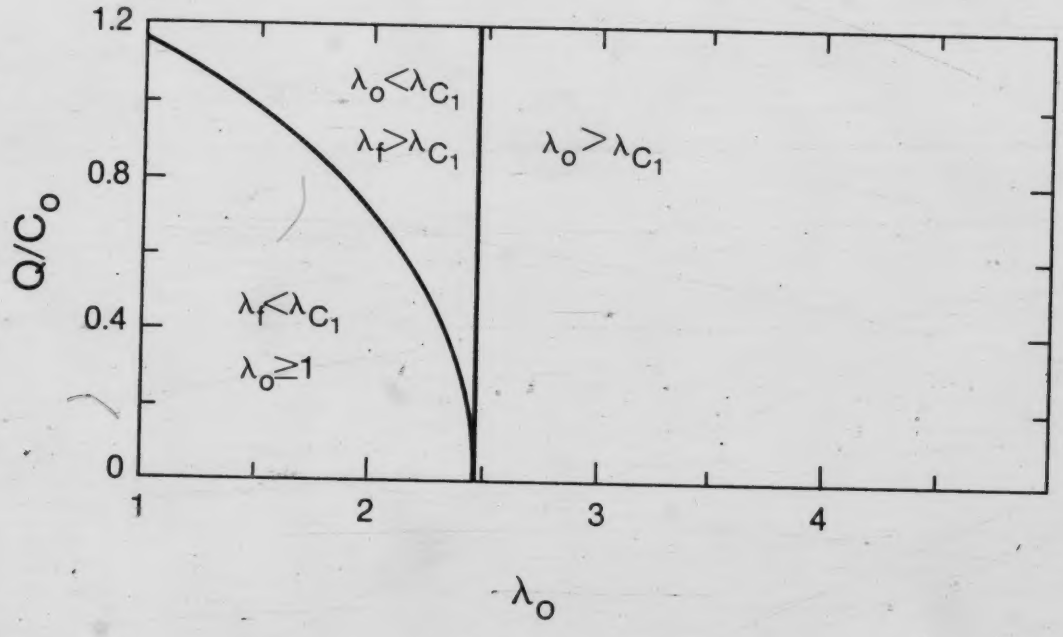

Figure 6.4 Transverse Impact Problem - Region of validity in (Q, λ_o) plane for solution of a Mooney-Rivlin string valid if $\lambda_f < \lambda_{c1}$.

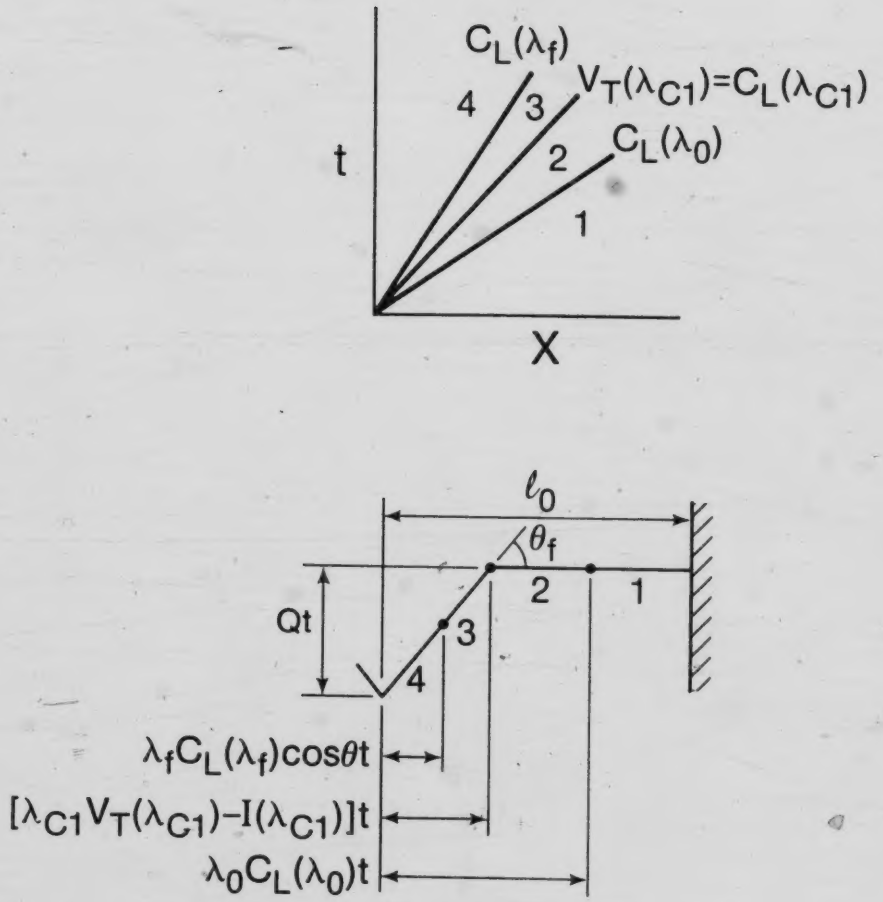

Figure 5.5 Transverse Impact Problem - Solution valid for Mooney-Rivlin string if $\lambda_o < \lambda_{c1}$ and $\lambda_f > \lambda_{c1}$.

$$X/t = c_L(\lambda), \quad \theta = \theta_f, \quad u = u_3^- - \int_{\lambda_{c1}}^{\lambda} c(\eta)d\eta \cos\theta_f,$$

$$v = v_3^- - \int_{\lambda_{c1}}^{\lambda} c(\eta)\, d\eta \sin\theta_f.$$

Region 4: $c_L(\lambda_f) \geq X/t \geq 0;$

$$\lambda = \lambda_f, \quad \theta = \theta_f, \quad u = 0, \quad v = -Q,$$

where the superscript - indicates values just behind $X = V_T(\lambda_{c1})t$, the subscript 3 refers to the corresponding region indicated in Figure 6.5, and,

$$u_3^- = \int_{\lambda_{c1}}^{\lambda_f} c_L(\eta)\, d\eta \cos\theta_f, \tag{6.10}$$

$$v_3^- = -Q + \int_{\lambda_{c1}}^{\lambda_f} c_L(\eta)\, d\eta \sin\theta_f. \tag{6.11}$$

Equations (6.9) are equivalent to equations (5.20) - (5.23) in Beatty and Haddow (1985) when $\phi = \pi/2$. It may be deduced from the jump relations across the shock that,

$$u_3^- = -V_T(\lambda_{c1})\lambda_{c1}(\cos\theta_f - 1) - I(\lambda_{c1}), \tag{6.12}$$

$$v_3^- = -V_T(\lambda_{c1})\lambda_{c1}\sin\theta_f. \tag{6.13}$$

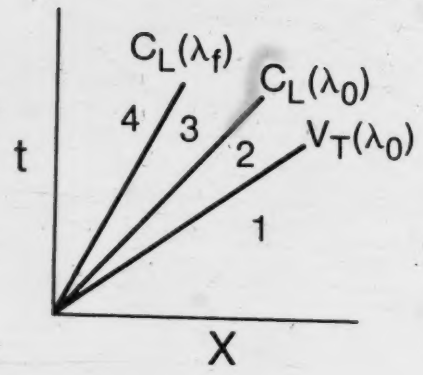

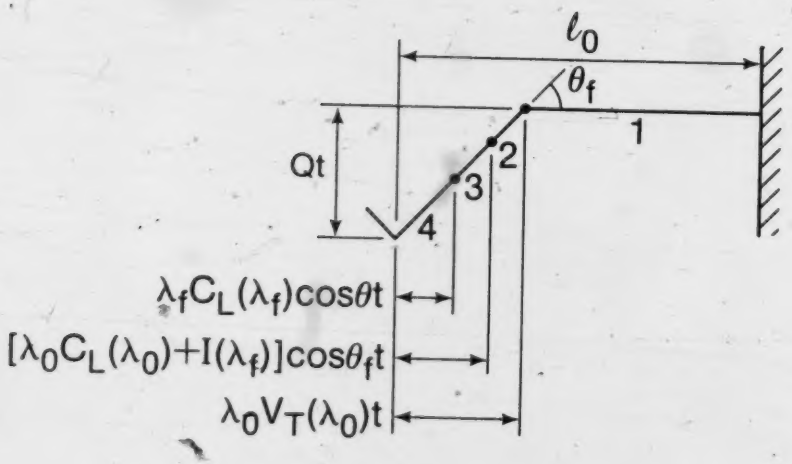

Figure 6.6 Transverse Impact Problem - Solution valid for Mooney-Rivlin string if $\lambda_o > \lambda_{cl}$.

If λ_o and Q are given, the unknowns can be obtained from equations (6.10) - (6.13).

The solutions for $\lambda_o > \lambda_{c1}$ is indicated in Figure 6.6, and consists of the following regions:

Region 1: $X/t > V_T(\lambda_o)$;

$\lambda = \lambda_o, \quad \theta = u = v = 0.$

Region 2: $V_T(\lambda_o) > X/t \geq c_L(\lambda_o)$;

$\lambda = \lambda_o$, $u = u_2$, $v = v_2$. (6.14)

Region 3: $c_L(\lambda_o) \geq X/t \geq c_L(\lambda_f)$;

$X/t = c_L(\lambda)$, $\theta = \theta_f$, $u = u_2 - I(\lambda) \cos\theta_f$,

$v = v_2 - I(\lambda) \sin\theta_f$.

Region 4: $c_L(\lambda_f) \geq X/t \geq 0$;

$\lambda = \lambda_f, \quad \theta = \theta_f, \; u = 0, \; v = -Q,$

where

$$u_2 = I(\lambda_f) \cos\theta_f, \tag{6.15}$$

$$v_2 = -Q + I(\lambda_f) \sin\theta_f. \tag{6.16}$$

It may be deduced from the jump relations across the shock that

$$u_2 = -\lambda_o V_T(\lambda_o)(\cos\theta_f - 1), \tag{6.17}$$

$$v_2 = -\lambda_o V_T(\lambda_o) \sin\theta_f. \tag{6.18}$$

If λ_o and Q are given, the unknowns can be obtained from equations (6.15) - (6.18).

6.1.2 Three Term S.E.F. String

Isothermal stress-stretch relation obtained from Ogden's 3 term strain energy function is

$$P = \frac{dW}{d\lambda} = \sum_{i=1}^{3} \mu_i \left(\lambda^{a_i - 1} - \lambda^{a_i/2 - 1} \right) ,$$

and the wave speeds c_L and c_T are,

$$c_L = \left\{ \frac{1}{\rho_o} \frac{dP}{d\lambda} \right\}^{1/2} = \left\{ \sum_{i=1}^{3} \frac{\mu_i}{\rho_o} \left[(a_i - 1)\lambda^{a_i - 2} + \left(\frac{a_i}{2} + 1 \right) \lambda^{-a_i/2 - 2} \right] \right\}^{1/2} , \quad (6.19)$$

$$c_T = |V_T| = \left\{ \frac{P}{\rho_o \lambda} \right\}^{1/2} = \left\{ \sum_{i=1}^{3} \frac{\mu_1}{\rho_o} \left[\lambda^{a_i - 2} - \lambda^{-a_i/2 - 2} \right] \right\}^{1/2} . \quad (6.20)$$

and the a_i and μ_i are given by (4.18), for the discussion which follows.

The relation between the non-dimensional nominal stress $\bar{P} = P/3\mu$ with λ is shown in Figure 6.7. It follows from (6.19) and (6.20) that $c_L > c_T$ if $\lambda < \lambda_{c1}$ or $\lambda > \lambda_{c2}$ and $c_L < c_T$ if $\lambda_{c1} < \lambda < \lambda_{c2}$ where $\lambda_{c1} = 2.1674$ and $\lambda_{c2} = 3.1674$. When $\lambda = \lambda_{c1}$ or $\lambda = \lambda_{c2}$, $c_L = c_T$.

We outline the possible solutions when the initial stretch λ_o is in each region (a) - (d), which are indicated in Figure 6.8.

First we present in detail the solution when λ_o is in region (d), that is $\lambda_o \geq \lambda_{c2}$. Solutions for the other cases are then indicated in the (X,t) plane. Referring to the (X,t) plane shown in Figure 6.9, the similarity solution is:

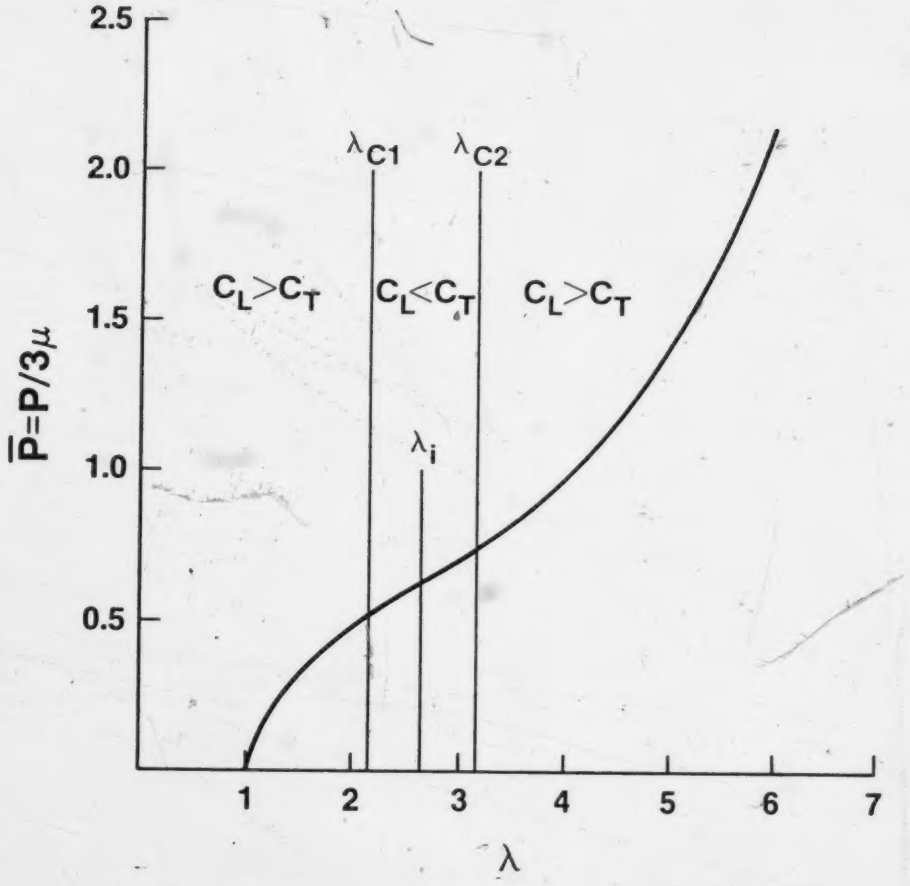

Figure 6.7 Isothermal stress-stretch relation for 3 term strain energy function with parameters (4.18).

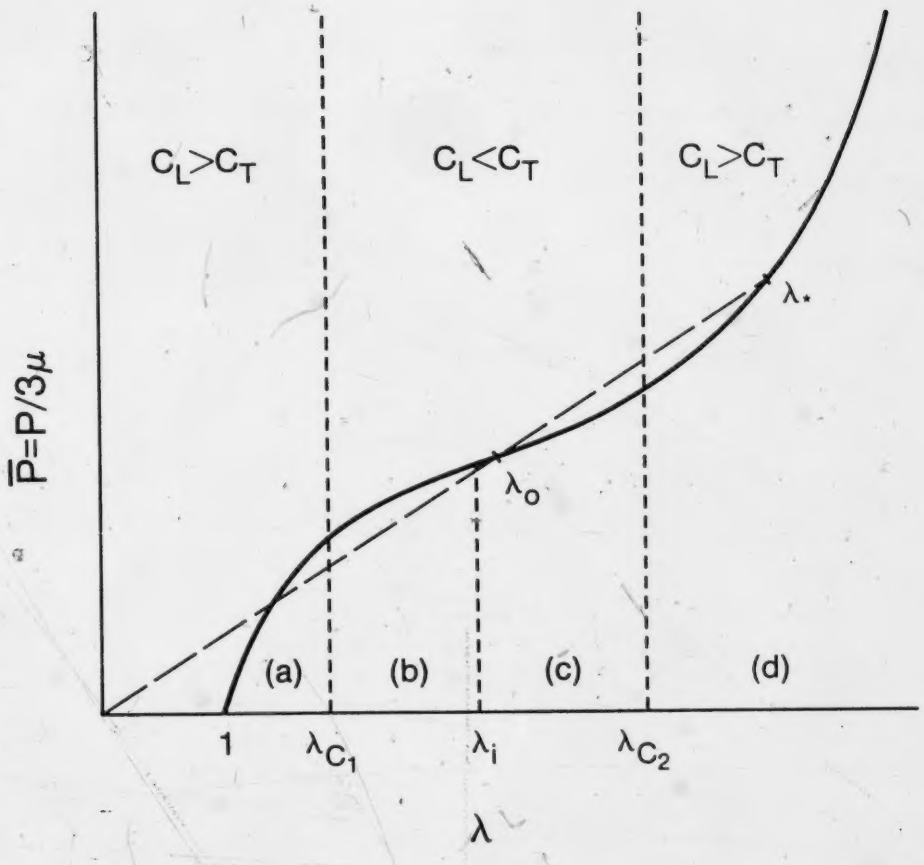

Figure 6.8 Isothermal stress-stretch relation (schematic) for 3 term strain energy function showing λ_o in region (c), that is $\lambda_i < \lambda_o < \lambda_{c2}$, and $V_T(\lambda_o) = V_T(\lambda_*)$.

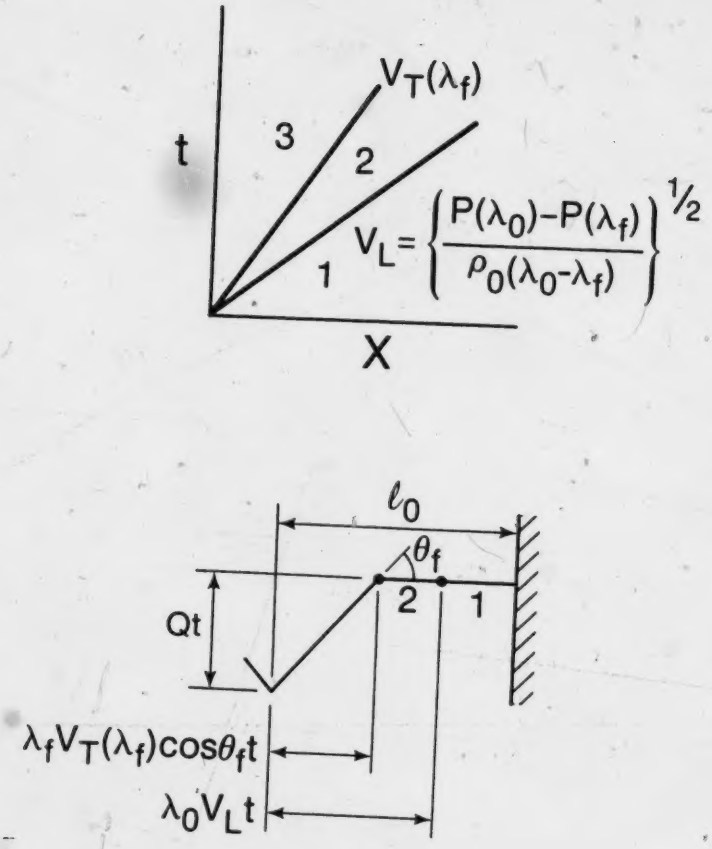

Figure 6.9 Transverse Impact Problem - Solution valid for 3 term Ogden string when $\lambda_o \geq \lambda_{c2}$.

Region 1: $X/t > V_L$;

$\lambda = \lambda_o, \quad \theta = u = v = 0.$

Region 2: $V_L > X/t > V_T(\lambda_f)$; (6.21)

$\lambda = \lambda_f, \quad \theta = 0, \quad u = u_2, \quad v = 0 .$

Region 3: $V_T(\lambda_f) > X/t \geq 0$;

$\lambda = \lambda_f \quad \theta = \theta_f, \quad u = 0, \quad v = -Q,$

where the subscript 2 refers to the corresponding region indicated in Figure 6.9, and

$$V_L = \left\{ \frac{P(\lambda_f) - P(\lambda_o)}{\rho_o(\lambda_f - \lambda_o)} \right\}^{1/2} . \tag{6.22}$$

Equation (6.22) is the same as equation (5.25) in Beatty and Haddow (1985) when $\phi = \pi/2$. It may be deduced from the jump relations across the shocks that

$$u_2 = -V_L(\lambda_f - \lambda_o) , \tag{6.23}$$

$$u_2 = \lambda_f V_T(\lambda_f)(\cos\theta_f - 1) , \tag{6.24}$$

$$\sin\theta_f = Q/(\lambda_f V_T(\lambda_f)) . \tag{6.25}$$

If λ_o and Q are given, the unknowns can be obtained from (6.22) - (6.25).

When λ_o is in region (c), that is $\lambda_i < \lambda_o < \lambda_{c2}$, where λ_i is the stretch at the inflection point as indicated in Figure 6.7, there are two possible solutions. If $\lambda_f > \lambda_*$, where $V_T(\lambda_*) = V_T(\lambda_o)$ as indicated in Figure 6.8, then $V_L > V_T$ and the solution is the same as that for

$\lambda_o \geq \lambda_{c2}$. If $\lambda_f < \lambda_*$, then $V_T > V_L$ and the solution is indicated in Figure 6.10.

Next consider the solutions when λ_o is in region (b), that is $\lambda_{c1} < \lambda_o < \lambda_i$. When $\lambda_f < \lambda_i$ the solution is of the same form as the Mooney-Rivlin s.e.f string when $\lambda_o > \lambda_{c1}$. When $\lambda_f > \lambda_*$, where $V_T(\lambda_*) = V_T(\lambda_o)$ as shown in Figure 6.11, the solution is as indicated in Figure 6.9. When $\lambda_i < \lambda_f < \lambda_*$, there are two possible solutions. The first solution occurs when $\lambda_{c1} < \lambda_o < \lambda_T$ where λ_T is the point of tangency of the tangent which passes through λ_f as shown in Figure 6.12, and

$$c_L(\lambda_T) = \left\{ \frac{P(\lambda_f) - P(\lambda_T)}{\rho_o(\lambda_f - \lambda_T)} \right\}^{1/2} = \left\{ \frac{1}{\rho_o} \frac{\partial P}{\partial \lambda} \right\}^{1/2}_{\lambda = \lambda_T} \tag{6.26}$$

The solution is indicated in Figure 6.13. The second solution occurs when $\lambda_o > \lambda_T$ and is indicated in Figure 6.10.

When $1 < \lambda_o < \lambda_{c1}$, shown as Region (a) in Figure 6.14, and $\lambda_f < \lambda_i$, the solutions are of the same form as those presented for the Mooney-Rivlin s.e.f. string. When $\lambda_i < \lambda_f < \lambda_{**}$, where $V_T(\lambda_{**}) = V_T(\lambda_{c1})$ as shown in Figure 6.14, the solution is as indicated in Figure 6.15, where λ_T is the point of tangency of the tangent which passes through λ_f as shown in Figure 6.14. When $\lambda_f > \lambda_{**}$, there are two possible solutions. The solution when $\lambda_o > \lambda_T$, where λ_T is the point of tangency of the tangent which passes through λ_f as shown in Figure 6.16, is indicated in Figure 6.9. The solution when $\lambda_o < \lambda_T$ consists of constant state regions 1, 3 and 4 and a centered simple wave region 2 as indicated in Figure 6.17. A longitudinal shock

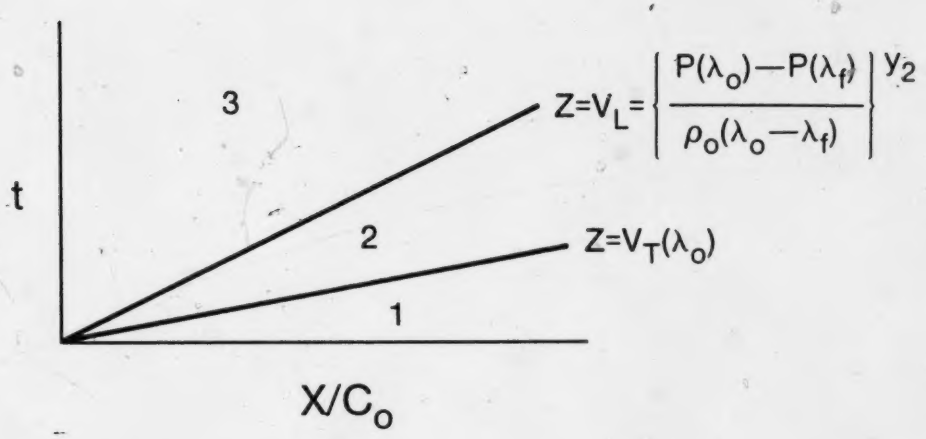

Figure 6.10 Transverse Impact Problem - Solution valid for 3 term Ogden string when $\lambda_i < \lambda_o < \lambda_{c2}$ and $\lambda_f < \lambda_*$.

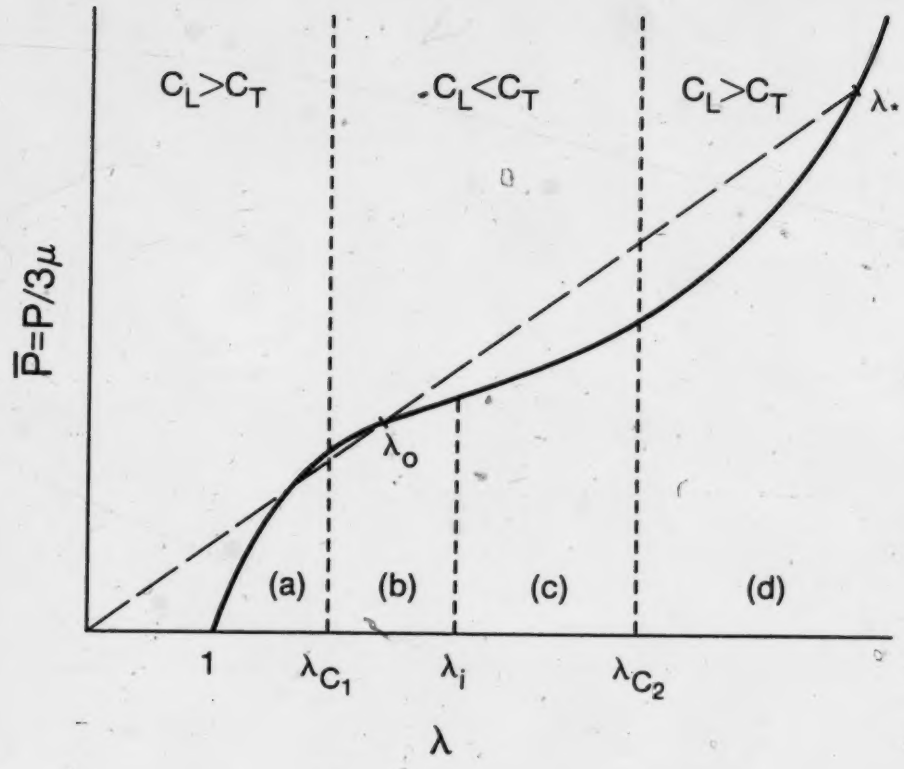

Figure 6.11 Isothermal stress-stretch relation (schematic) for 3 term strain energy function. showing λ_o in region (b), that is $\lambda_{c1} < \lambda_o < \lambda_i$, and $V_T(\lambda_o) = V_T(\lambda_*)$.

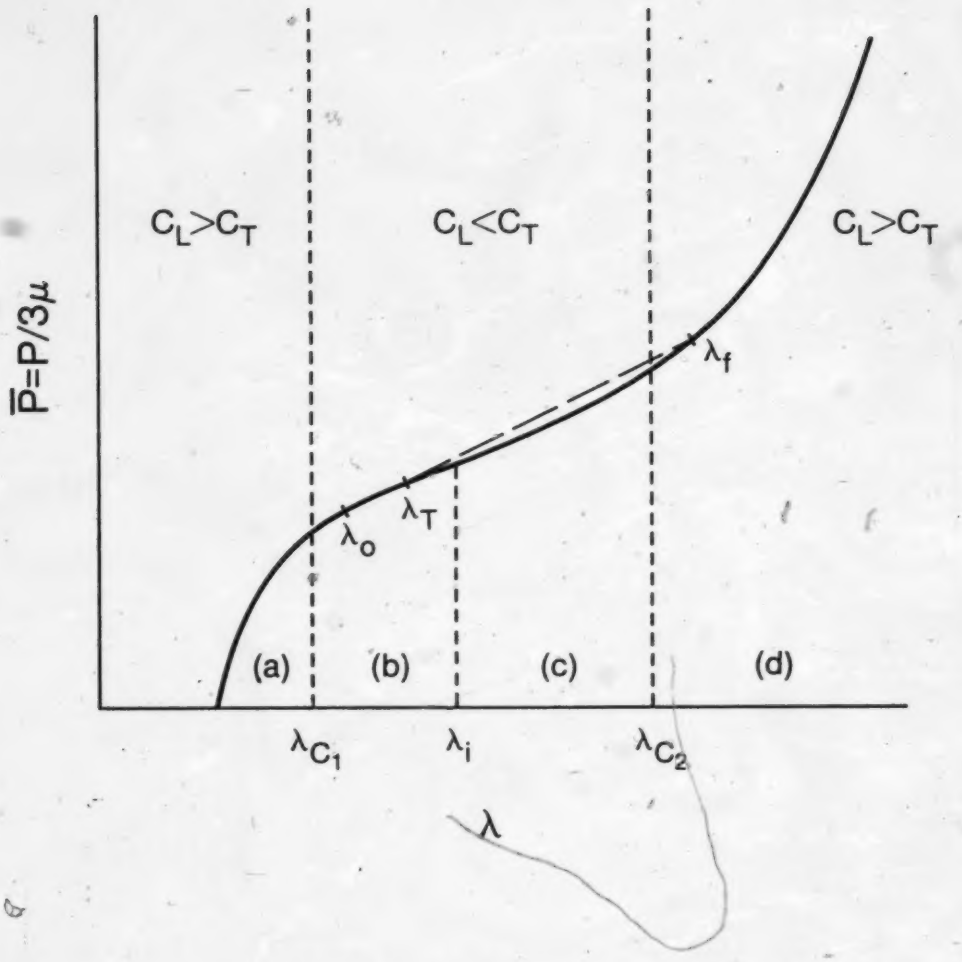

Figure 6.12 Isothermal stress-stretch relation (schematic) for 3 term strain energy function showing λ_o in region (b), that is $\lambda_{c1} < \lambda_o < \lambda_i$, and $\lambda_f < \lambda_*$.

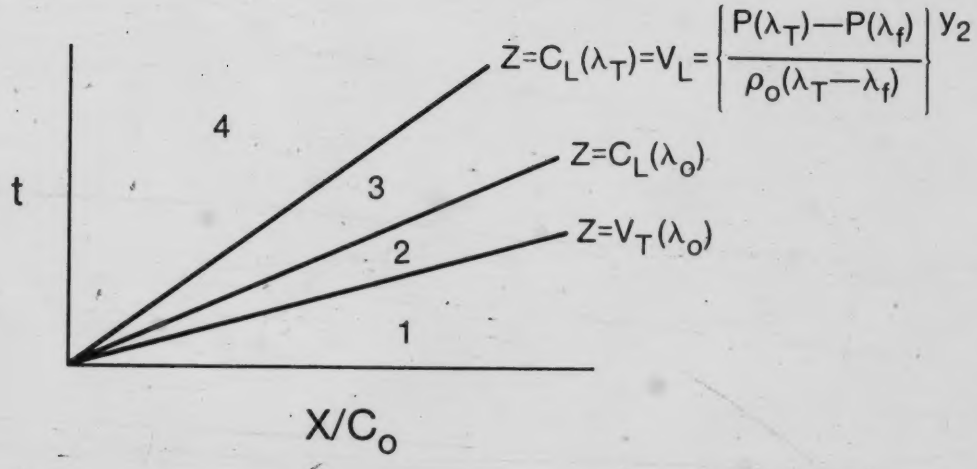

Figure 6.13 Transverse Impact Problem - Solution valid for 3 term Ogden string when $\lambda_{c1} < \lambda_o < \lambda_T$ and $\lambda_f < \lambda_*$.

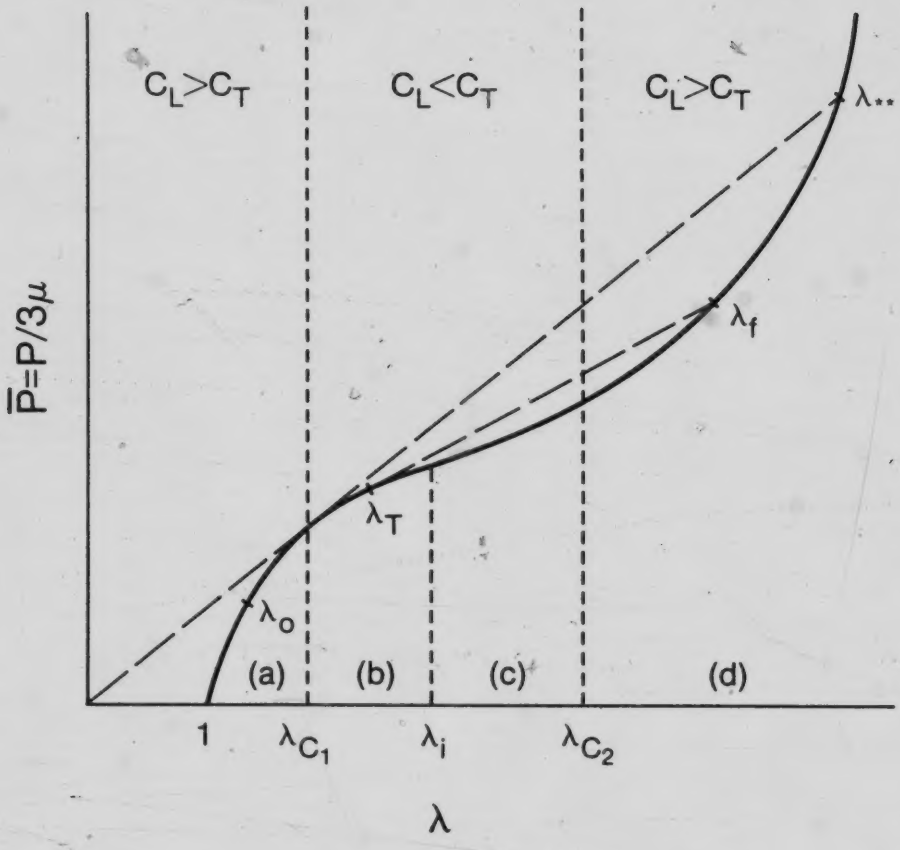

Figure 6.14 Isothermal stress-stretch relation (schematic) for 3 term strain energy function showing λ_o in region (a), that is $1 < \lambda_o < \lambda_{c1}$, and $V_T(\lambda_{c1}) = V_T(\lambda_{**})$.

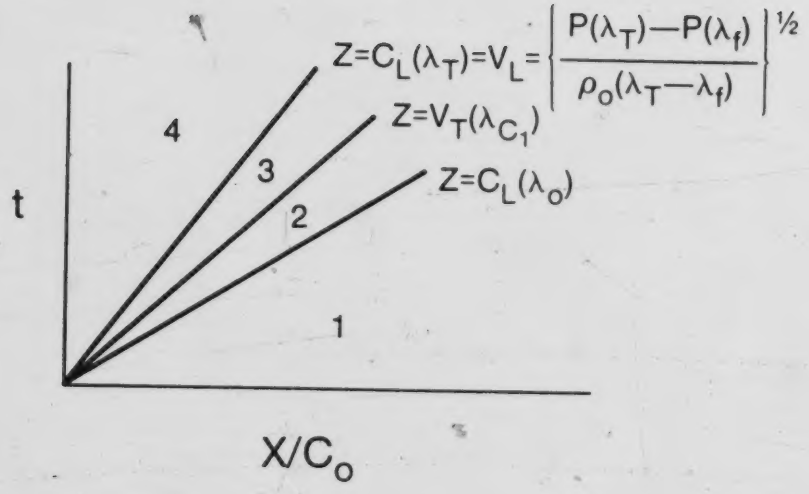

Figure 6.15 Transverse Impact Problem - Solution valid for 3 term Ogden string when $1 < \lambda_o < \lambda_{cl}$ and $\lambda_i < \lambda_f < \lambda_{**}$.

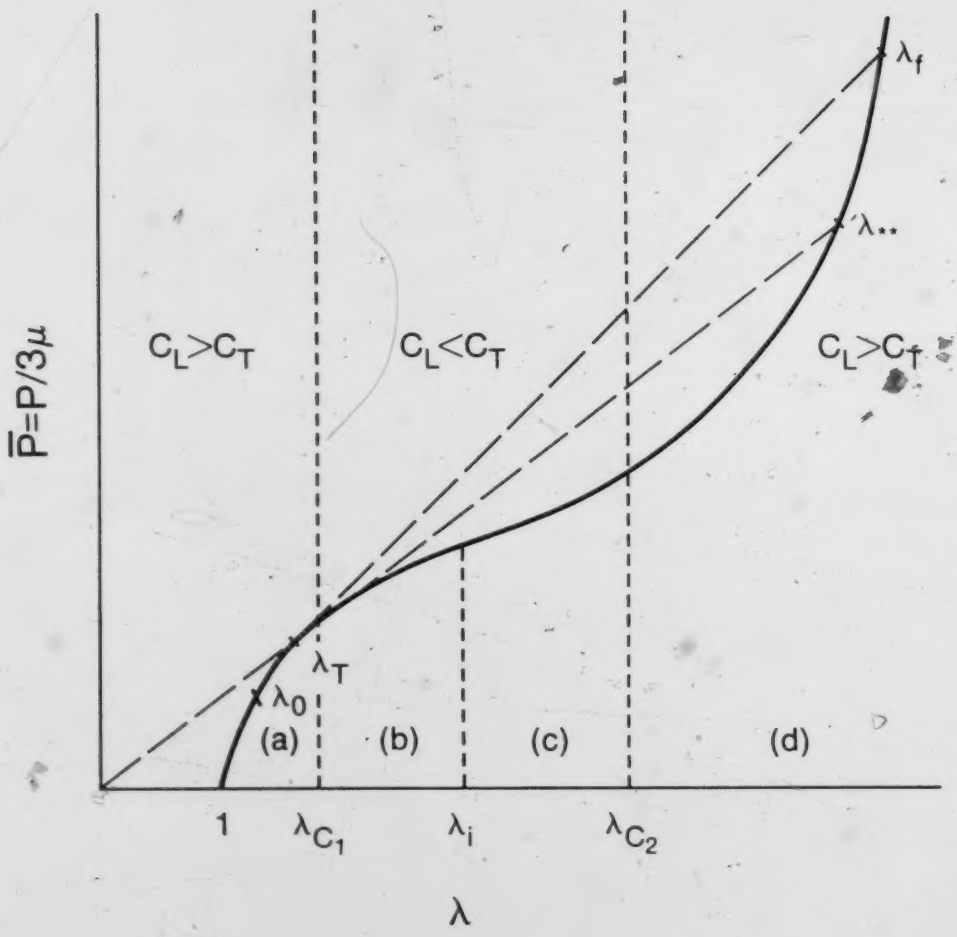

Figure 6.16 Isothermal stress-stretch relation (schematic) for 3 term strain energy function showing λ_o in region (a), that is $1 < \lambda_o < \lambda_{c1}$, and $\lambda_f > \lambda_{**}$.

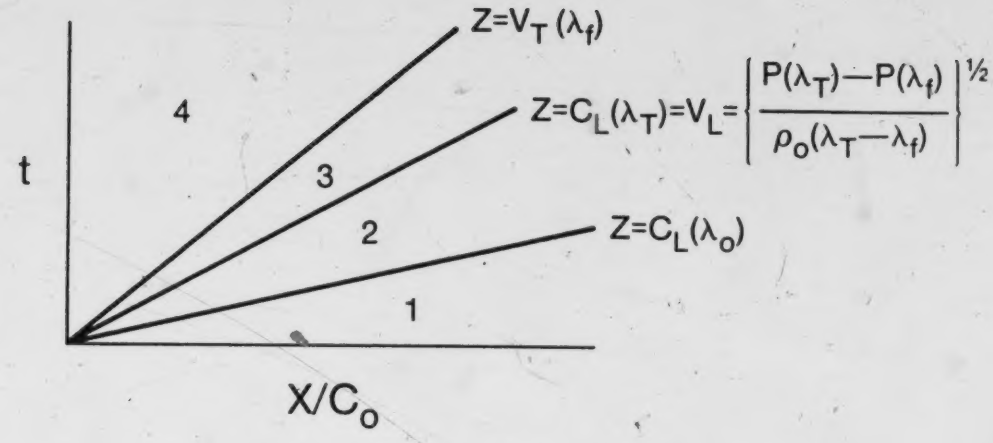

Figure 6.17 Transverse Impact Problem - Solution valid for 3 term Ogden string when $1 < \lambda_o < \lambda_T < \lambda_{c1}$ and $\lambda_f > \lambda_{**}$.

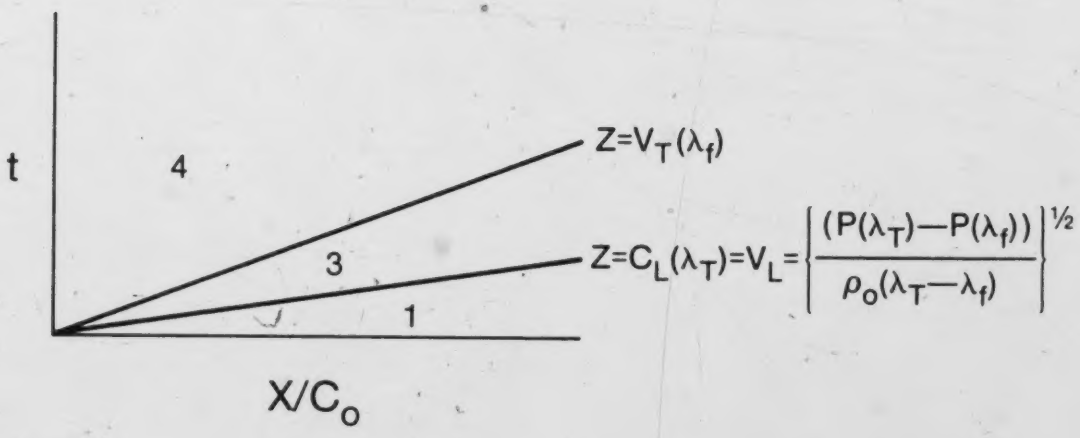

Figure 6.18 Transverse Impact Problem - Solution valid for 3 term Ogden string when $1 < \lambda_o = \lambda_T < \lambda_{c1}$ and $\lambda_f > \lambda_{**}$.

coincides with a characteristic. When $\lambda_f > \lambda_{**}$ and $\lambda_o = \lambda_T < \lambda_{c1}$ the centered simple wave region 2 vanishes, as indicated in Figure 6.18. Consider the case when $\lambda_o = \lambda_T = \lambda_{c1}$. Region 3 in Figure 6.18 vanishes and $V_T = V_L$. The solution is then found from jump conditions (5.20) and (5.21) and is a limiting case of the solution indicated in Figure 6.18.

6.2 Symmetrically Plucked String

We consider a string fixed at points, $x = \pm\ell_o$ of the x_1 axis. The natural reference configuration occupies the interval $[-L,L]$ of the x_1 axis and the x_1 coordinate of a particle in the reference configuration is $X\epsilon[-L,L]$. At time $t = 0$ the string is released from the symmetrically deformed configuration given by

$$x_1(X,0) = \frac{\ell_o}{L} X, \quad x_2(X,0) = -\ell_o \frac{(L-X)}{L} \tan\theta_1 \tag{6.27}$$

for $X\epsilon[0,L]$, where θ_1 is the angle the string makes with the x_1 axis as shown in Figure 6.19. The stretch λ_1 at $t = 0$ is given by

$$\lambda_1 = \lambda_o/\cos\theta_1 > 1 \tag{6.28}$$

where $\lambda_o = \ell_o/L$. If $0 \le \ell_o/L < 1$, the string is slack before the deformation (6.27) is applied and $\theta_1 > \cos^{-1}(\ell_o/L)$. After the string is suddenly released from the deformed configuration (6.27), it is assumed that the subsequent deformed shape of the string is symmetrical about the x_2 axis, consequently only the part $X\epsilon[0,L]$ is considered.

Similarity solutions are presented for Mooney-Rivlin and three term s.e.f. strings, and these solutions are valid until the first

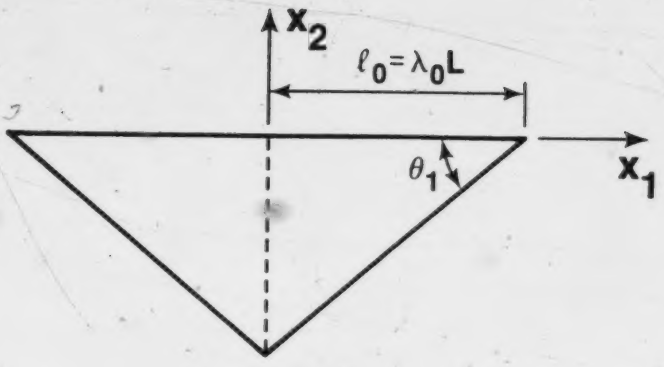

Figure 6.19 Deformed configuration of the string before it is released at time t = 0.

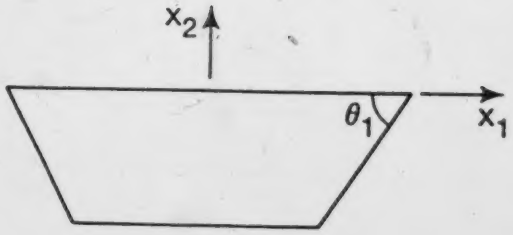

Figure 6.20 Deformed configuration of the string for time t > 0.

reflection occurs at X = L. For certain values of λ_o and θ_1, no longitudinal reflected wave is possible since the string cannot sustain compression and this is discussed later. It was shown in Chapter V, that $c_T = V_T$, consequently a discontinuity of θ is propagated along characteristics with slopes c_T in the (X,t) plane. There is no characteristic parallel to the t axis of the (X,t) plane for $\lambda \neq 1$, consequently after the string is suddenly released, the subsequent deformed shape of the string is as indicated in Figure 6.20.

6.3.1 Mooney-Rivlin String

We first present similarity solutions for a Mooney-Rivlin S.E.F. string with $\alpha = 0.6$ where the wave speeds c_L, c_T are given by equations (6.3), (6.4). The similarity solutions consist of three constant state regions in the (X,t) plane, separated by shocks $Z = V_T$ and $Z = V_L$, where V_T and V_L are determined by λ_o and θ_1. The initial values θ_1 and λ_o determine whether $V_L > V_T$ or $V_T > V_L$. First we consider the case with $V_L > V_T$, as indicated in the (X,t) plane in Figure 6.21. The following solution is valid if $\lambda_1 < \lambda_{c1}$ or if $\lambda_1 > \lambda_{c1}$ and $\lambda_f < \hat{\lambda_T}$, where $V_T(\hat{\lambda_T}) = V_T(\lambda_1)$ and λ_f is the unloaded stretch.

Region 1: $X/t > V_L$;

$$u = v = 0, \ \lambda = \lambda_1, \ \theta = \theta_1.$$

Region 2: $V_L > X/t > V_T(\lambda_f)$;

$$u = u_2, \ \ v = v_2, \ \ \lambda = \lambda_f, \ \ \theta = \theta_1,$$

Region 3: $V_T(\lambda_f) > X/t \geq 0$;

$$u = 0, \ \ v = v_3, \ \ \lambda = \lambda_f, \ \ \theta = 0 \ ,$$

where

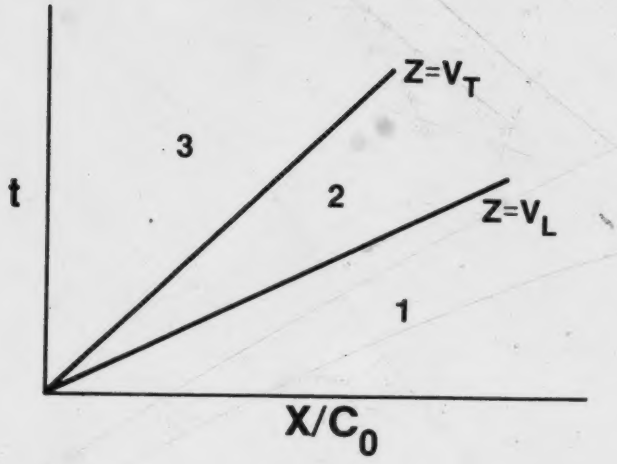

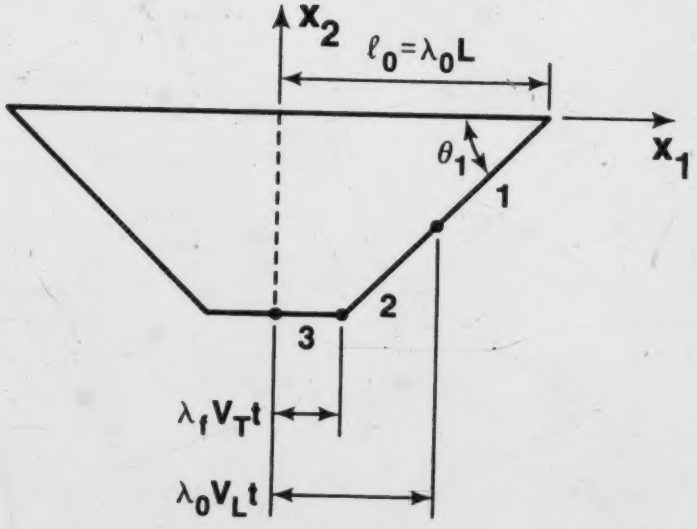

Figure 6.21 Plucked String Problem - Solution valid for Mooney-Rivlin string if $\lambda_1 < \lambda_{c1}$ or if $\lambda_1 > \lambda_{c1}$ and $\lambda_f < \lambda_T^{\wedge}$.

$$V_L = \left\{ \frac{P(\lambda_f) - P(\lambda_1)}{\rho_o(\lambda_f - \lambda_1)} \right\}^{1/2} \tag{6.29}$$

It may be deduced from the jump relations across the shocks,

$$u_2 = V_L \cos\theta_1 \, (\lambda_1 - \lambda_f) \, , \tag{6.30}$$

$$v_2 = V_L \sin \theta_1 \, (\lambda_1 - \lambda_f) \, , \tag{6.31}$$

$$u_2 = \lambda_f V_T(\lambda_f)(1 - \cos\theta_1) \, , \tag{6.32}$$

$$v_2 = -\lambda_f V_T(\lambda_f)\sin \theta_1 + v_3 \, . \tag{6.33}$$

If λ_o and θ_1 are given the unknowns can be obtained from (6.29) - (6.33), and (6.28).

Next we consider the case, $V_T > V_L$ as indicated in Figure 6.22. The solution given is valid if $\lambda_f > \lambda_{c1}$ or if $\lambda_1 > \lambda_{c1}$ and $\lambda_f > \hat{\lambda_T}$.

Region 1: $X/t > V_T(\lambda_1)$;

$u = v = 0, \ \lambda = \lambda_1, \ \theta = \theta_1.$

Region 2: $V_T(\lambda_1) > X/t > V_L$; (6.34)

$u = u_2, \ v = v_2, \ \lambda = \lambda_1, \ \theta = 0.$

Region 3: $V_L > X/t \geq 0$;

$u = 0, \ v = v_2, \ \lambda = \lambda_f, \ \theta = 0,$

where V_L is given by (6.29). From the jump relations across the shocks,

$$u_2 = -\lambda_1 V_T(\lambda_1)(1 - \cos\theta_1), \tag{6.35}$$

$$v_2 = \lambda_1 V_T(\lambda_1)\sin\theta_1, \tag{6.36}$$

$$u_2 = V_L(\lambda_f - \lambda_1). \tag{6.37}$$

If λ_o and θ_1 are given, the unknowns can be obtained from (6.29), (6.35)-(6.37) and (6.28).

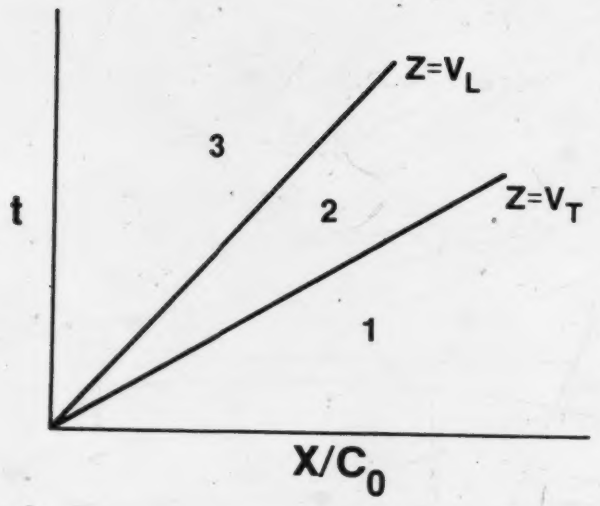

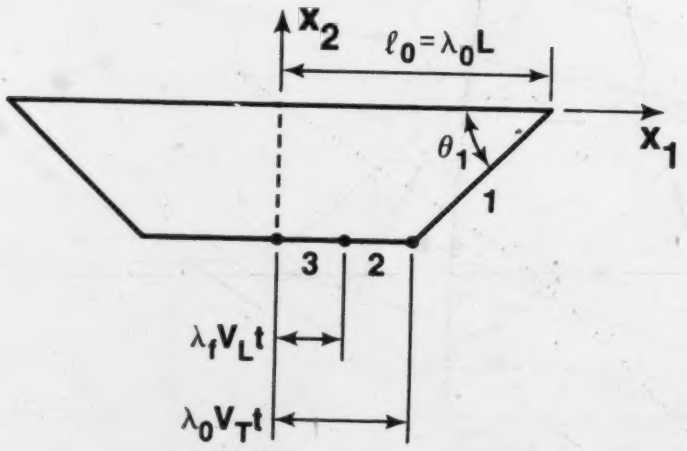

Figure 6.22 Plucked String Problem - Solution valid if $\lambda_f > \lambda_{c1}$ or if $\lambda_1 > \lambda_{c1}$ and $\lambda_f > \hat{\lambda_T}$.

The regions of validity in the (θ_1,λ_o) plane for the above solutions are shown in Figure 6.23.

For the limiting cases of these solutions as $\lambda_f \to \lambda_T^{\wedge}$ so that $V_L \to V_T$ and region 2 in Figure 6.21 and 6.22 becomes vanishingly small, a solution is readily obtained from jump relations (5.20) and (5.21). This solution is particularly simple since $\lambda_f = \lambda_T^{\wedge} = \lambda_o$.

6.3.2 Three Term Ogden String

We present solutions for a three term S.E.F. string where the wave speeds c_L and c_T are given by equations (6.19) and (6.20). Solutions for $\lambda_1 < \lambda_i$ are of the same form as those for the Mooney-Rivlin string. We present two solutions, one which is valid if $\lambda_1 > \lambda_f > \lambda_{c2}$ and one which is valid if $\lambda_1 > \lambda_{c2} > \lambda_f > \lambda_i$. The first solution consists of constant state regions 1,3,4 and a centered simple wave region 2 as indicated in Figure 6.24 and is as follows:

Region 1: $X/t \geq c_L(\lambda_1)$;

$$u = v = 0, \quad \lambda = \lambda_1, \quad \theta = \theta_1 . \tag{6.38}$$

Region 2: $c_L(\lambda_1) \geq X/t \geq c_L(\lambda_f)$;

$$X/t = c_L(\lambda), u = -\hat{I}(\lambda)\cos\theta_1, \quad v = -\hat{I}(\lambda)\sin\theta_1, \quad \theta = \theta_1.$$

Region 3: $c_L(\lambda_f) \geq X/t > V_T(\lambda_f)$

$$\lambda = \lambda_f, \; u = u_3 = -\hat{I}(\lambda_f)\cos\theta_1, \; v = v_3 - \hat{I}(\lambda_f)\sin\theta_1, \; \theta = \theta_1.$$

Region 4: $V_T(\lambda_f) < X/t \geq 0$;

$$u = 0, \quad v = v_4, \quad \lambda = \lambda_f, \quad \theta = 0,$$

where

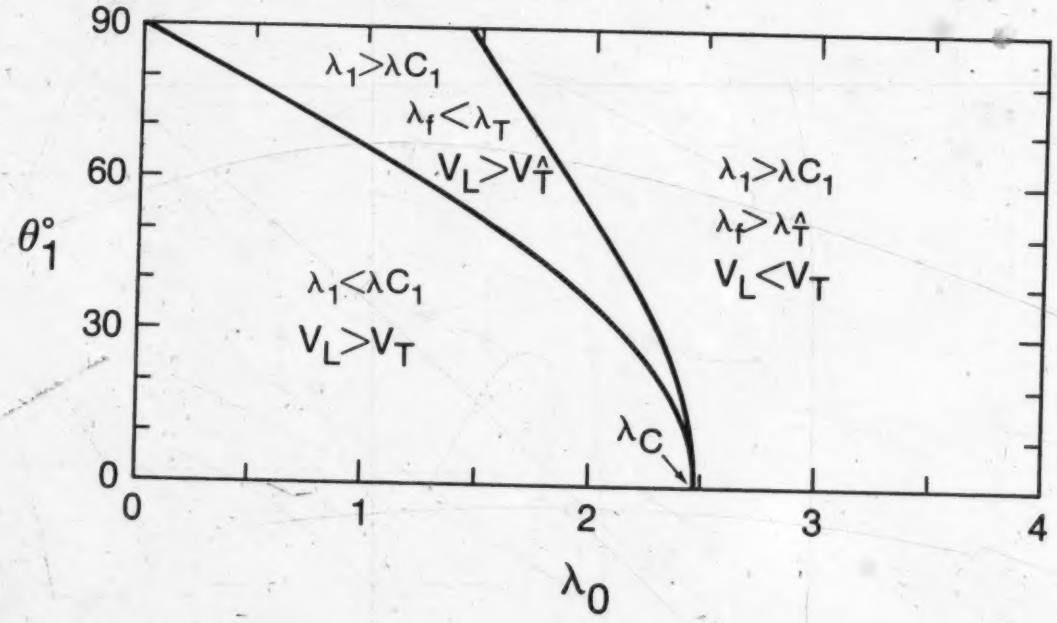

Figure 6.23 Plucked String Problems - Regions of validity for Mooney-Rivlin s.e.f. string with $\alpha = 0.6$. Note that λ_o is the prestretch when $\lambda_o \geq 1$, when $\lambda_o < 1$ the string is slack and $\lambda_o = \ell_o/L$ is not the stretch.

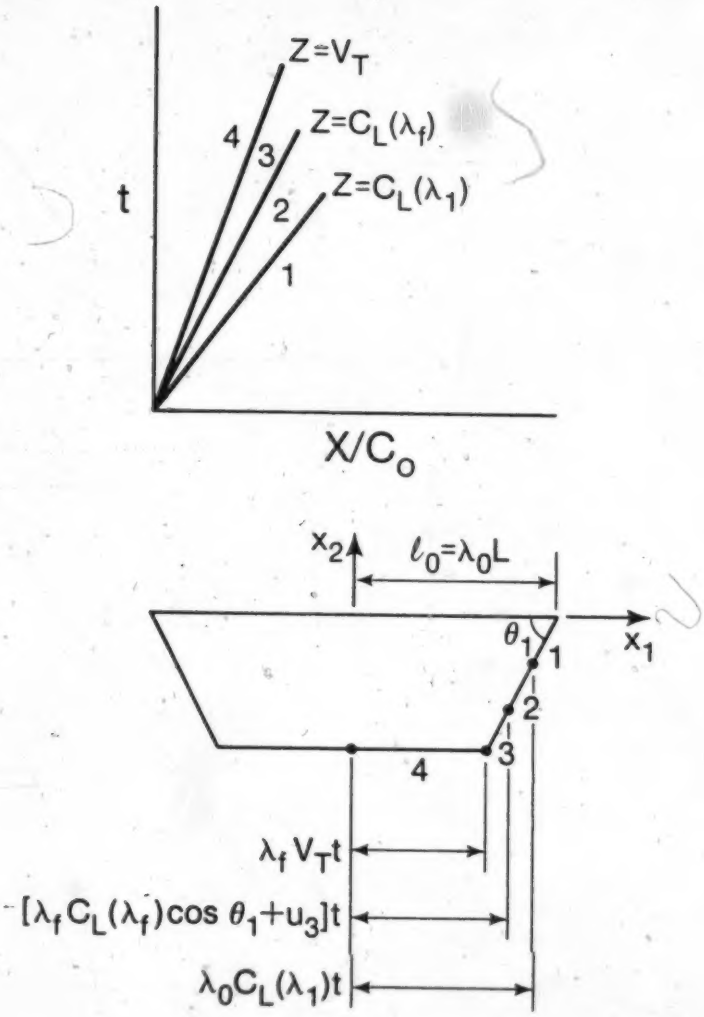

Figure 6.24 Plucked String Problem - Solution valid for 3 term Ogden string if $\lambda_1 > \lambda_f > \lambda_{c2}$.

$$\hat{I}(\lambda) = \int_{\lambda_1}^{\lambda} c_L(\eta)\, d\eta ,$$

and

$$v_4 = v_3 + \lambda_f V_T(\lambda_f)\sin\theta_1, \tag{6.39}$$

is obtained from the jump relation across the transverse shock. If λ_o and θ_1 are given the unknowns can be obtained from (6.38), (6.39) and (6.28).

As λ_f approaches λ_{c2} region 3 shrinks and for $\lambda_f = \lambda_{c2}$ the characteristics bounding region 3 coincide. A small modification to the above solution is required.

When $\lambda_1 > \lambda_{c2} > \lambda_f > \lambda_i$ the solution consists of constant state regions 1 and 4 and centered simple wave regions 2 and 3 as shown in Figure 6.25 and is as follows:

Region 1: $X/t \geq c_L(\lambda_1)$;

$$u = v = 0, \quad \lambda = \lambda_1, \quad \theta = \theta_1. \tag{6.40}$$

Region 2: $c_L(\lambda_1) \geq X/t > V_T(\lambda_{c2})$;

$$X/t = c_L(\lambda),\ u = -\hat{I}(\lambda)\cos\theta_1,\ v = -\hat{I}(\lambda)\sin\theta_1,\ \theta = \theta_1.$$

Region 3: $V_T(\lambda_{c2}) > X/t \geq c_L(\lambda_f)$;

$$X/t = c_L(\lambda),\quad u = \bar{u}_3 - \int_{\lambda_{c_2}}^{\lambda} c_L(\eta)d\eta,\quad v = \bar{v}_3,\ \theta = 0,$$

Region 4: $c_L(\lambda_f) \geq X/t \geq 0$;

$$u = 0,\quad v = \bar{v}_3,\ \lambda = \lambda_f,\quad \theta = 0,$$

where

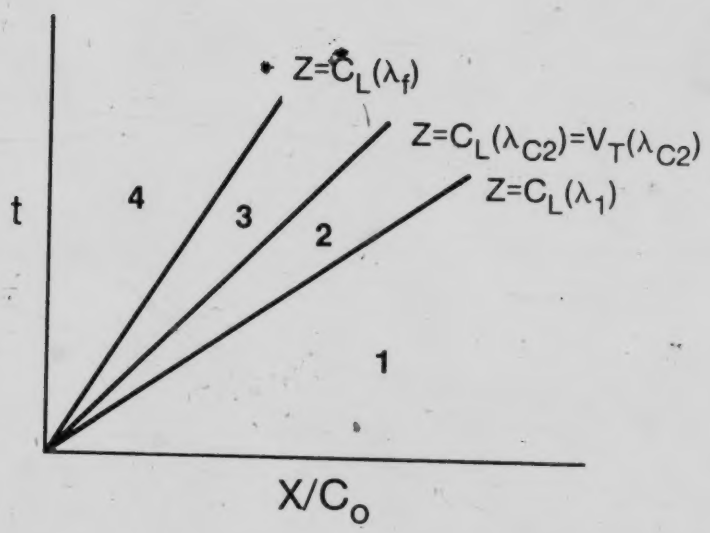

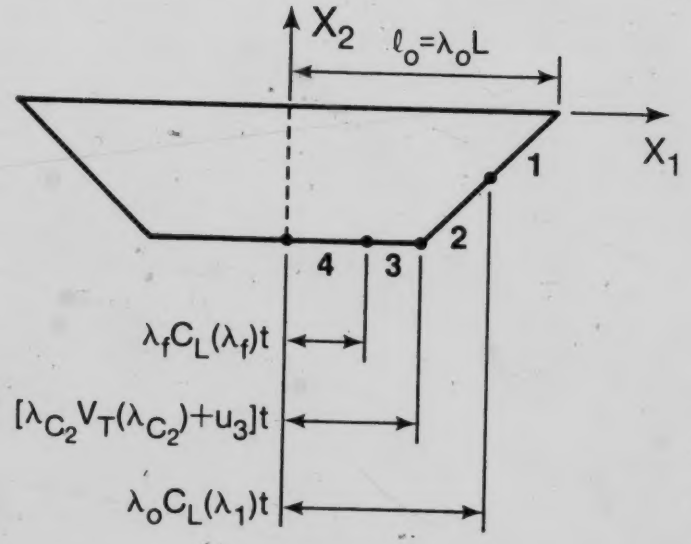

Figure 6.25 Plucked String Problem - Solution valid for 3 term Ogden string if $\lambda_1 > \lambda_{c2} > \lambda_f > \lambda_i$.

$$\bar{u}_3 = -\hat{I}(\lambda_{c2})\cos\theta_1 - \lambda_{c2}V_T(\lambda_{c2})(1 - \cos\theta_1), \tag{6.41}$$

$$\bar{v}_3 = -\hat{I}(\lambda_{c2})\sin\theta_1 + \lambda_{c2}V_T(\lambda_{c2})\sin\theta_1 \tag{6.42}$$

are obtained from the jump relations across the transverse shock. If λ_o and θ_1 are given, the unknowns can be obtained from (6.40) - (6.42), (6.28) and,

$$\bar{u}_3 = \int_{\lambda_{c2}}^{\lambda_f} c_L(\lambda)d\lambda \ . \tag{6.43}$$

The region of validity in the (λ_o, θ_1) plane is shown in Figure 6.26.

Solutions can be obtained in a similar manner when λ_1 and λ_f are in other regions of the isothermal nominal stress-stretch curve shown in Figure 6.7.

6.3 Analogy with Propagation of Waves in Elastic Half Space

Collins (1966) has considered the problem of propagation of waves in an incompressible elastic half space, when the surface is given a uniform motion by the sudden application of shearing stress. When an isotropic solid is considered this problem is analogous to the string problem.

The deformation field for the shear problem for propagation of transverse waves in the x_3 direction is,

$$x_1 = X_1 + \xi_1(X_3,t), \quad x_2 = X_2 + \xi_2(X_3,t), \quad x_3 = X_3, \tag{6.44}$$

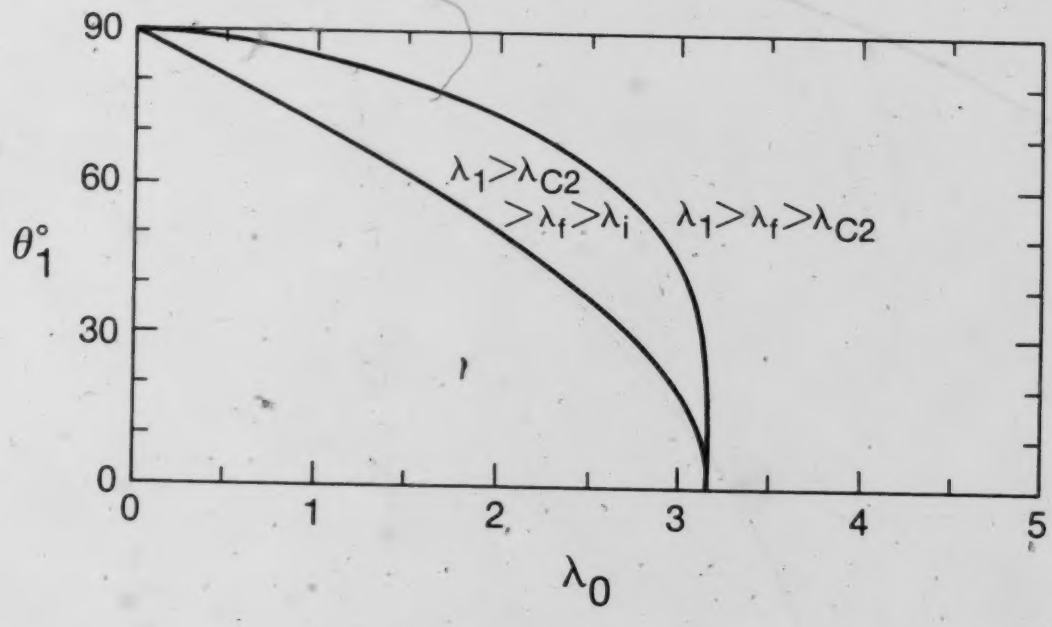

Figure 6.26 Plucked String Problem - Regions of validity for 3 term Ogden string with parameters (4.18).

and the physical components of the deformation gradient tensor are,

$$[\underset{\sim}{F}] = \begin{bmatrix} 1 & 0 & \alpha_1 \\ 0 & 1 & \alpha_2 \\ 0 & 0 & 1 \end{bmatrix}, \tag{6.45}$$

where $\alpha_1 = \partial\xi_1/\partial X_3$, $\alpha_2 = \partial\xi_2/\partial X_3$. The resultant simple shear is $\alpha = (\alpha_1^2 + \alpha_2^2)^{1/2}$, and $\alpha_1 = \alpha\cos\theta$, $\alpha_2 = \alpha\sin\theta$, where θ is the angle the resultant simple shear makes with the x_1 axis.

It follows that,

$$\frac{\partial(\alpha\cos\theta)}{\partial t} = \frac{\partial v_1}{\partial X_3}, \quad \frac{\partial(\alpha\sin\theta)}{\partial t} = \frac{\partial v_2}{\partial X_3}, \tag{6.46}$$

where $v_1 = \dfrac{\partial\alpha_1}{\partial t}$ and $v_2 = \dfrac{\partial\alpha_2}{\partial t}$.

The strain energy function for an isotropic solid can be expressed as $W = W(\alpha_1,\alpha_2) = \hat{W}(\alpha)$, and the resultant shearing stress on a plane X_3 = constant is given by

$$\tau = \frac{d\tilde{W}}{d\alpha}. \tag{6.47}$$

The components S_{31} and S_{32} of the nominal stress tensor are given by,

$$S_{31} = \tau\cos\theta, \quad S_{32} = \tau\sin\theta,$$

consequently the Lagrangian equations of motion are,

$$\frac{\partial(r\cos\theta)}{\partial X_3} = \rho_o \frac{\partial v_1}{\partial t}, \quad \frac{\partial(r\sin\theta)}{\partial X_3} = \rho_o \frac{\partial v_2}{\partial t}. \tag{6.48}$$

The system of equations (6.46) and (6.48) is in conservation form and is analogous to (5.4) with

$$\underset{\sim}{G} = (\alpha\cos\theta_1, \alpha\sin\theta, v_1, v_2)^T, \quad \underset{\sim}{H} = -(v_1, v_2, r\cos\theta, r\sin\theta)^T.$$

It is evident that $\alpha, r, \theta, v_1, v_2$ in the shear problem are analogous to λ, P, θ, u, v, respectively, in the string problem.

Collins has shown that in the shear problem a pair of transverse simple waves or shocks and a pair of circular waves can propagate. The transverse simple waves and circular waves are analogous to the longitudinal and transverse waves, respectively, of the string problem. However the analogy is not complete, since unlike P, λ curves an r, α curve passes through the origin and r is an odd function of α. Collins (1966,1967) considered strain energy functions for which

$$\frac{dr}{d\alpha} > 0$$

$$\text{and } \frac{d^2r}{d\alpha^2} \lessgtr 0 \text{ for } \alpha \gtrless 0, \text{ or } \frac{d^2r}{dt^2} \gtrless 0 \text{ for } \alpha \gtrless 0. \tag{6.49}$$

The shear problem then results in a strictly hyperbolic system with distinct eigenvalues $\pm c_L$ and $\pm c_T$ where

$$c_L = \left(\frac{1}{\rho_o}\frac{dr}{d\alpha}\right)^{1/2} \text{ and } c_T = \left(\frac{1}{\rho_o}\frac{r}{\alpha}\right)^{1/2}.$$

If inequality $(6.49)_1$ is satisfied, $c_T > c_L$ for all $\alpha \neq 0$, and if $(6.49)_2$ is satisfied $c_L > c_T$ for all $\alpha \neq 0$. Collins did not consider an "S" shaped τ, α curve, which would result in $c_T = c_L$ at an isolated point as indicated in Figure 6.27. Similarity solutions for the shear problem are of similar form to those of the string problem. In his second paper (Collins, 1967), Collins gives some non similarity solutions which involve interaction of the c_L and c_T characteristics. These solutions are approximate and are valid only for moderate finite deformation.

A further partial analogy is the problem of propagation of a line polarized transverse wave in a compressible hyperelastic half space. This problem has been considered by Davison (1966) and involves the coupling of longitudinal waves with transverse waves, due to the Poynting effect. The governing system of first order partial differential equations is of the same form as (5.5) with matrix (5.6) however all four characteristic fields are genuinely nonlinear unlike those for the shear problem considered by Collins and the string problem.

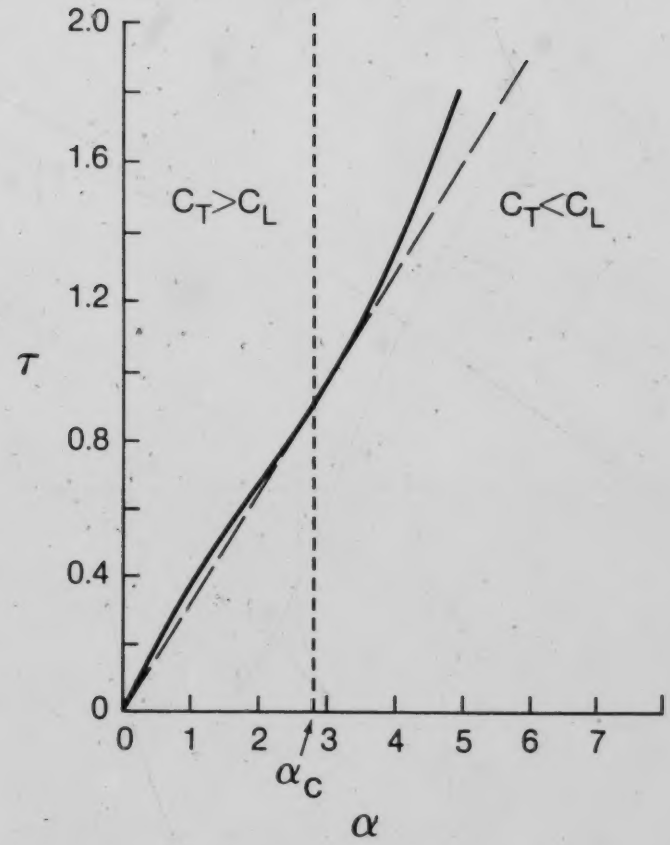

Figure 6.27 Relation between resultant shear stress and shear strain due to Treloar (1975).

Chapter VII

Experimental Results

7.1 Experimental Procedure

Previous experimental work has been done by Riegal and Nowinski (1976) for the impact problem. We are not aware of published work on the plucking problem. For completeness, experimental work on the impact problem is included in this thesis and the results are in broad agreement with those of Riegal and Nowinski (1976). In the above mentioned paper, the experimental results are compared with some theoretical considerations and this is also done in greater detail in this thesis.

7.1.1 Transverse Impact Problem

The apparatus is shown in Figure 7.1 and 7.2 An elastic string is stretched with the desired initial stretch between two adjustable clamps. A 5.56 mm calibre pneumatic gun with a rifled barrel is then loaded with an air gun pellet of mass 0.99 g and an air reservoir is charged to the pressure required to produce the desired muzzle velocity. This pressure is in the range of 700 to 7,000 kPa and produces a muzzle velocity of 30 to 100 m/s. The gun is discharged by opening a solenoid valve, and the pellet passes through three photo detectors which can be seen in Figure 7.2. The first two photo detectors are 30.5 mm apart and are used for timing the projectile for velocity determination. This is accomplished by an electronic frequency counter used in period mode, the first sensor starts the

Figure 7.1 Experimental setup for transverse impact problem.

Figure 7.2 Another view of the experimental setup for transverse impact problem.

count and the second sensor stops the count. The counting frequency is10 MHz giving a 0.1 μs resolution which translates to approximately ± .31 m/s resolution. The third photo detector is used to trigger a delay generating device which controls the stroboscopic light source. If the velocity of the pellet is known, the delay can be calculated to place the projectile in the desired location for the photograph. After the delay, a pulse is sent from the delay generator to the stroboscopic light source, and an exposure is taken. The camera used is a Nikon FM, with a 55 mm lens and is used at f 1:4 and the film is Kodak T-max 400-400 A.S.A. When a photograph is taken, the room is darkened and the shutter of the camera is opened. The solenoid valve is then opened and the gun discharged. After the exposure is taken the shutter of the camera closes. The elapsed time is less than one second, consequently the exposure is from the strobe light only, and the ambient light has little or no effect on the exposure. The duration of flash of the stroboscopic light is approximately 1.2 μs.

7.1.2 Plucked String

The equipment setup is shown in Figure 7.3. An elastic string is held between two adjustable clamps with the desired initial stretch. The string is then stretched and clamped in a modified telephone relay. The relay is operated and the string is held in place at the midpoint as shown in Figure 7.4. When the string is released from the deformed configuration shown in Figure 7.4, it passes through a photo detector which is used to trigger the same delay generator as was used for the

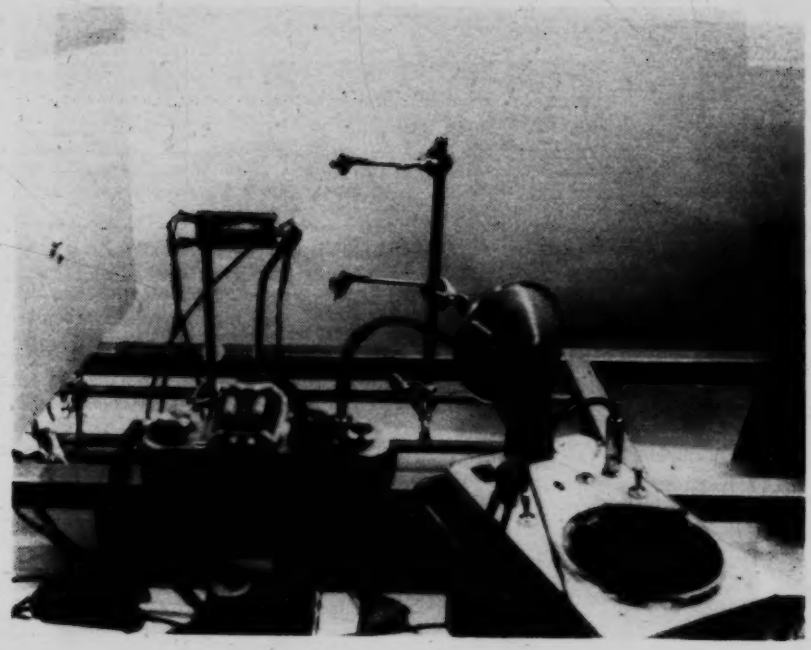

Figure 7.3 Experimental setup for plucked string problem.

Figure 7.4 Deformed configuration of the string before it is released at time $t = 0$.

Figure 7.5 An example of a photograph with double exposure which is used to calculate the velocity of the central flat portion of the string.

impact experiments. The photographic procedure is the same as outlined for the impact experiments. The room is darkened, and the relay is released. The elastic cord passes through the photo detector and the stroboscopic light source flashes after the delay. The camera shutter is held open until the flash has occurred.

Double exposures are used to calculate the velocity of the central flat portion of the deformed configuration of the string after it has been released. An example of a photograph is shown in Figure 7.5. To obtain a double exposure, a second delay generator and a strobe light are required. As the string passes through the photo detector, the signal triggers both of the delay generators which are set to two different delays. The time between the flashes is simply the longer delay minus the shorter delay. The velocity can be calculated by measuring from the photographs the distance the central flat portion of the string has travelled in the time between the two exposures.

7.2 Results for Transverse Impact Problem

Experimental results are presented and compared to theoretical results obtained from similarity solutions which were outlined in Chapter VI. The similarity solutions are valid only until the first reflection, and the experimental results presented are for times before the first reflection occurs at the fixed ends of the string. Special cases of reflection in the plucked string problem are considered and are discussed in the next section.

The strings used in the experiments are carefully selected commercial rubber bands of cross section 1.69 x 1.15 mm. The

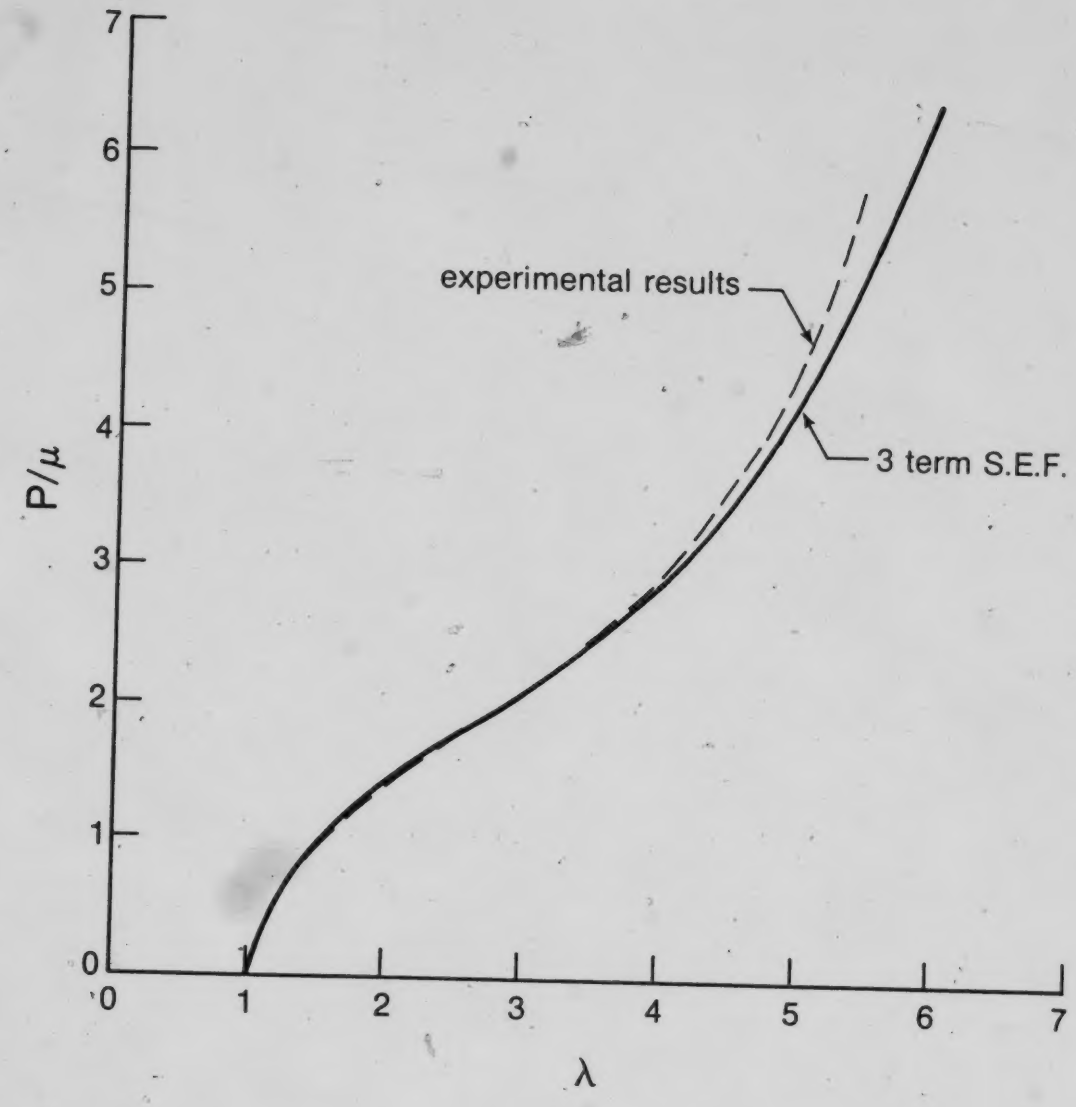

Figure 7.6 Isothermal nominal stress-stretch relation obtained from 3 term strain energy function with parameters (4.18) compared to experimental values. Young's modulus for infinitesimal deformations was experimentally determined to be equal to 1570 kPa.

numerical stress-stretch curve for these bands is in close agreement, up to a stretch of about 4, with that given by Ogden's 3 term strain energy function with parameters (4.18), as indicated in Figure 7.6. This curve is also in acceptable agreement with that obtained from the Mooney-Rivlin strain energy function with $\alpha = 0.6$ for stretches up to 3. A value of 1570 kPa was obtained for Young's modulus for infinitesimal deformation from the natural reference state. Since incompressibility is assumed we take $3\mu = 1570$ kPa. It is reasonable to neglect any viscoelastic effects, since an increase in stretch of only 3% was observed when a band was stretched initially to $\lambda = 7$ and held under constant load for 20 hours. The density of the bands is 1020 kg/m^3.

Results are presented for impact velocities of approximately 85 m/s and 49 m/s with an initial stretch $\lambda_o = 3.2$. Examples of photographs taken for a time before the first reflection occurs, are shown in Figures 7.7 and 7.8 for the impact velocities of 85.1 m/s and 48.6 m/s respectively. The final angle θ_f is measured from the photographs and compared to theoretical values obtained from similarity solutions outlined in Chapter 6. The experimental and theoretical results obtained are tabulated in Table 7.1.

Table 7.1 Transverse Impact Problem: Measured final angle θ_f for impact velocities Q = 85 and 49 m/s, and $\lambda_o = 3.2$.

Impact Velocity Q(m/s)	Final Stretch λ_f	Final Angle θ_f (degrees)	
		Measured	Theoretical
84.0	5.00	54.0	53.9
85.1	5.03	53.0	54.5
48.6	4.02	40.7	38.7
48.6	4.02	40.5	38.7
48.6	4.02	41.0	38.7
49.8	4.06	42.0	39.4
49.8	4.06	41.5	39.4

A simple calculation shows that the slowing of the pellet due to the resistance of the band is negligible.

7.3 Results for Plucked String Problem

Experimental results are presented for times before the first reflection occurs and compared to theoretical results obtained from similarity solutions which were outlined in Chapter VI. The string is given an initial stretch λ_o, and then held at the midpoint with an initial angle θ_1 before it is released. Figure 7.9 is a photograph with two exposures showing the initial deformed shape of the string before it is released at time t = 0, and the subsequent deformed shape of the string after it is released. The experimental results verify the mathematical model which predicts that the angle θ is zero at the midpoint of the cord for times $t > 0$. This is evident in Figure 7.9 by the central flat portion of the string after it is released. Results

Figure 7.7 Transverse Impact Problem - Example of a photograph taken for a time before the first reflection occurs with impact velocity Q = 85.1 m/s.

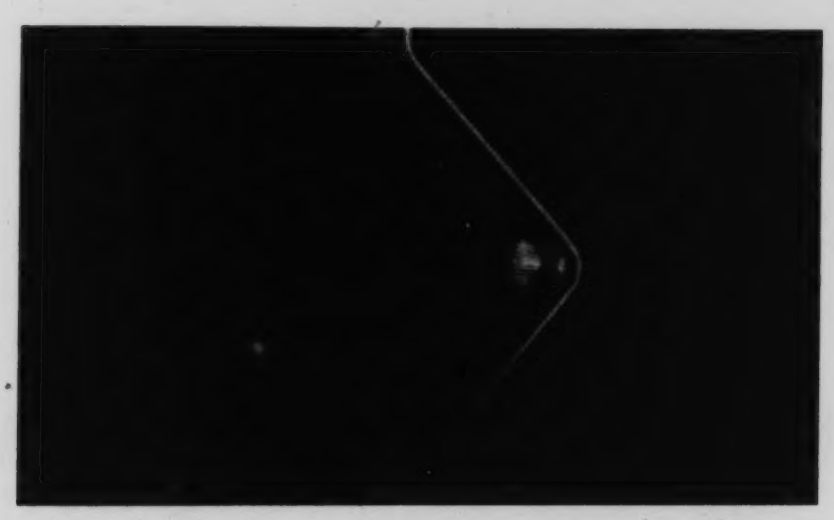

Figure 7.8 Transverse Impact Problem - Example of a photograph taken for a time before the first reflection occurs with impact velocity Q = 48.6 m/s.

are presented when $\lambda_o = 2.0$ and $\theta_1 = 45°$ so that the stretch $\lambda_1 = 2.83$, consequently it is reasonable to compare these results with those predicted by the solutions based on the Mooney-Rivlin strain energy function with $\alpha = 0.6$. An example of the photographs taken is shown in Figure 7.10, where the double exposure is used to obtain v_f the velocity of the flat portion of the elastic cord. The experimental values of v_f obtained from different photographs are tabulated in Table 7.2, and compared to the theoretical value.

Table 7.2 Experimental values of velocity of the central flat portion of the string, v_f, compared to the theoretical value of v_f, with $\lambda_o = 2.0$, $\theta_1 = 45°$ and $\lambda_1 = 2.83$.

Theoretical velocity v_f (m/s)	Experimental velocity v_f (m/s)
38.13	36.40
	36.00
	38.22
	39.50
	39.60

The similarity solutions presented in Chapter VI are valid only until the first reflection occurs at the fixed end of the string. An exact solution can be obtained for a special case of reflection in the plucked string problem. First we consider the similarity solution for plucking of a Mooney-Rivlin string with $\alpha = 0.6$, when the final stretch λ_f and λ_1 satisfy condition $V_T(\lambda_f) = V_T(\lambda_1)$, that is the solution consists of two constant state regions 1 and 2, indicated in Figure 7.11, and the discontinuities of λ and θ coincide. This solution is

Figure 7.9 Plucked String Problem - A photograph with double exposure showing the initial deformed shape of the string before it is released at time t = 0, and the subsequent deformed shape of the string after it is released.

Figure 7.10 Plucked String Problem - An example of a photograph taken at a time before the first reflection occurs. The double exposure is used to determine the velocity of the central flat portion of the string.

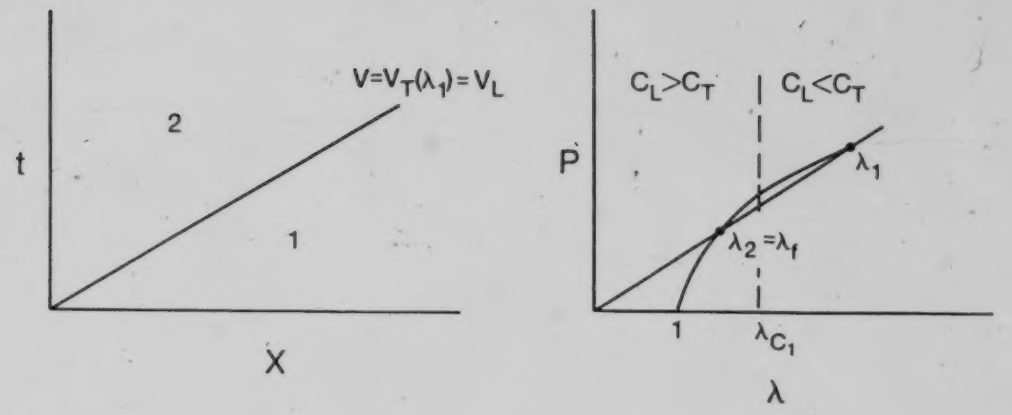

Figure 7.11 Plucking String Problem - the final stretch λ_f and λ_1 satisfy condition $V_T(\lambda_f) = V_T(\lambda_1)$ and the discontinuities of λ and θ coincide. This solution is valid for $tV_T(\lambda_1) \leq 1$.

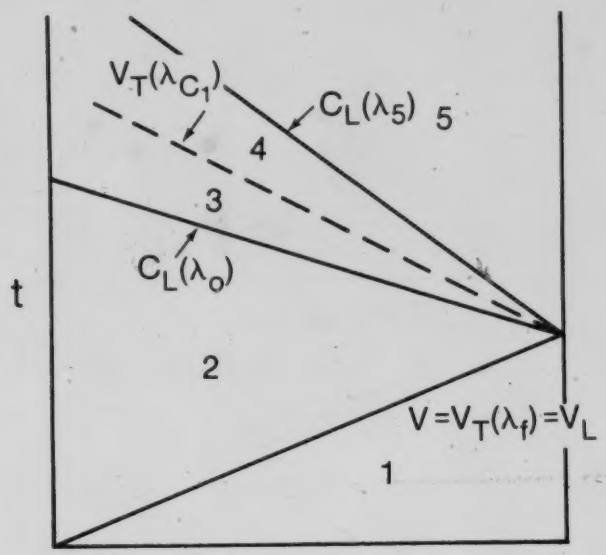

Figure 7.12 Plucking String Problem - The solution with reflection for $0 \leq t \leq L/c_L(\lambda_o) + L/V_T(\lambda_1)$, when $V_T(\lambda_f) = V_T(\lambda_1)$ and the discontinuities of λ and θ coincide for $tV_T(\lambda_1) \leq 1$.

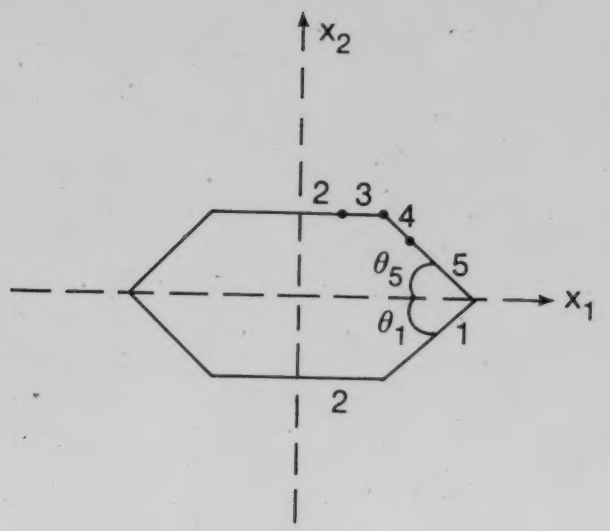

Figure 7.13 Plucking String Problem - Deformed configuration of the string when $V_T(\lambda_f) = V_T(\lambda_1)$, shown before and after the first reflection occurs.

Figure 7.14 Plucking String Problem - experimental results taken for a time after the first reflection occurs, with $\lambda_o = 2$ and $\theta_1 = 45°$. The form after the reflection is similar to that before the reflection.

readily obtained from the jump relations (5.20) and (5.21) and since $\lambda_f = \lambda_o$, the angle θ_1 required for a given $\lambda_o < \lambda_{c1}$ is obtained from $V_T(\lambda_f) = V_T(\lambda_1)$ and $\lambda_o = \lambda_1 \cos\theta_1$. At time $t = L/V_T(\lambda_1)$, which is the limit of validity of the similarity solution, the uniform stretch is λ_o and the uniform velocity has components,

$$u_2 = 0, \quad v_2 = \lambda_1 V_T(\lambda_1) \sin\theta_1 \quad \text{for } 0 \le X < L.$$

If a velocity in the negative x_2 direction and of magnitude v_2 is superimposed, the problem becomes identical to the transverse impact problem with the string initially at rest at time $t_* = 0$, where $t_* = t - L/V_T(\lambda_1)$, and with boundary condition,

$$v(L, t_*) = -\lambda_1 V_T \sin\theta_1.$$

This means that we can use the solution given by (6.10) - (6.13) to obtain the response for $L/V_T(\lambda_1) < t < L/c_L(\lambda_o) + L/V_T(\lambda_1)$ as indicated in Figure 7.12.

Results for a specific case are as follows:

$$\lambda_1 = 3, \quad \lambda_f = \lambda_2 = \lambda_o = 2.12726, \quad \theta_1 = 44.84°$$

$$v_2 = 1.0263\ c_o, \quad V_T(\lambda_1) = 0.48517\ c_o,$$

$$\theta_2 = \theta_3 = 0, \quad v_3 = v_2 = 1.0263\ c_o, \quad \theta_4 = \theta_5 = 44.838,$$

$$\lambda_5 = 3.00024$$

where the subscripts 1,2,3,4 refer to the corresponding regions shown in Figure 7.12. It is interesting to note that $\theta_5 \simeq \theta_1$, $\lambda_1 \simeq \lambda_5$, and the form after the first reflection is similar to that before the

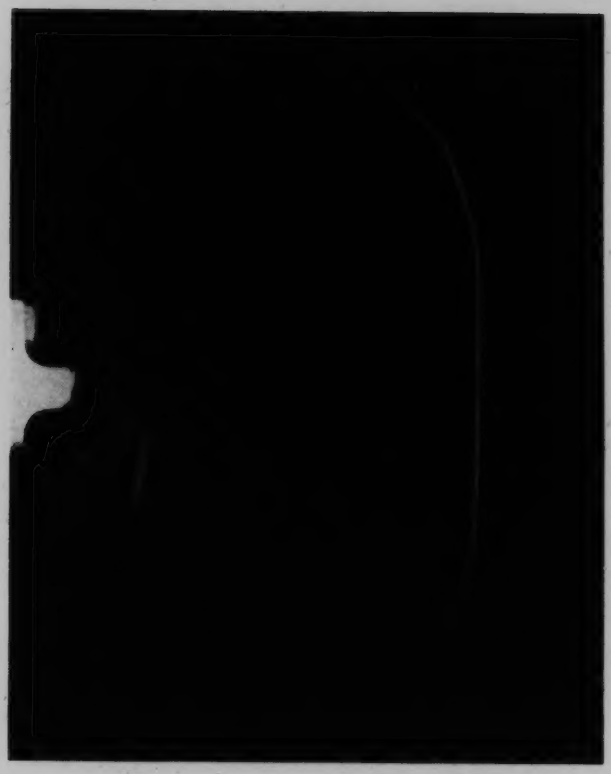

Figure 7.15 Plucking String Problem - Experimental results taken for a time after the first reflection occurs, with evidence of a double kink.

Figure 7.16 Plucking String Problem - Experimental results taken for a time after the first reflection occurs, with evidence of a double kink.

reflection as indicated in Figure 7.13. Experimental results for λ_o = 2 and θ_1 = 45° shown in Figure 7.14 indicate that $\theta_1 \simeq \theta_5$. However, experimental results shown in Figures 7.15, 7.16 indicate that a double kink develops after the first reflection. This is because of the interaction of the reflected longitudinal shock and the incident transverse shock.

Since the string is assumed to be perfectly flexible so that it cannot withstand compressive stress, no reflected longitudinal wave is possible, for certain values of λ_o and θ_1, when the wave front reaches X = L. An example is as follows, based on the similarity solution for a Mooney-Rivlin string with α = 0.6, and $\lambda_1 < \lambda_{c1}$. The similarity solution for λ_o = 1 and θ_1 = 45° is of the form indicated in Figure 7.17 and equations (6.29), (6.30) and (6.28) give the following results,

$$\lambda_1 = \sqrt{2}\,, \qquad \lambda_2 = \lambda_3 = 1.1792\,,$$

$$V_L = 0.7291\ c_o, \qquad V_T = 0.3498\ c_o\,.$$

The longitudinal shock reaches X = L at $t = L/V_L$. If we consider the reflection from the fixed end X = L a solution valid until the reflected shock meets the θ discontinuity can be obtained from the solution given in (5.7) for the simple tension problem of a reflected unloading shock at a fixed end. This solution is indicated in Figure (7.18) and is valid if the value of λ_4 is greater than 1 so that the string is still in tension. For the example considered the solution gives λ_4 = 0.623 with a corresponding nominal compressive stress $P/3\mu$ = -0.81, no reflected longitudinal wave is possible. An

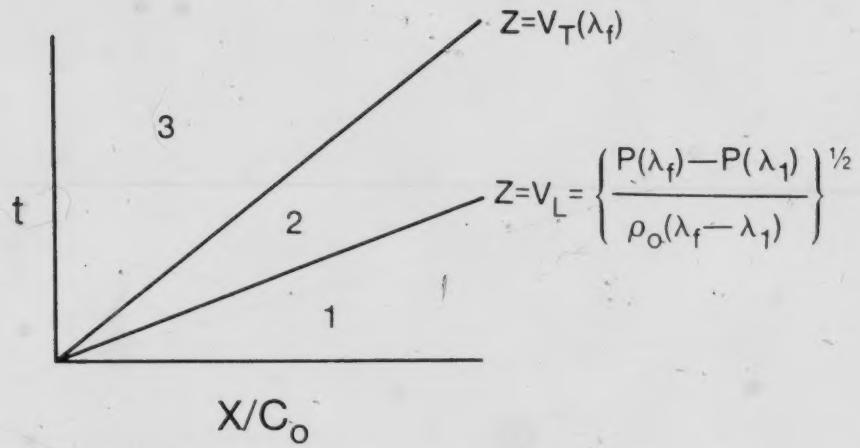

Figure 7.17 Plucking String Problem - Solution for Mooney-Rivlin string with $\alpha = 0.6$, and $\lambda_1 = \lambda_{c1}$. The solution is valid for $tV_L \leq 1$.

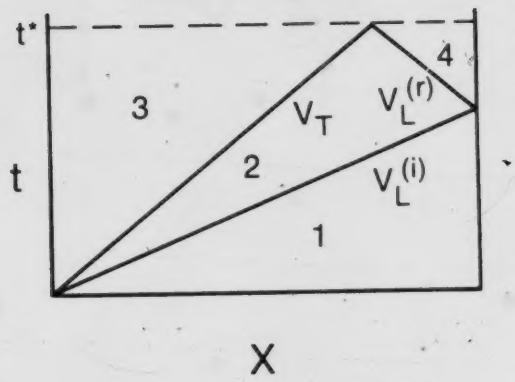

Figure 7.18 Plucking String Problem - Solution with reflection for Mooney-Rivlin string with $\alpha = 0.6$, and $\lambda_1 < \lambda_{c1}$. The solution is valid for $t \leq t^*$.

Figure 7.19. Plucking String Problem - Experimental results for $\lambda_o = 1$, $\theta = 45°$, at time t = 3.9 ms. The longitudinal shock has reflected from the ends resulting in instability since the string cannot sustain compression.

experimental verification of this is shown in Figure 7.19 which is for a plucked string with $\lambda_o = 1$ and released with $\theta_1 = 45°$. Using the experimentally determined properties of the string and noting that L = 64 mm the time of arrival of the longitudinal shock of X = L is found to be 2.237 ms. The picture shown in Figure 7.19 was taken at t = 3.9 ms, that is after the arrival of the longitudinal shock and indicates that the string does not withstand compressive stress resulting from the reflection.

7.4 Concluding Remarks

The experimental results confirm the validity of the theoretical analysis for both the transverse impact and plucking problems. The numerical results obtained are based on the use of an isothermal stress-stretch relation, however, there is no difficulty in principle in using an adiabatic stress-stretch relation and taking the effect of the jump in entropy across a longitudinal shock into account. This has been done in Chapter V for the particular case of the simple tension unloading problem and the indications are that the additional complications involved are not justified. The errors resulting from the thermodynamic approximations used are likely to be small compared to the experimental errors in determining material properties.

Bibliography

Anderson, D.A., Tannehill, J.C., Pletcher, R.H., Computational Fluid Mechanics and Heat Transfer, Series in Computational Methods in Mechanics and Thermal Sciences, McGraw Hill Book Company, 1984.

Beatty, M.F., Haddow, J.B., "Transverse Impact of a Stretched String", Trans. ASME, J. Appl. Mech., v. 107, pp. 137-143, 1985.

Bland, D.R., Nonlinear Dynamic Elasticity, Blaisdell Publishing Company, Waltham, Massachusetts, 1969.

Bracewell, R.N., The Fourier Transform and Its Applications, 2nd Edition, McGraw-Hill Book Co., 1986.

Brigham, E.O., The Fast Fourier Transform, Prentice Hall Inc., 1974.

Burden, R.L., Faires, J.D., Reynolds, A.C., Numerical Analysis, 2nd Edition, Prindle, Weber and Schmidt, Boston, Massachusetts, 1981.

Chadwick, P., "Thermo-Mechanics of Rubberlike Materials", Phil. Trans. R. Soc., A1260, pp. 371-403, 1974.

Chadwick, P., Continuum Mechanics: A Concise Theory, George Allen and Unwin Ltd., 1976.

Chadwick, P., Creasy, C.F.M., "Modified Entropic Elasticity of Rubberlike Materials", J. Mech. Phys. Solids, v32, No. 5, pp. 337-357, 1984.

Christensen, R.M., Theory of Viscoelasticity An Introduction, 2nd Edition, Academic Press, 1982.

Collins, W.D., "The Propagation and Interaction of One-Dimensional Non-Linear Waves in an Incompressible Isotropic Elastic Half-Space", Q. Jl. Appl. Math., v 20, Pt. 4, pp. 429-452, 1967.

Collins, W.D., "One-Dimensional Non-Linear Wave Propagation in Incompressible Elastic Materials", Q. Jl. Mech. Appl. Math., v. 19, pp. 259-328, 1966.

Courant, R., Freidrichs, K.O., Supersonic Flow and Shock Waves, Springer-Verlag, 1976.

Cristescu, N., "Rapid Motions of Extensible Strings", J. Mech. Phys. Solids, v 12, pp. 269-278, 1964.

Davison, L., "Propagation of Plane Waves of Finite Amplitude in Elastic Solids", J. Mech. Phys. Solids, v 14, pp. 249-270, 1966.

Earnshaw, S., "On the Mathematical Theory of Sound", Phil. Trans. v. 150, pp. 133-148, 1858.

Gerald, C.F., Wheatley, P.O., Applied Numerical Analysis, 3rd Edition, Addison-Wesley Publishing Company, Inc., 1984.

Glauz, R.D., Lee, E.H., "Transient Wave Analysis in a Linear Time-Dependent Material", J. Appl. Phys., v. 25, pp. 947-953, 1954.

Gottleib, D., Turkel, E., "Boundary Conditions for Multi-Step Finite Difference Methods for Time Dependent Equations", J. Comp. Physics, v. 26, pp. 181-196, 1978.

Havelock, T.H., The Propagation of Disturbances in Dispersive Media, Cambridge Tracts in Mathematics and Mathematical Physics, Cambridge University Press, 1914.

Jeffrey, A., Quasilinear Hyperbolic Systems and Waves, Research Notes in Mathematics, Pitman Publishing Co., 1976.

von Karmen, T., Duwez, P., "The Propagation of Plastic Deformation in Solids", J. Appl. Phys., v. 21, pp. 987-994, 1950.

Lorimer, S.A., Haddow J.B., "MacCormack's Scheme Applied to Plane Wave Propagation in a Linear Viscoelastic Solid", Comm. Appl. Num. Methods, v. 2, pp. 563-569, 1986.

Morse, P.M., Ingard, K.O., Theoretical Acoustics, McGraw Hill, 1968.

Nowinski, J.L., "On the Propagation of Finite Disturbances in Bars of Rubberlike Materials," ASME Journal of Engineering for Industry, v. 87, pp. 523-529, 1965.

Ogden, R.W., "Large Deformation Isotropic Elasticity: on the Correlation of Theory and Experiment for Incompressible Rubberlike Solids," Proceedings of the Royal Society of London, Series A, Vol. 326, pp. 565-584, 1972.

Ogden, R.W., "Nearly Isochoric Elastic Deformations: Application to Rubberlike Solids," Journal of the Mechanics and Physics of Solids, Vol. 26, pp. 37-57, 1978.

Ogden, R.W., "Elastic Deformations of Rubberlike Solids," in Mechanics of Solids, The Rodney Hill 60th Anniversary Volume (Eds. H.G. Hopkins and M.J. Sewell), pp. 499-537, Pergamon Press, 1982.

Ogden, R.W., Nonlinear Elastic Deformations, Ellis Harwood Limited, Chichester, England, 1984.

Ogden, R.W., Private Communication, 1988.

Pipkin, A.C., Lectures on Viscoelasticity Theory, Springer-Verlag, New York, 1972.

Rayleigh, "Aerial Plane Waves of Finite Amplitudes," Phil. Trans. R. Soc., A84, pp. 247-284, 1910.

Riegel, C., Nowinski, J.L., "An Experimental Investigation of Wave Propagation in a Rubber String Impacted by Projectile," Int. J. Nonlinear Mechanics, v. 11, 229-237, 1976.

Riemann, B.H., "Uber die Fortpflanzung ebener Luftwellen," Abh. Kon. Ges. Weiss. Gottingen 8 (1860), Werke (2nd ed), pp. 156ff, English Translation in, A Source Book in Classical Analysis, Harvard University Press, 1973.

Sod, G.A., Numerical Methods in Fluid Dynamics, Cambridge University Press, 1985.

Spencer, A.J.M., Continuum Mechanics, Longman Inc., New York, 1980.

Taylor, G.I., "The Plastic Wave in a Wire Extended by an Impact Load," The Scientific Papers of G.I. Taylors, Vol. I, Cambridge University Press, pp. 567-579, 1958.

Treloar, L.R.G., The Physics of Rubber Elasticity, 3rd edition, Oxford University Press, 1975.

Whitham, G.B., Linear and Nonlinear Waves, Pure and Applied Mathematics: A Wiley Interscience Series of Texts, Monographs and Tracts, John Wiley and Sons Ltd., 1974.